AFFDL-TR-75-85

ADA018885

CRITICAL REVIEW OF STAGNATION POINT HEAT TRANSFER THEORY

LOCKHEED PALO ALTO RESEARCH LABORATORY
3251 HANOVER STREET
PALO ALTO, CALIFORNIA 94304

JULY 1975

TECHNICAL REPORT AFFDL-TR-75-85
FINAL REPORT FOR PERIOD 15 JANUARY 1975 — 15 JULY 1975

AIR FORCE FLIGHT DYNAMICS LABORATORY
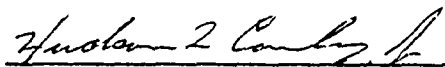Air Force Systems Command
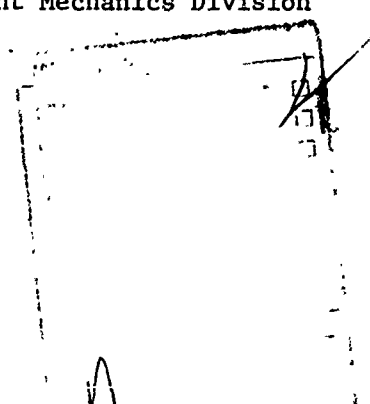Wright-Patterson Air Force Base, Ohio 45433

NOTICE

When Government drawings, specifications, or other data are used for any purpose other than in connection with a definitely related Government procurement operation, the United States Government thereby incurs no responsibility nor any obligation whatsoever; and the fact that the government may have formulated, furnished, or in any way supplied the said drawings, specifications, or other data, is not to be regarded by implication or otherwise as in any manner licensing the holder or any other person or corporation, or conveying any rights or permission to manufacture, use, or sell any patented invention that may in any way be related thereto.

This technical report has been reviewed and is approved for publication.

HUDSON L. CONLEY, JR., Project Engineer
Research and Development Group
Experimental Engineering Branch

FOR THE COMMANDER

ALFRED C. DRAPER
Asst for Research and Technology
Flight Mechanics Division

Copies of this report should not be returned unless return is required by security considerations, contractual obligations, or notice on a specific document.

REPORT DOCUMENTATION PAGE		READ INSTRUCTIONS BEFORE COMPLETING FORM
1. REPORT NUMBER AFFDL-TR-75-85	2 GOVT ACCESSION NO.	3. RECIPIENT'S CATALOG NUMBER
4. TITLE *(and Subtitle)* Critical Review of Stagnation Point Heat Transfer Theory.		5 TYPE OF REPORT & PERIOD COVERED Final Report, 15 Jan - 15 Jul 75 6. PERFORMING ORG. REPORT NUMBER
7 AUTHOR(s) H. Hoshizaki, Y. S. Chou, N. G. Kulgein J. W. Meyer		8 CONTRACT OR GRANT NUMBER(s) F33615-75-C-3032
9 PERFORMING ORGANIZATION NAME AND ADDRESS Lockheed Palo Alto Research Laboratory 3251 Hanover Street Palo Alto, Calif. 94304		10. PROGRAM ELEMENT, PROJECT, TASK AREA & WORK UNIT NUMBERS 62201F 142601
11 CONTROLLING OFFICE NAME AND ADDRESS Flight Mechanics Division Air Force Flight Dynamics Laobratory Wright-Patterson Air Force Base, Ohio 45433		12 REPORT DATE July 1975
		13. NUMBER OF PAGES 108 p.
14 MONITORING AGENCY NAME & ADDRESS(*If different from Controlling Office*)		15. SECURITY CLASS. *(of this report)* Unclassified
		15a. DECLASSIFICATION/DOWNGRADING SCHEDULE

16. DISTRIBUTION STATEMENT *(of this Report)*

Approved for public release; distribution unlimited.

17. DISTRIBUTION STATEMENT *(of the abstract entered in Block 20, if different from Report)*

18 SUPPLEMENTARY NOTES

19 KEY WORDS *(Continue on reverse side if necessary and identify by block number)*

Arc Heated Re-entry Facilities
Stagnation Point Heat Transfer
Free Stream Turbulence
Aerodynamic Heating

20 ABSTRACT *(Continue on reverse side if necessary and identify by block number)*

The discrepancy between the bulk enthalpy obtained from an arc chamber heat balance and the test section bulk enthalpy derived from stagnation point heat transfer measurements is investigated. Free stream turbulence is a possible cause of discrepancy. Copper particle impingement may also be a possible cause if the copper mass loading is greater than 0.1%. Enthalpy fluctuations, radial enthalpy gradients, chemical nonequilibrium, swirl flow, and transport property uncertainties were all found to be unimportant.

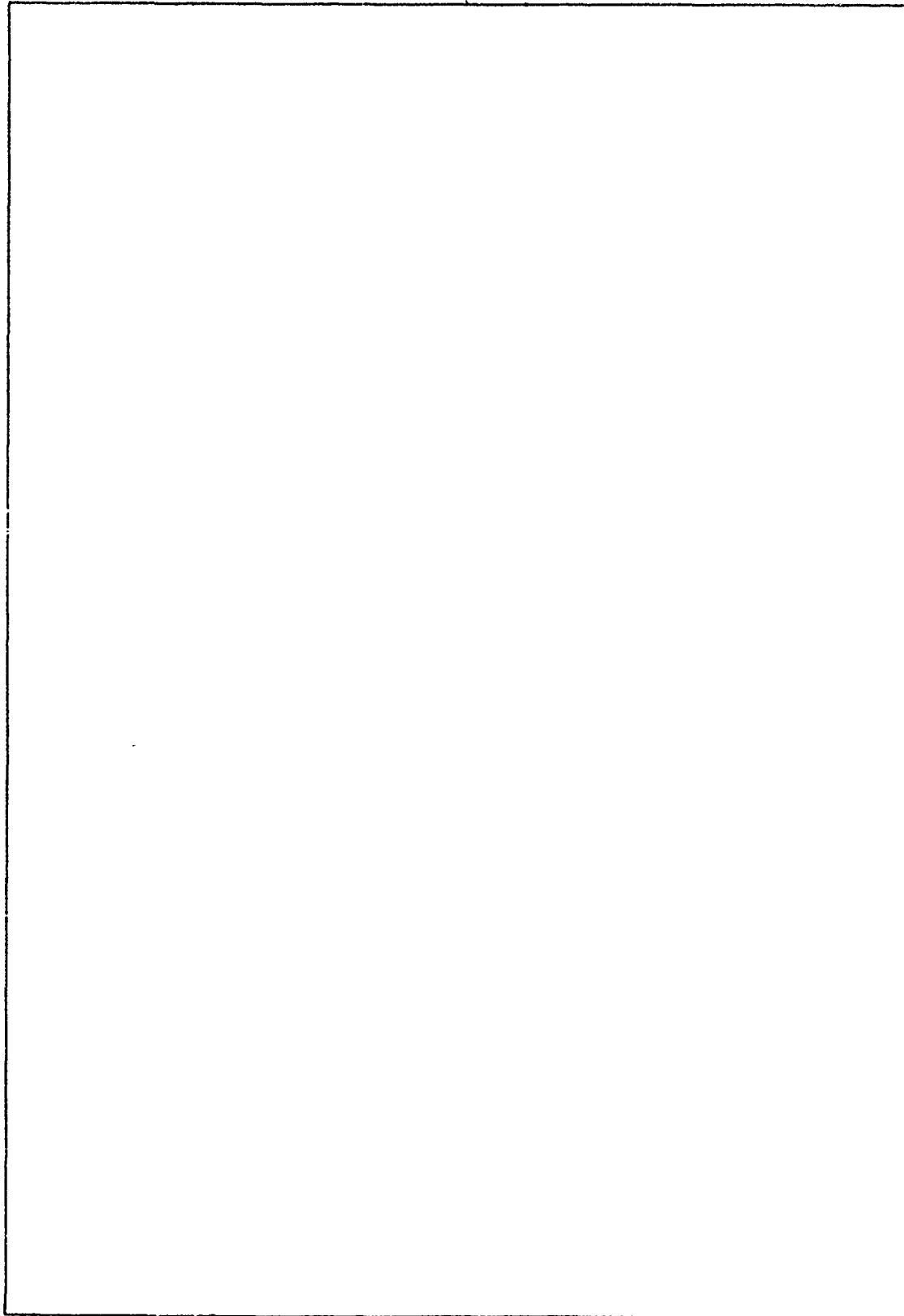DD $_{1\ JAN\ 73}^{FORM}$ 1473 EDITION OF 1 NOV 65 IS OBSOLETE

FOREWORD

This report was prepared by Lockheed Palo Alto Research Laboratory of Palo Alto, California, and summarizes their work under Contract F33615-75-C-3032. The developments reported were carried out under Project 1426, "Experimental Simulation of Flight Mechanics", Task 142601, "Diagnostic, Instrumentation and Similitude Technology", and work unit 14260140, "Critical Review of Stagnation Point Heat Transfer Theories Applicable to Arc Tunnel Flows". Mr. Hudson L. Conley, Jr., of the Air Force Flight Dynamics Laboratory (AFFDL/FXN) was the contract monitor.

This development effort was initiated in January, 1975, and was completed in June, 1975.

The technical report was released by the authors in July, 1975, for publication.

iii

TABLE OF CONTENTS

LIST OF TABLES

LIST OF ILLUSTRATIONS

LIST OF ILLUSTRATIONS (Cont)

LIST OF ILLUSTRATIONS   (Cont)

Section 1
INTRODUCTION

The basic problem addressed in this report is the uncertainty in measured stagnation enthalpy in the Reentry Nose Tip (RENT) Leg of the AFFDL 50 Megawatt Facilities. The values of local stagnation enthalpy derived from stagnation point heat transfer measurements appear to be significantly higher than those obtained from heat balance measurements on the arc heater and from direct measurements of local stagnation enthalpy. These discrepancies may be due to possible errors in instrumentation or due to some of the assumptions contained in stagnation-point heat transfer theories being violated. The basic objective of this program was to investigate the latter possibility, namely, the possibility that there are some important physical phenomena present in the RENT, such as enthalpy gradients, free-stream turbulence, etc., which are not taken into account by the Fay and Riddell type of stagnation-point heat transfer theories.

The technical approach to this problem was to critically review stagnation point heat transfer theories and other papers and reports which may be relevant to a possible cause of measured discrepancies in stagnation enthalpy. Two groups of papers and reports were considered. The first group consisted of stagnation point heat transfer theories defined in a narrow sense, i.e., theories treating the heat transfer from a dissociated gas to blunt bodies in a supersonic stream (e.g., Fay and Riddell). The second group consisted of papers and reports which deal with phenomena such as particle impingement, free stream turbulence, etc., which are excluded from stagnation point heat transfer theories as defined in the above narrow sense, but which may be present in the RENT facility and may be a possible cause of the observed discrepancies in local stagnation enthalpy measurements. This second group is referred to as "possible cause" theories. Also included in the "possible cause" group are reports and papers containing data and information on facility operating conditions and facility test data which are useful in evaluating the relevancy of possible cause phenomena. The technical approach included, in addition to that described above, analyses to determine the relevancy of a possible cause and investigations to determine cause and effect relationship. Analytical investigations of the possible effects of timewise fluctuation of flow properties, radial

enthalpy gradients and swirl flow on heat transfer were conducted. A cause and effect relationship between free stream turbulence and heat transfer enhancement was established.

A total of eight possible causes were investigated in depth. The findings from these investigations are summarized in Table 1-1. (Radiative heat transfer was also briefly investigated and dismissed as being negligible). The major conclusions of these investigations are that, 1) the discrepancy between the arc chamber heat balance enthalpy and derived free stream enthalpy is between 20% and 50%, and 2) the possible cause which may be responsible is free stream turbulence.

Recommendations for additional efforts to further investigate this problem are two-fold. The first recommendation is to experimentally determine the free stream turbulence level and the copper mass loading in the RENT facility. These flow properties are critical to the quantitative evaluation of potentially important possible causes. The second recommendation is to develop two theoretical models. The first model would predict the flow properties in the test section (free stream turbulence, total pressure, enthalpy, etc.), including the effects of swirl in the arc chamber. The second model is a turbulent viscous, shock layer model which will predict the heat transfer enhancement and change in heat transfer distribution due to free stream turbulence by properly accounting for the interaction between free stream turbulence and the turbulence generated in the boundary layer.

Table 1-1 Summary of Possible Cause Investigations

Possible Cause	Report Section	Findings
Stagnation Point Heat Transfer Theories	2	Stagnation point heat transfer theories which include the effect of free stream turbulence in a subsonic flow show significant enhancement can occur if the free stream turbulence times the square root of the Reynolds Number $(T\sqrt{Re})$ is sufficiently large.
Mass Flux and Bulk Enthalpy	3	Calculation of test section mass flux and bulk enthalpy using measured heat rate and total pressure data indicate that the discrepancy between the arc chamber heat balance enthalpy and the test section bulk enthalpy is between 20% and 50%.
Free Stream Turbulence	4	Subsonic heat transfer data to spheres and cylinders show that free stream turbulence can increase the stagnation point heat transfer by as much as 1.8. In the RENT facility, a 5% turbulence level may increase heat transfer by 50%.
Copper Particle Impingement	5	A 0.1% copper mass loading will increase the stagnation region heat transfer by 5 percent by particle impingement. This heat transfer augmentation is proportional to the RENT flow field copper mass loading which is not reliably known.
Enthalpy Fluctuations and Gradients	6	Analytical results show that enthalpy fluctuations increase heat transfer by about 6% in the RENT facility. Analysis also shows that radial enthalpy gradients can increase or decrease heat transfer. The maximum effect in the RENT facility is about 1%.
Swirling Flow	7	Analysis of the effect of a swirl component in an otherwise uniform flow on heat transfer shows that swirl effects in the RENT facility are negligible. Subsonic data on swirl effects verify this conclusion.

Table 1-1 (Cont)

Possible Cause	Report Section	Findings
Chemical Nonequilibrium	8	Chemical kinetic analyses and computations show that the effects of chemical nonequilibrium on heat transfer in RENT facility are negligible.
Transport Properties	9	The effect of transport property uncertainties on heat transfer is of the order of a few percent and cannot be considered to be a significant error source.

Section 2

STAGNATION POINT HEAT TRANSFER THEORIES

In this section, conventional stagnation point heat transfer theories and heat transfer theories which attempt to account for the effect of free-stream turbulence are described. Although the examination of conventional heat transfer theories has contributed little to the understanding of the RENT stream enthalpy discrepancy, a brief summary of these theories are included for the sake of completeness.

2.1 Conventional Stagnation Point Heat Transfer Theories

Conventional stagnation point heat transfer theories are defined as those theories which predict the heat transfer at the stagnation point of a body immersed in a uniform flow which is free of gradients of any type, has no free stream turbulence, and is devoid of any type of particulate matter. These theories have been developed over the past 20 years and are generally valid for supersonic and hypersonic flight velocities, dissociated and ionized gases and for flows that are in or out of chemical equilibrium.

In this section, only a general description of stagnation point heat transfer theories are presented. A detailed discussion of chemical non-equilibrium effects is presented in Section 8 and the effects of transport properties variations on heat transfer are discussed in Section 9.

Conventional stagnation point heat transfer theories which are of interest to the present program are typified by Fay and Riddell (Ref. 2-1),

------

Ref. (2-1) Fay, J. A., and Riddell, F. R., "Theory of Stagnation Point Heat Transfer in Dissociated Air", J. Aeronaut. Sci., Vol. 25, No. 2, Feb. 1985, pp. 73-85, 121

-5-

Hoshizaki (Ref. 2-2) and others (Refs. 2-3 to 2-5). In all of these theoretical treatments of stagnation point heat transfer, it is implicitly assumed that the free stream is uniform and turbulence is negligible. The oncoming flow is assumed to be supersonic or hypersonic so tha. a bow shock is formed. The Reynolds number is assumed to be sufficiently high that the stagnation point boundary layer thickness is much less than the shock detachment distance. Under these conditions, the vorticity generated by the curved shock can be neglected and the flow at the edge of the boundary layer can be assumed to be free of gradients normal to the surface.

The high flight velocities considered generate stagnation temperatures large enough to dissociate and ionize the gas. The gas is assumed to be a mixture of perfect gases and in most treatments it is assumed to be either a binary mixture or a multicomponent mixture with equal mass diffusion properties. Transport properties such as viscosity and thermal conductivity are assumed to vary across the boundary layer.

At the stagnation point, the flow is locally similar and partial differential equations for the conservation of mass (overall and species) momentum and energy can be reduced to a set of total differential equations with the similarity variable as the independent variable. Numerical solutions to these equations require iteration on either the initial conditions

-----

Ref. (2-2) Hoshizaki, H., "Heat Transfer in Planetary Atmospheres at Super-Satellite Speeds", ARS J., Vol. 32, No. 10, Oct. 1962, pp. 1544-1552

Ref. (2-3) Pallone, Adrian and Van Tassell, Wm., "Effects of Ionization on Stagnation Point Heat Tra sfer in Air and in Nitrogen", Phys. Fluids, Vol. 6, No. 7, July 1963, pp. 983-986

Ref. (2-4) Marvin, J. G., and Deiwert, G. S., "Convective Heat Transfer in Planetary Gases", NASA TR R-224, 1965

Ref. (2-5) Sutton, K., and Graves, R. A., Jr., "A General Stagnation Point Convective Heating Equation for Arbitrary Gas Mixtures", NASA TR R-376, No. 1971

at the wall (for integrating from the wall to infinity, in similarity coordinate) or on entire profiles if the equations are cast in integral form (method of successive approximations).

The transport of chemical enthalpy can be handled in two ways in these solutions. One can retain the terms which account for chemical energy transport in the energy equation and solve the equations in this form (Fay and Riddell, Ref. 2-1), or one can define a total thermal conductivity which is the sum of the thermal conductivity due to molecular collisions and the thermal conductivity due to diffusion of atoms or ions (Koshizaki, Ref. 2-2). The latter method is restricted to thermochemical equilibrium and a fixed elemental gas composition.

It has been a common practice to correlate the numerical results with total enthalpy or flight velocity, fluid properties evaluated at the wall, or stagnation pressure. The correlations that have been published are all quite similar in form and all yield stagnation point heat transfer predictions which vary by about 5 to 10 percent. These differences are usually attributed to slight differences in transport properties and numerical methods of solution.

Analysis of these theories leads to the conclusion that the RENT enthalpy discrepancy cannot be explained on the basis of gross inaccuracies in the theories. The theories have been verified by comparison to laboratory and flight test data and have been employed in the analysis and development of many successful reentry vehicles. The theories are valid within the framework of the assumptions and restrictions for which they were developed.

2.2 Stagnation Point Heat Transfer Theories with Free Stream Turbulence

The stagnation point heat transfer enhancement due to free stream turbulence has been studied theoretically for incompressible flow by Galloway (Ref. 2-6) and Traci and Wilcox (Ref. 2-7). Galloway includes a Reynolds

-----

Ref. (2-6)   T. R. Galloway, "Enhancement of Stagnation Flow Heat and Mass Transfer Through Interactions of Free Stream Turbulence", AIChE Journal, Vol. 19, No. 3, 1973

Ref. (2-7)   R. M. Traci and D. C. Wilcox, "Analytical Study of Freestream Turbulence Effects on Stagnation Point Flow and Heat Transfer", AIAA 7th Fluid and Plasma Dynamics Conf., Palo Alto, Ca., June 17-19, 1974, AIAA Paper No. 74-515

stress term in the otherwise laminar boundary layer questions. This Reynolds stress was modeled by a somewhat modified mixing-length eddy viscosity turbulence model. It was assumed by Galloway that the velocity fluctuations

$$|u'| \sim |v'| = \ell \frac{\partial u}{\partial y} \qquad (2\text{-}1)$$

where ℓ is the Prandtl's mixing length $\ell = ky$ and k is a constant. It was also assumed that the Reynolds stress $\overline{u'v'}$ is proportional to

$|\overline{u'}| \; |\overline{v'}|$. Thus

$$\overline{u'v'} \sim |\overline{u'}| \; |\overline{v'}| = |u'| \; ky \frac{\partial u}{\partial y} = \epsilon_m \frac{\partial u}{\partial y} \qquad (2\text{-}2)$$

where c_m is defined as the eddy viscosity. Unlike the conventional mixing length turbulence model, which, according to Eqs. (2-1) and (2-2), should be given as

$$\epsilon_m = k^2 y^2 \; (\frac{\partial u}{\partial y}), \qquad (2\text{-}3)$$

Galloway created a relationship between ϵ_m and the free stream turbulence as

$$\epsilon_m = k \; IU_\infty y \qquad (2\text{-}4)$$

where I is the free stream turbulence intensity and U_∞ is the free stream velocity. It is to be noted that should Eq. (2-3) be used, there would be no relation between boundary layer Reynolds stress and the free stream turbulence. Also there would be no stagnation heat transfer enhancement due to the fact that $u = 0$, $\epsilon_m = 0$ at the stagnation region. Hence, the conventional mixing length model is not an applicable turbulence model for the study of free stream turbulence.

Based on the eddy viscosity of Eq. (2-4), enhancement in heat transfer at the stagnation point was found by Galloway as shown in Figure 1. In this figure, the temperature profiles normal to the surface are shown as a function of the parameter X which is equal to $kL\sqrt{R_e}$, where R_e is the Reynolds number based on nose radius R. The Nusselt number is also tabulated in Figure 1.

$$\theta = \frac{T - T_\infty}{T_O - T_\infty}$$

CIRCULAR CYLINDER

x	Nu/$\sqrt{\text{Re}}$
8.0	3.937
1.0	1.6040
0.0	1.1494

$$\eta = Y/R \cdot \text{Re}^{1/2}$$
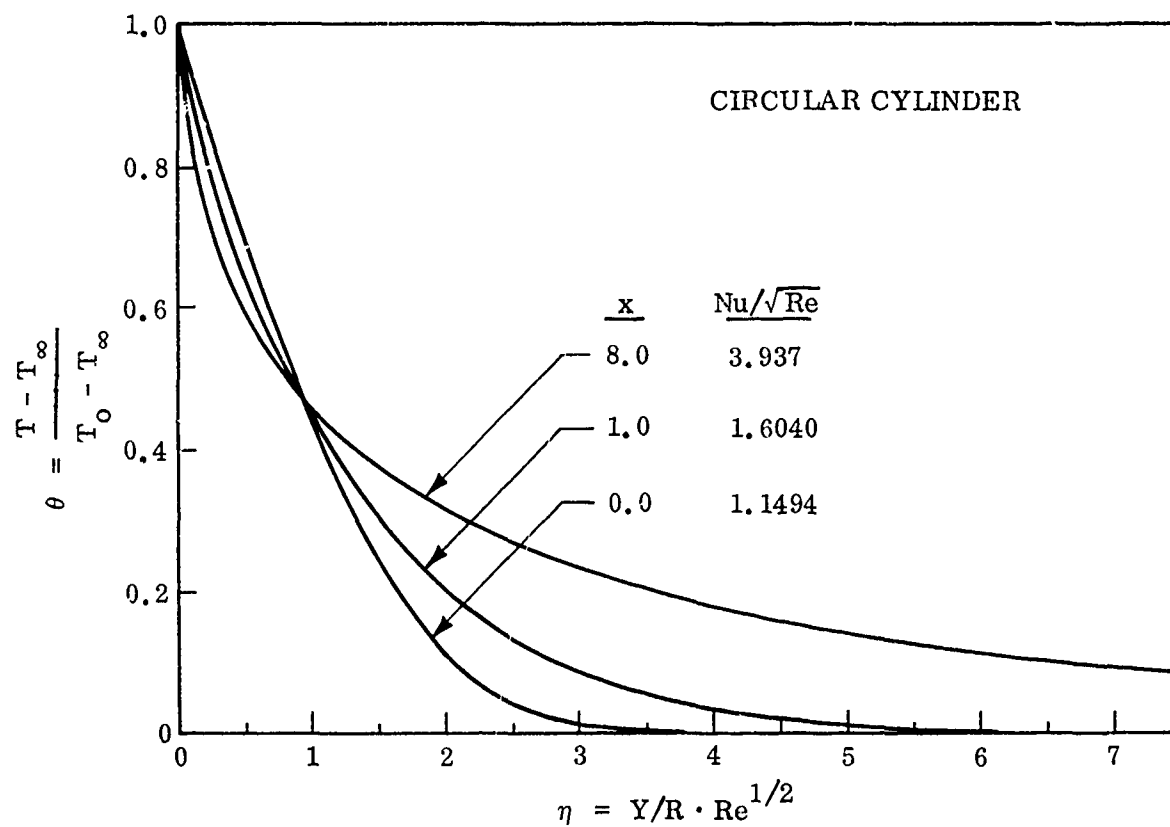
Figure 1   Profiles Normal to the Surface

Comparisons with experimental results were also made by Galloway. By choosing the right value of the constant k (Eq. 2-2), good agreement between theory and experiments were found as discussed in Section 4 (Free Stream Turbulence) of this report.

Based on the work of Ref. (2-6), we may conclude that free stream turbulence significantly enhances the heat transfer, the relevant parameter for this enhancement is $I\sqrt{Re}$.

Traci and Wilcox (Ref. 2-7), on the other hand, used a turbulent kinetic energy (TKE) model in their study. The TKE model they used was developed by Saffman (Ref. 2-8). In this model the relation between Reynolds stress and the mean rate of strain tensor is given as

$$\tau_{ij} = 2(\nu + \epsilon_m) S_{ij} - \frac{2}{3} e \, \delta_{ij} \qquad (2-5)$$

where τ_{ij} is the Reynolds stress tensors. S_{ij} is the mean rate of strain tensor which is related to the gradients of the mean flow, δ_{ij} is the Kronecker delta (i.e., $\delta_{ij} = 0$, if $i \neq j$, $\delta_{ij} = 1$ if $i = j$), ν is the molecular viscosity, ϵ_m is the eddy viscosity and e is the turbulent kinetic energy density.

ϵ_m is related to the turbulent kinetic energy e and the so-called turbulent pseudovorticity, ω, as

$$\epsilon_m = \frac{e}{\omega} \qquad (2-6)$$

The turbulent pseudovorticity can be related to the turbulent length scale as

$$\ell_t = \frac{\sqrt{e}}{\alpha^* \omega} \qquad (2-7)$$

where α^* is a constant.

To complete the model, partial differential equations for e and ω are derived. These equations state the conservation of turbulent kinetic energy and turbulent pseudovorticity along a streamline. The solution is to be sought by coupling these equations with the flow equations.

Ref. (2-8)   P. G. Saffman, "A Model for Inhomogeneous Turbulent Flows, Proceedings of Royal Society, A317, p. 417, 1970

-10-

Since the TKE model yields the turbulence structure (energy and length scale) along a streamline, it is the proper model for the study of free stream turbulence. In the Traci and Wilcox paper, the stagnation point problem was solved by dividing the flow field into three regions. Region I consists of a uniform mean flow with the flow unperturbed by the presence of a body. The turbulence is convected by the mean flow and at the same time, decays by dissipation. Differential equations which govern this decay process are obtained from the conservation equations for e and ω. The turbulence level obtained near the body is used as the free stream turbulence level. In Region II, the mean flow is assumed to be undisturbed by the turbulence and is given by the laminar stagnation point inviscid solution. The turbulence level is enhanced by the mean flow strain (even though small) in this region as shown in Figure 2. (In this figure, the constant c is the inviscid flow velocity gradient). The solution to the turbulence differential equations (note the mean flow is assumed to be known in these equations) near the wall will be the turbulence level at the boundary layer edge which is the input value to Region III. Region III is the viscous boundary layer region where the flow equations are completely coupled to the turbulence equations. Solutions for this region yield the heat transfer to the wall. A numerical method of solution was employed in this region. The match or patch point between Region II and III was, however, somewhat arbitrary.

Solutions for both the cylinder and the sphere were obtained by Traci and Wilcox as shown in Figures 3 and 4. Again significant heat transfer enhancement was found, the amount of enhancement depends on the parameters $I_x \overline{Re_D}$ where D is the nose diameter and Re_D is the Reynolds number based on D.

In summary, theoretical studies for the stagnation point heat transfer enhancement in incompressible flow have been made. The theoretical results agree well with experimental data and show a significant increase in heat transfer due to free stream turbulence. Corresponding heat transfer theories for supersonic flow with free stream turbulence do not seem to be available in the open literature.
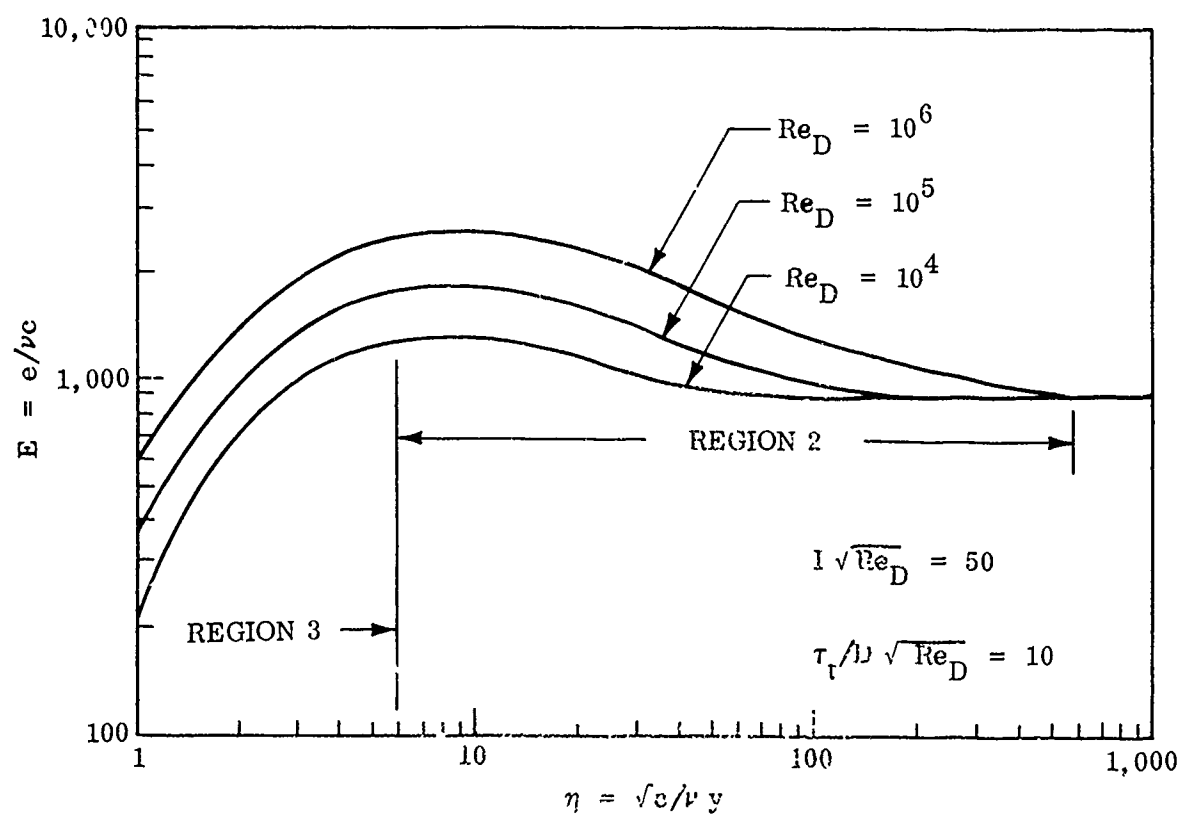
Figure 2   Variation of Turbulent Energy Approaching the
Stagnation Point
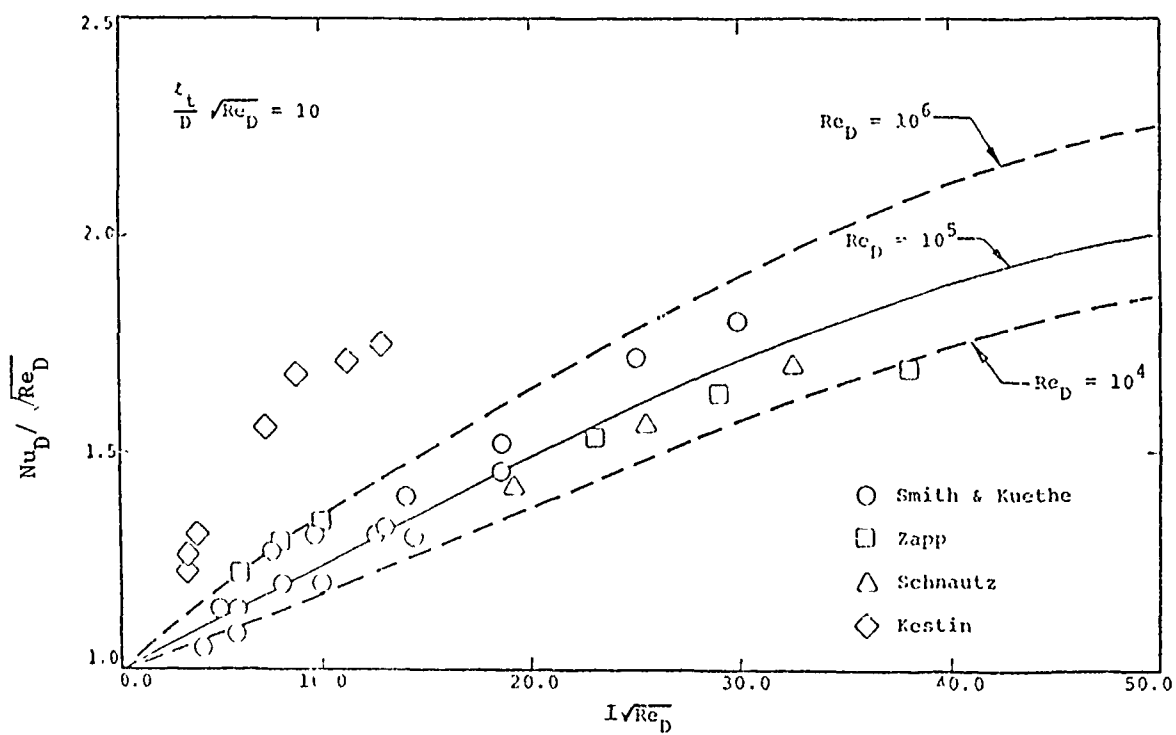
Figure 3 Stagnation Point Heat Transfer to a Cylinder in a Turbulent Cross Flow
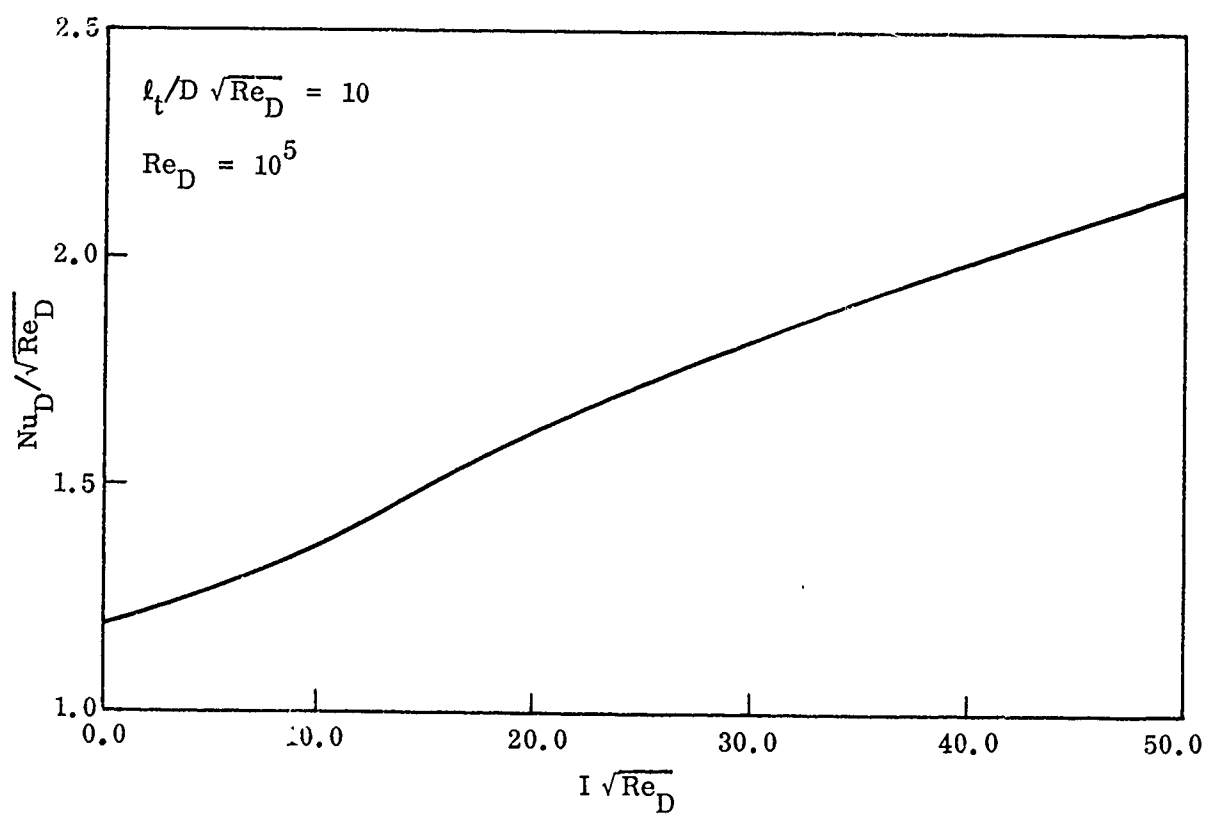
Figure 4 Stagnation Point Heat Transfer for a Sphere in a
Turbulent Flow

Section 3

MASS FLUX AND BULK ENTHALPY

The heat transfer rates measured near the centerline of the RENT nozzle are roughly 2 to 2.5 times higher than those computed using the enthalpy obtained from an arc chamber heat balance. It should not be inferred from these types of comparisons that the stagnation point heat transfer theory predictions are low by a factor of 2 to 2.5. The heat rate distribution across the nozzle suggests that there is an enthalpy distribution across the nozzle. In order to determine the mass-averaged enthalpy at the test section, the enthalpy flux across the nozzle must be integrated. A comparison of this mass-averaged enthalpy with the enthalpy obtained from the heat balance should then reveal the true discrepancy between the measured and predicted heat transfer rate. It is conceivable that this discrepancy between theory and data is not a constant, but varies across the test section. It does not appear possible to determine this fact until the entire problem has been sorted out.

The mass flux and the mass-averaged enthalpy can be computed if the free stream total pressure, the total pressure behind the shock and the corresponding stagnation point heat transfer rates are known. It should be noted that in order to obtain accurate results, the profile of the total pressure behind the shock should match the heat rate profile. Unfortunately, the total pressure and heat rate data available for analysis during this program were not perfectly matched and the results presented below must be considered approximate.

The mass flux at the test section is given by

$$\dot{m} = \pi \int_{-r_e}^{+r_e} \rho u r dr$$

where the test cross section is considered to consist of two semi-circles ($-r_e$ to 0, 0 to $+r_e$) which may or may not by symmetric. The mass-averaged or bulk enthalpy is given by

$$H_B = \frac{\pi \int_{-r_e}^{+r_e} \rho u \, H \, r dr}{\dot{m}}$$

The above expression can be rewritten as

$$\dot{m} = \pi \int_{-r_e}^{+r_e} pM\sqrt{0.604\frac{\gamma}{ZT}} \; r \, dr$$

$$H_B = \frac{\pi \int_{-r_e}^{+r_e} pM\sqrt{0.604\frac{\gamma}{ZT}} \; H r dr}{\dot{m}}$$

All of the above quantities are free stream values. The Mach number, M, is obtained from the ratio of total pressures; p, the static pressure is computed as a function of M and the free stream total pressure; the static temperature, T, is obtained from H, the local total enthalpy, and M, the compressibility, Z, is obtained from the static temperature pressure. The local total enthalpy is determined from the Fay-Riddell heat transfer relation

$$\dot{q} = C_w\sqrt{\frac{P_{t_2}}{r_n}} \; (H - h_w)$$

It is this last relationship which requires that the total pressure (behind the shock) profile accurately match the heat rate profile in order to obtain accurate values of H.

The mass flux and bulk enthalpy were computed using the above relations and the total pressure and heat rate data reported by Brown-Edwards (Ref. 3-1). In these calculations the total pressure behind the shock was assumed ɔ be constant across the test section at the centerline value for the purpose of obtaining the total enthalpy from the heat rate data. This approximation was necessary since the total pressure profiles did not accurately match the heat rate profiles.

Ref. 3-1 Brown-Edwards, E.G., "Fluctuations in Heat Flux as Observed in the Expanded Flow from the RENT Facility Arc Heater", AFFDL TR-73-102, Nov. 1973

In the determination of the Mach number, the actual total pressure profiles were used.

The mass flux and bulk enthalpy computed from the profile data are shown in Figure 5 for three nozzles. The approximation discussed above causes the mass flux to be high and the bulk enthalpy to be low. It is difficult to determine the actual error, but it is estimated that the computed mass flux is probably about 10 to 20 percent higher than the value an accurate computation would yield and the bulk enthalpy is probably 10 to 20 percent too low. The three computation points shown for the 1.11" dia. nozzle correspond to the average, high and low level heat rates. There appears to be no significant difference between these three points. Also shown in Figure 5 are the bulk enthalpies derived from arc chamber heat balances as reported by Brown-Edwards (Ref. 3-1) and Conley (Ref. 3-2). The computed bulk enthalpies a:e about 10 and 30 percent higher than the heat balance enthalpies reported by Brown-Edwards and Conley, respectively.

It appears from these calculations that the discrepancy between the measured and predicted heat rates or equivalently, the derived local enthalpy, may be somewhere between 20 and 50 percent.

Ref. 3-2 Conley, H. L., "Enthalpy Measurements in the RENT Facility Using the AEDC Transient Enthalpy Probe", AFFDL-TM-74-124-FXN, May 1974
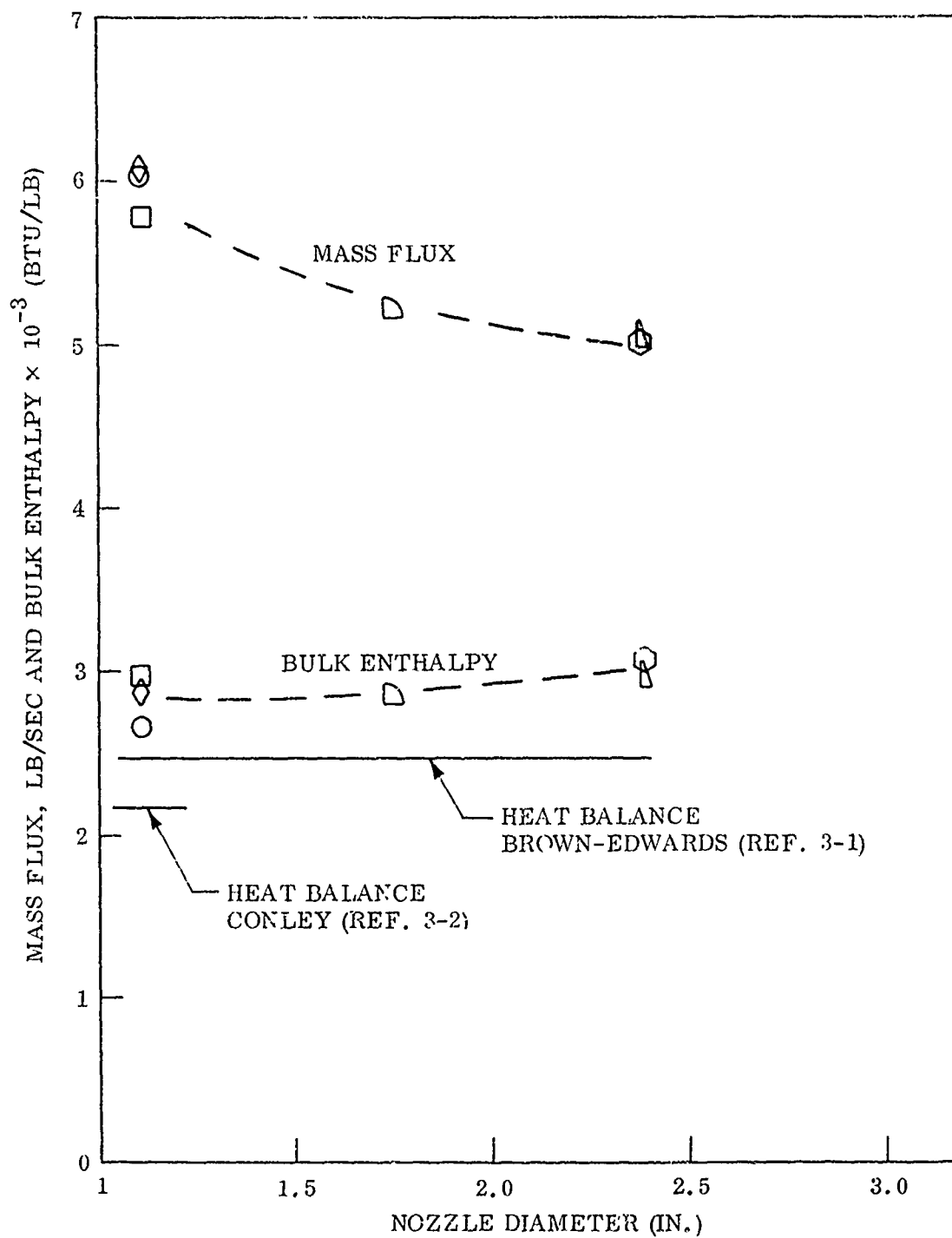
Figure 5   Mass Flux and Bulk Enthalpy

Section 4
FREE STREAM TURBULENCE

4.1 Overview

This section considers the potential effects of free stream turbulence on stagnation point heat transfer. One may correctly anticipate that such added disturbances will increase the rate of heat transfer over what is predicted by a laminar theory like Fay & Riddell's classic formula (Ref. 4-1). Although there have been no direct measurements of turbulence in the RENT flow, some recent work by Humphreys (Ref. 4-2) on heat transfer from a rotated arc, which also has added swirl because of the mode of gas injection into the arc chamber, shows that heat transfer to a downstream constraining tubular enclosure is increased. Their conclusion was that "Large increases in the heat transfer rates to the tube were observed with rotation and it was shown that these increases were due to the swirling flow and turbulence caused by the arc's rotation". The Reynolds number of the RENT jet for say the 1.11" nozzle is about 8×10^5, an extremely high value. Such a jet would be completely turbulent a short distance from the exit plane, a process which could be further shortened by the known arc instabilities (Ref. 4-3) or the turbulent boundary layer that probably exists near the exit plane of the arc chamber. Because the model diameter may be as much as one-half the exit nozzle diameter, fluctuations in the jet from any of the flow conditions may affect the boundary layer and its immediate

------

Ref. (4-1) Fay & Riddell, "Stagnation Point Heat Transfer in Dissociated Air", J.A.S. <u>25</u>, pp 73-85 (1958)

Ref. (4-2) Humphreys, J. F., and Lawton, J., "Heat Transfer for Plasma Systems Using Magnetically Rotated Arcs", Journal of Heat Transfer, p. 397-402, Nov. 1972

Ref. (4-3) Kesten, J., and Wood, R., "The Influence of Turbulence on Mass Transfer from Cylinders", Journal of Heat Transfer, p. 321-327, Nov. 1971

external flow. The Reynolds number based on model diameter is also very high, e.g., 4×10^5, for a quarter inch nose radius model so that, as will be shown, effects of external stream turbulence would be accentuated. It is therefore worthwhile to at least attempt to give reasonable bounds on the effect of turbulence on stagnation point heat transfer so possible measurements of this quantity during RENT operations can be quickly evaluated.

Our discussion will first center on the extensive experimental results for subsonic flow, then go on to the limited data available for supersonic flow, then show available theoretical results, and finally make recommendations for future experimental programs.

4.2 Experimental Results for Subsonic Flow

Experiments on effects of free stream turbulence have been made for cylinders, spheres, and jets impinging against plates. One of the most important results of these studies is that the effects of turbulence are magnified if some relevant Reynolds number is large. If the turbulence level is expressed by the definition $T \equiv u'/U_\infty$, where u' is the fluctuating level of free stream velocity and U_∞ its mean value, then increases in heat transfer relative to $T = 0$ are expressed in terms of the variable $T(Re)^{1/2}$ or $T \times Re$ where Re is the Reynolds number based on cylinder or sphere diameter or discharge nozzle diameter. Some investigators have used mass transfer instead of heat transfer to gage the effects of turbulence and found comparable results.

Kestin & Wood (Ref. 4-3) have summarized results for a cylinder as shown in Figure 6. The value of $Nu/R_e^{1/2}$ at $T = 0$ is about 0.94 so that the maximum measured effect at the stagnation point is (roughly) a factor of 1.8 increase in the Nusselt number hD/k. A curve fit to the data is shown and follows (Eq. 4-1).

$$\frac{Nu}{(R_e)^{1/2}} = 0.945 + 3.48 \left(\frac{TR_e^{1/2}}{100} \right) - 3.99 \left(\frac{TR_e^{1/2}}{100} \right)^2 \tag{4-1}$$

This expression peaks at a value of $TR_e^{1/2}$ of 43.6. The Reynolds number for a model with a half inch diameter placed in the exit of the Mach 1.8 nozzle has an R_e of 4×10^5 so that $R_e^{1/2} \cong 600$. A 7% free stream turbulence level could then produce this maximum effect on the stagnation line of a cylinder in cross flow if the effect of free stream turbulence is

-20-
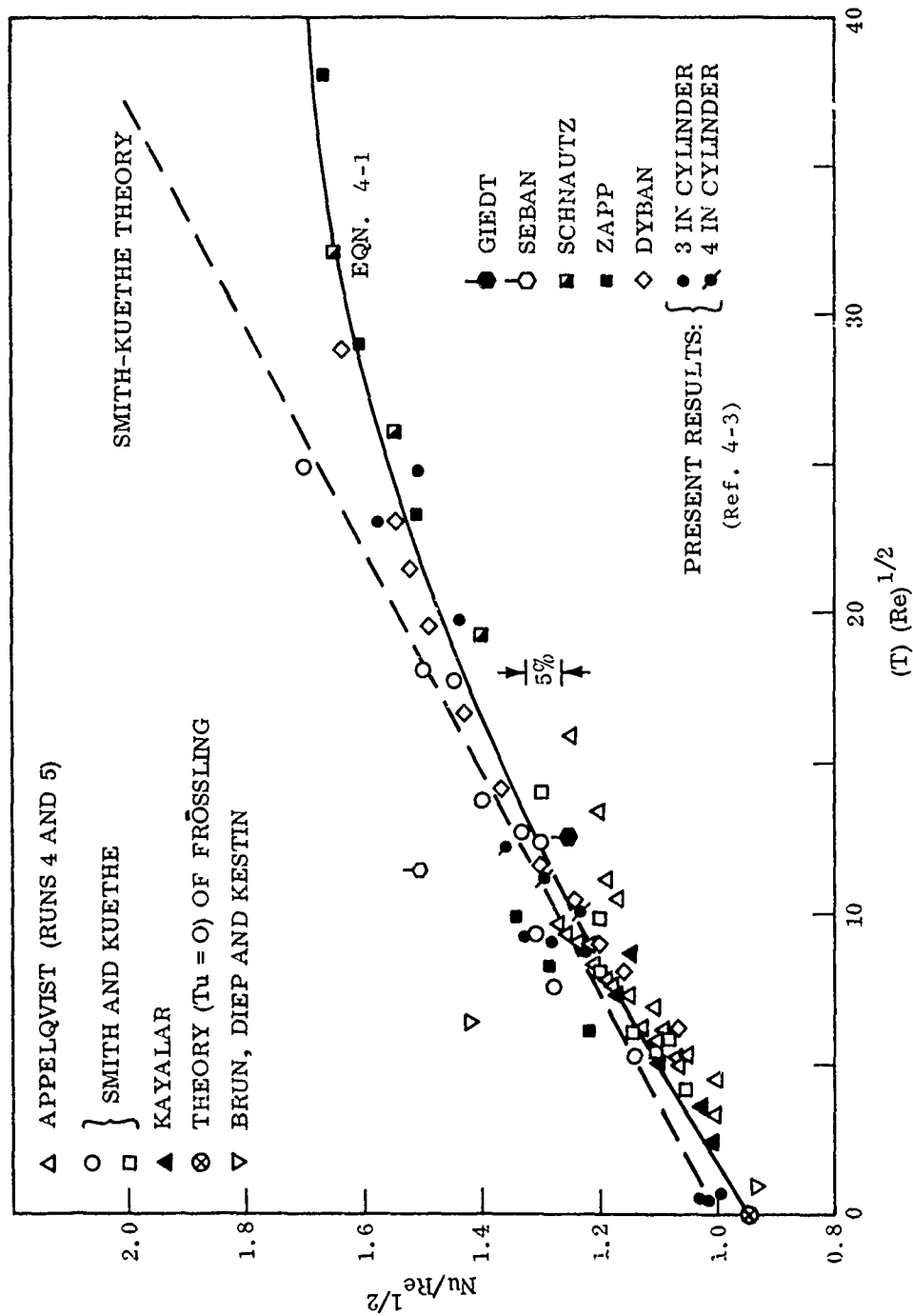
Figure 6   Measurements for the Local Rate of Heat (Mass) Transfer at the
Stagnation Line of Cylinders in Cross Flow

independent of Mach number.

An important feature of this heat (or mass) transfer augmentation is that the distributions of the effect around the stagnation point seem to follow a "displaced" laminar law. This is illustrated for a cylinder in Figure 7 from Ref. 4-3. Only at the separation point at $\theta \cong 105$ degrees is there a difference in the curves. This result suggests that most of the boundary layer is dominated by viscous forces and that turbulence represents an additional "outer flow" transport term which steepens the relevant wall gradients.

Early work by Smith & Kuethe (Ref. 4-4) shows the same trends and, for clarity, these and other data are given in Figure 8. One of the key features of the data is that the greatest increment in heat transfer experimentally observed was a factor of 1.7. The early data of Keston (indicated by the ◇) appears to jump to this value for very low turbulence levels. Therefore, one is led to suspect that a maximum value may indeed exist and that the simple linear trend of the "theory" is not correct.

Results for the augmentation of stagnation point heating on a sphere demonstrate the importance of having the turbulent Reynolds number greater than a value of about 7×10^2. Since the RENT model Reynolds numbers are about 10^5, this condition could be met if free stream turbulence exceeded 7%.

Some results from Gostkowski (Ref. 4-5) are shown in Figure 9. The largest measured increment of heat transfer was 2.5/1.4 or 1.8 which is in apparent agreement with the results found for cylinders. The straight line showing an ever increasing effect would appear to be a tenuous extrapolation of the data.

Ref. (4-4) Smith, M., and Kuethe, A., "Effects of Turbulence on Laminar Skin Friction and Heat Transfer", Physics of Fluids 9, No. 5, p. 2337-2344, Dec. 1966

Ref. (4-5) Gostkowski, V., and Costello, F., "The Effect of Free Stream Turbulence on the Heat Transfer from the Stagnation Point of a Sphere", Int. J. Heat and Mass Transfer, 13, pp. 1382-1386 (1970)

Figure 7   Effect of Turbulence on Mass-Transfer Rate Around a
Cylinder   Reynolds Number: Re = 125,000 (nominal)
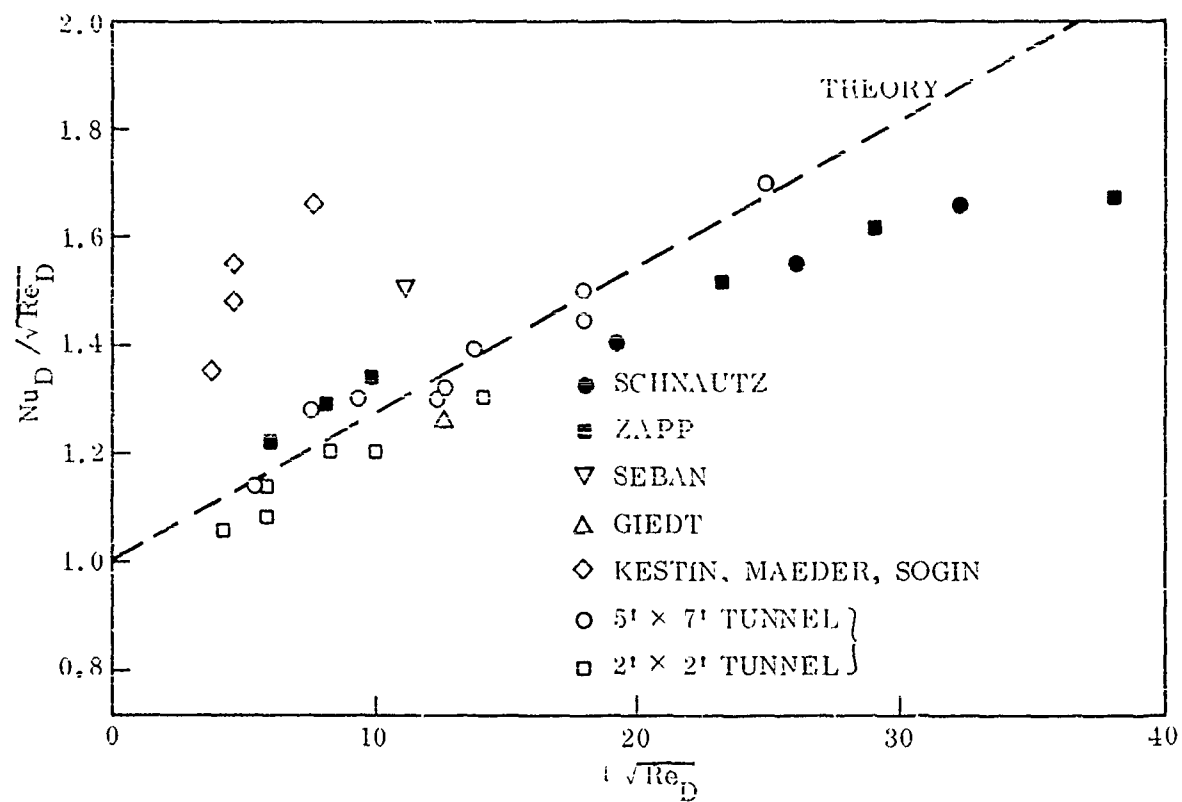
Figure 8   Heat Transfer Data at Stagnation Point of Cylinders
Compared with Data from Other Sources and With Theory
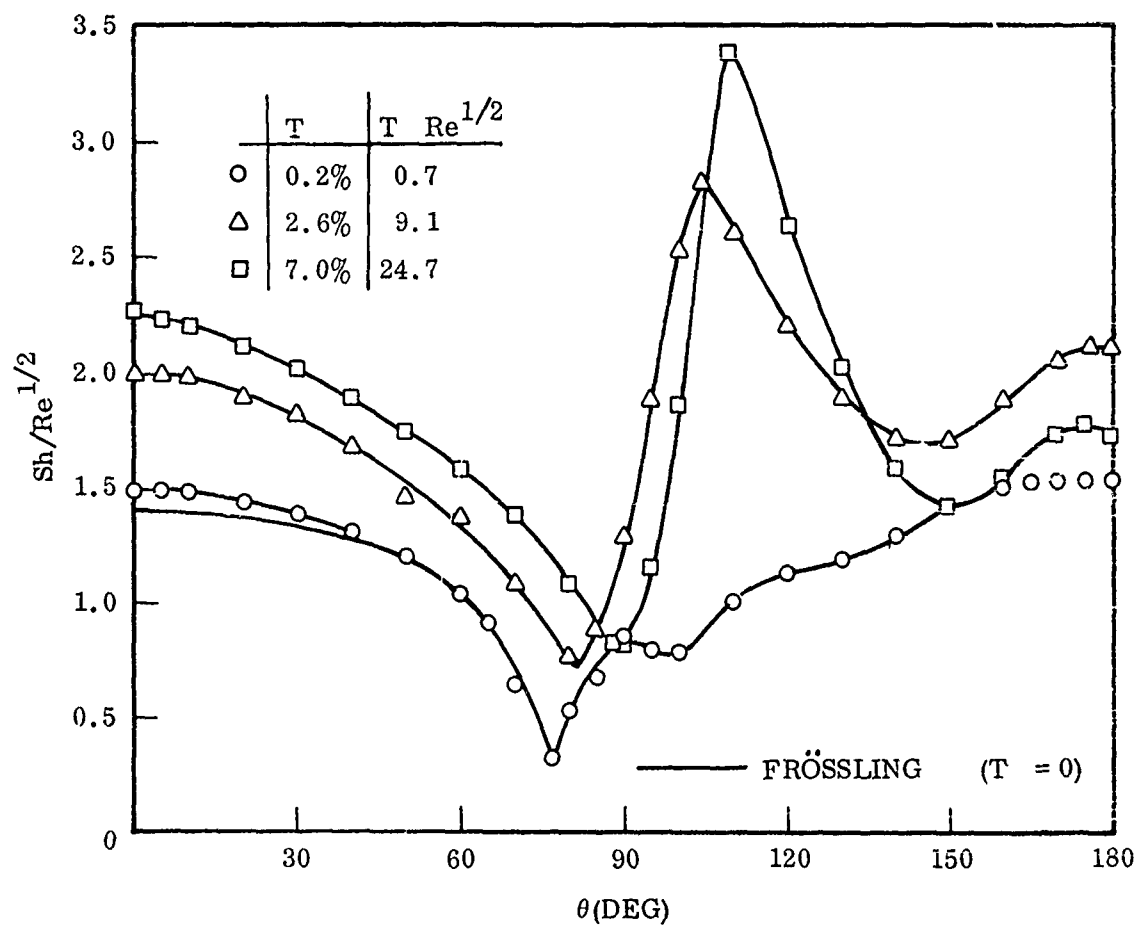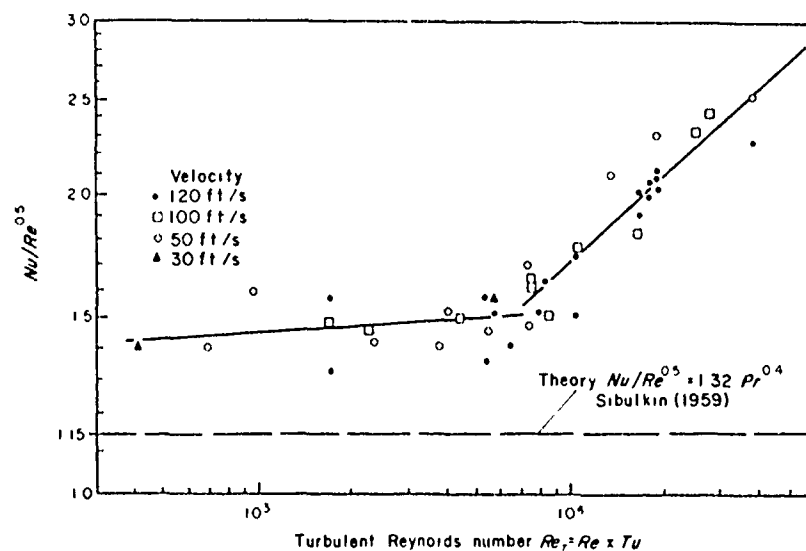
Figure 9 Correlation of Free-Stream Turbulence Effects on Heat-Transfer
         to Sphere

Galloway and Sage (Ref. 4-6) have made extensive measurements around a spherical body as well as at the stagnation point. Some of their results are given in Figures 10 and 11.

The Frossling number is $\dfrac{Nu - 2}{\sqrt{R_e}\; P_r^{1/3}}$ so that, because Nu >> 2, ratios between the quantity yield the combined effects of turbulence and Reynolds number. The quantity α_t is identical to T, the ratio u'/U_∞. Notice from Figure 10 that, at the largest Reynolds number, 68,000, the distribution of Nusselt number for all turbulence levels follows qualitatively the distribution for the 1.3% nominal level of the experimental tunnel. Therefore, the increased heat transfer level at the stagnation point followed by a monotomic decline is valid up to the vicinity of separation. After about the 70° angle from the stagnation point there are differences in behavior depending on turbulence level. (It should be noted that these and other investigators have checked for possible effects of the wake and separated flow region on stagnation point heat transfer and found none. This is done, for example, by attaching faired streamline shapes to the rear of the body which suppress the recirculating region). The maximum increase in stagnation point heat transfer was 1.55/1.15 = 1.35. Looking at Figure 11, the maximum change in heat transfer at fixed turbulence (α_t = 0.256) level but with changing Reynolds number was found to be 1.55/1.05 = 1.48. There seems to be no evidence from these results that the effect of free stream turbulence is to trip the laminar boundary layer and make it turbulent. Rather, the transport in the usual laminar boundary layer seems to be augmented. Aside from the simple "displaced" form of the distribution, this conclusion is also supported by the $Nu/\sqrt{R_e}$ scaling law which applies even with the added free stream turbulence level.

These increases of heat transfer appear to be smaller than those encountered for the cylindrical case. However, this is not necessarily accurate as shown by the results of Ref. (4-6) given in Table 4-1.

Ref. (4-6)   Galloway, T.R., and Sage, B. II., "Local and Macroscopic Thermal Transport from a Sphere in a Turbulent Air Stream", A.I.Ch.E. Journal, 18, No. 2, pp. 287-293 (March 1972)
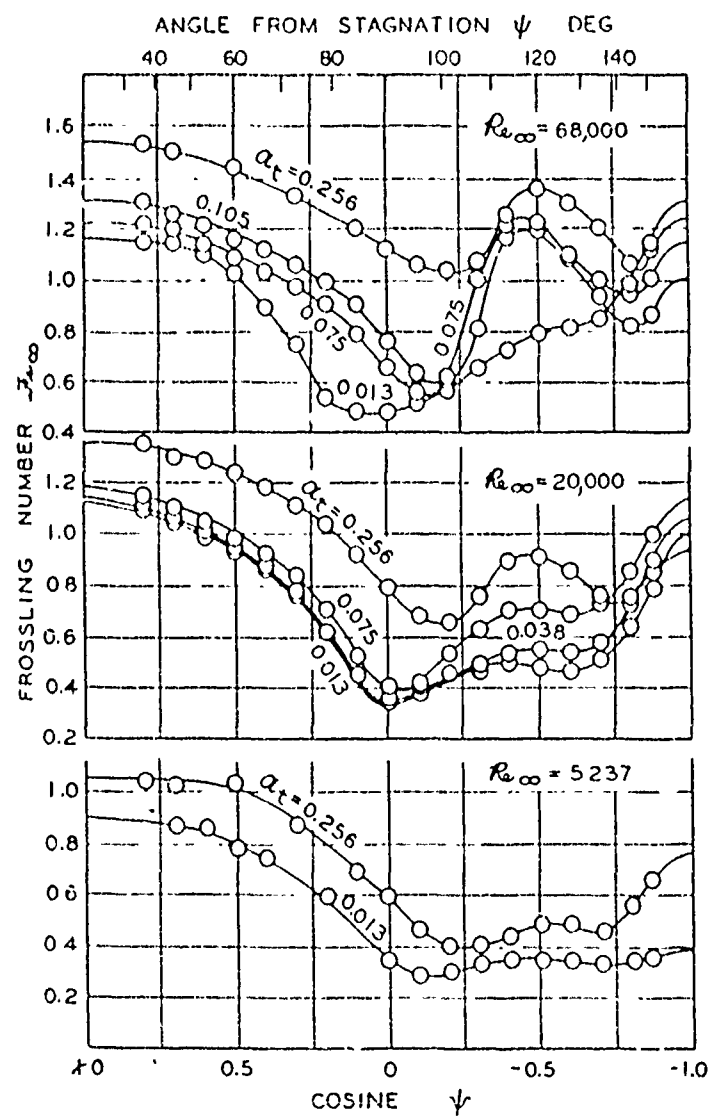
Figure 10   Local Transport from the 1.5-in. Sphere at Several
            Reynolds Numbers
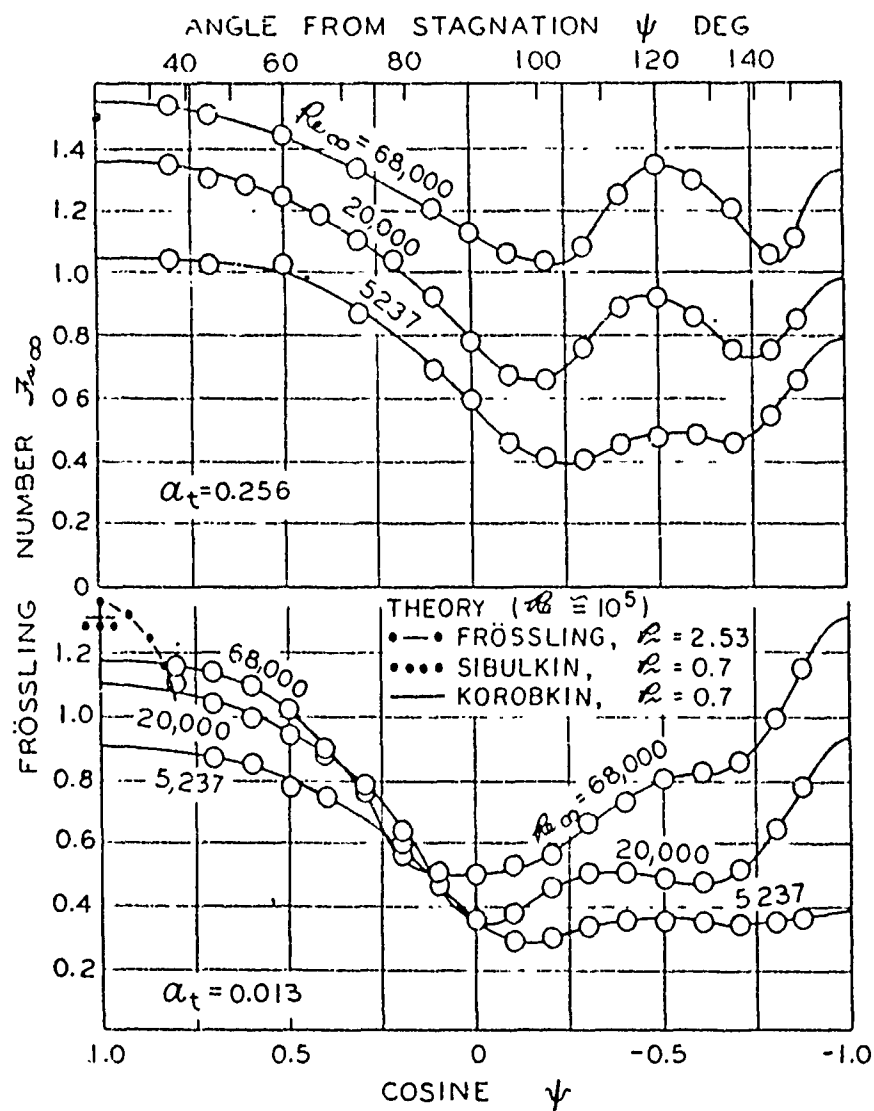
Figure 11   Local Transport from the 1.5-in. Sphere at
             Low and High Turbulence

Table 4-1: Values of $F = (\dfrac{Nu - 2}{\sqrt{R_e}\ P_r^{1/3}})$

R_e	T = 25.6%	T = 1.3%
68,000	1.55	1.19
20,000	1.38	1.10
5,237	1.05	0.9

The very high (1.3%) level of tunnel turbulence has itself interacted with the variation in Reynolds number to produce the overall variability shown in the second column. If the low value of 0.9 for F is used as a reference then the increase if $1.55/0.9 = 1.72$ which for the $T\sqrt{R_e} = .256\sqrt{68,000} =$ 66.8 compares with cylinder results for asymptotic values of this parameter. When the low value of 0.9 is used, the data for the sphere can be plotted as shown in Figure 12. The low point has a turbulent Reynolds number of only 1340 which apparently confirms the results given in Figure 9.

The situation of a free jet impinging normal to a flat surface has been studied in great detail by Donaldson, C.D., et al., Ref. (4-7). They show the ratio of heat transfer to its laminar value as a function of distance from the nozzle exit plane. Since the jet was becoming turbulent, the results represent the effects of turbulent intensity on heat transfer. They are shown in Figure 13, where R_{e_5} is the local jet Reynolds number = $\rho_c \bar{w}_c r_5 / \mu_c$. The subscript c denotes jet centerline values and r_5 is the jet radius at the impingement location corresponding to the point where the jet velocity is one-half the centerline velocity. Notice that the asymptotic value, corresponding to the fully developed turbulent jet is a ratio of 2.2 which is slightly higher than the values observed for spheres and cylinders. One may speculate that these systematic differences are caused by the more severe stagnation point pressure gradient encountered by normal flat surfaces, cylinders, and spheres in that order. When these

-----

Ref. (4-7) Donaldsons, C.D., et al., "A Study of Free Jet Impingement: Part 2 Free Jet Turbulent Structure and Impingement Heat Transfer", Journal of Fluid Mechanics (1971) 45, Part 3, pp. 477-512
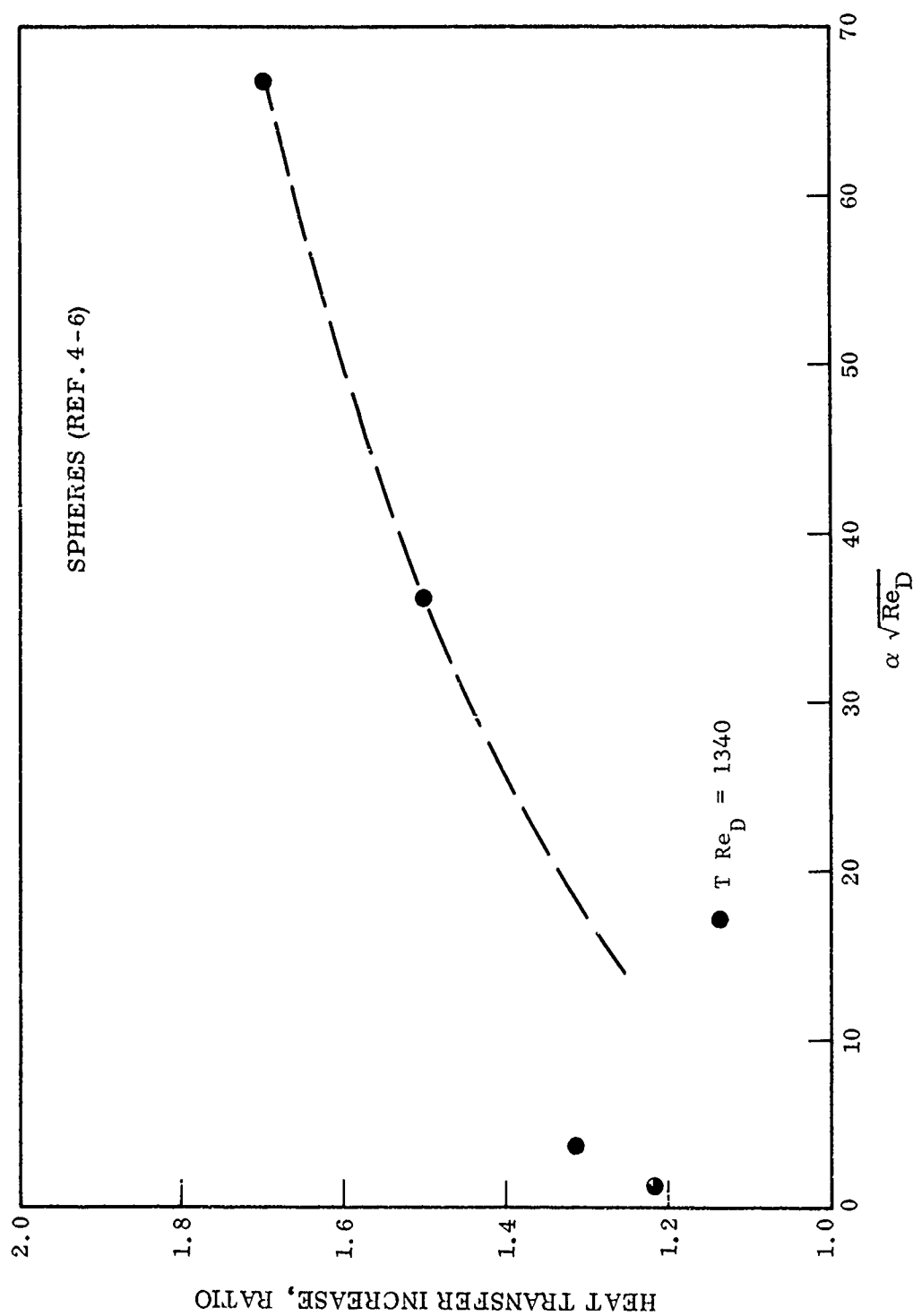
Figure 12   Sphere Stagnation Point Heat Transfer Enhancement
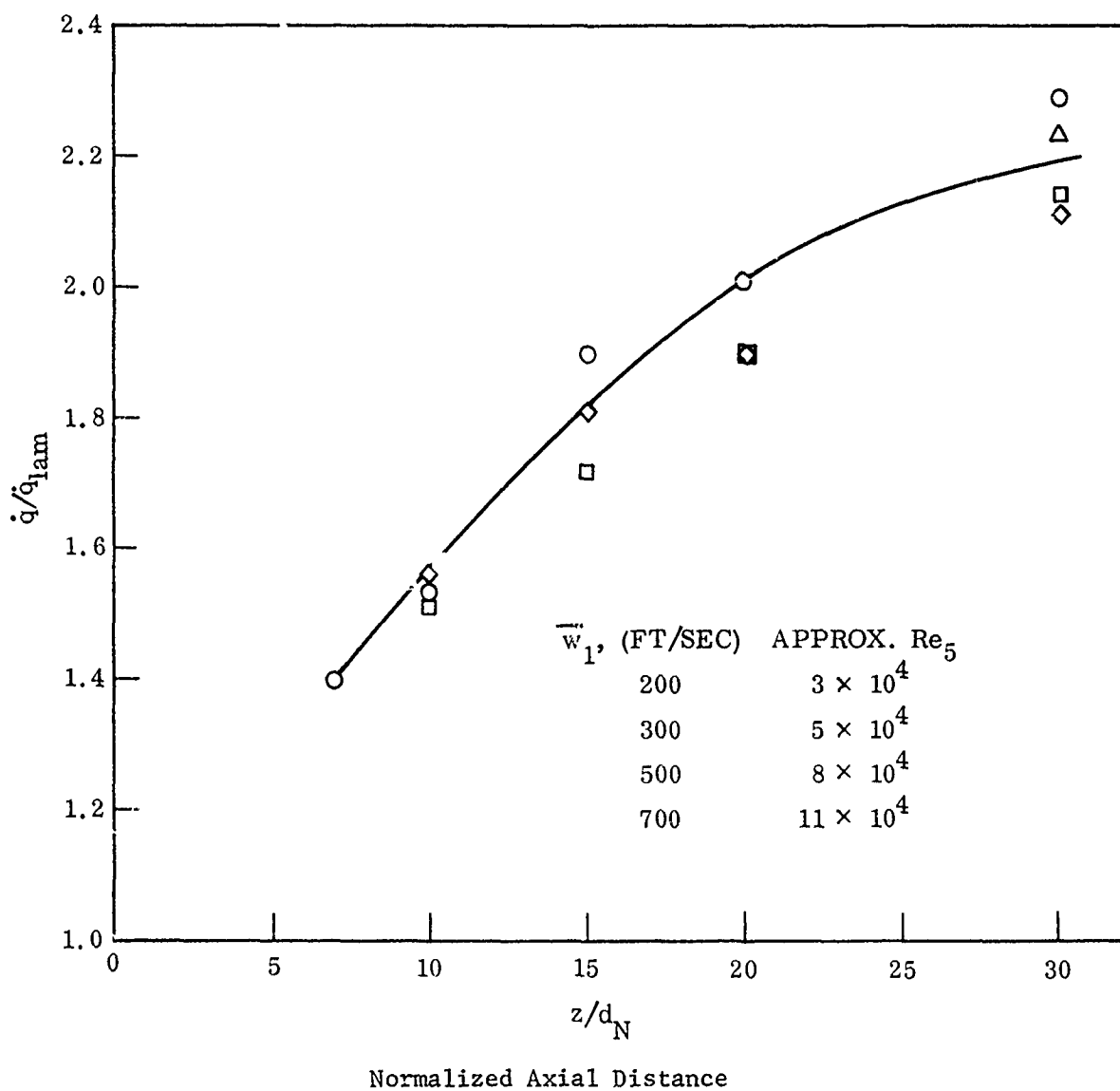
Figure 13   Ratio of Measured Heat Transfer to That Predicted by Laminar Theory at the Stagnation Point of the Impinging Jet

flat surface results are cast into the form used for cylinders and spheres the results are as shown in Figure 14. The general trend and values are in agreement with those found previously for spheres and cylinders. The scatter of data indicates that the parameter $T\sqrt{R_e}$ is insufficient to correlate results. It may be that the turbulence scale ℓ expressed in some typical nondimensional factor like (ℓ/D) $(\sqrt{R_e}$ may also be important. If the RENT facility turbulence level is connected with the size of the exit jet, then this factor would be important when comparing heat transfer results at the different Mach numbers.

A final point is that the distribution of heat transfer coefficient follows a laminar type behavior away from the stagnation point as shown in Figure 15. Most of the data seem to be shifted by a factor of about 2. The authors recommend that "for most engineering computations at large Reynolds numbers, sufficient accuracy will be achieved by applying the stagnation point turbulence correction factor to the normal laminar heat transfer rates ... it will be found that the heat transfer in the region near the stagnation point will be proportional to the square root of Reynolds number".

Bearman (Ref. 4-8) shows that when turbulence scales in the free stream flow are very much less than the body (model) dimension the longitudinal component of turbulence is amplified because of vortex stretching. This means that the stagnation region of a model does not always "damp out" turbulent external flow fluctuations.

There is no experimental doubt that if as much as 5% turbulence exists in the RENT free stream, then $T\sqrt{R_e} \approx 35$, and substantial increases in stagnation point heat transfer should be expected. This conclusion is not changed because of compressibility or the presence of a bow shock wave in front of the model. The shock wave represents an adverse pressure gradient to the stagnation region streamline. Some directly measured turbulence data are given in Ref. (4-9) and given in Figures 16 and 17.

Ref. (4-8) Bearman, P. W., "Some Measurements of the Distortion of Turbulence Approaching a Two-Dimensional Blunt Body", Journal of Fluid Mechanics, 53, pt. 3, pp. 451-467 (1972)

Ref. (4-9) Rose, W.C., "Turbulence Measurements in a Compressible Boundary Layer, AIAA Journal, 12, No. 8, pp. 1060-1064 (1974)
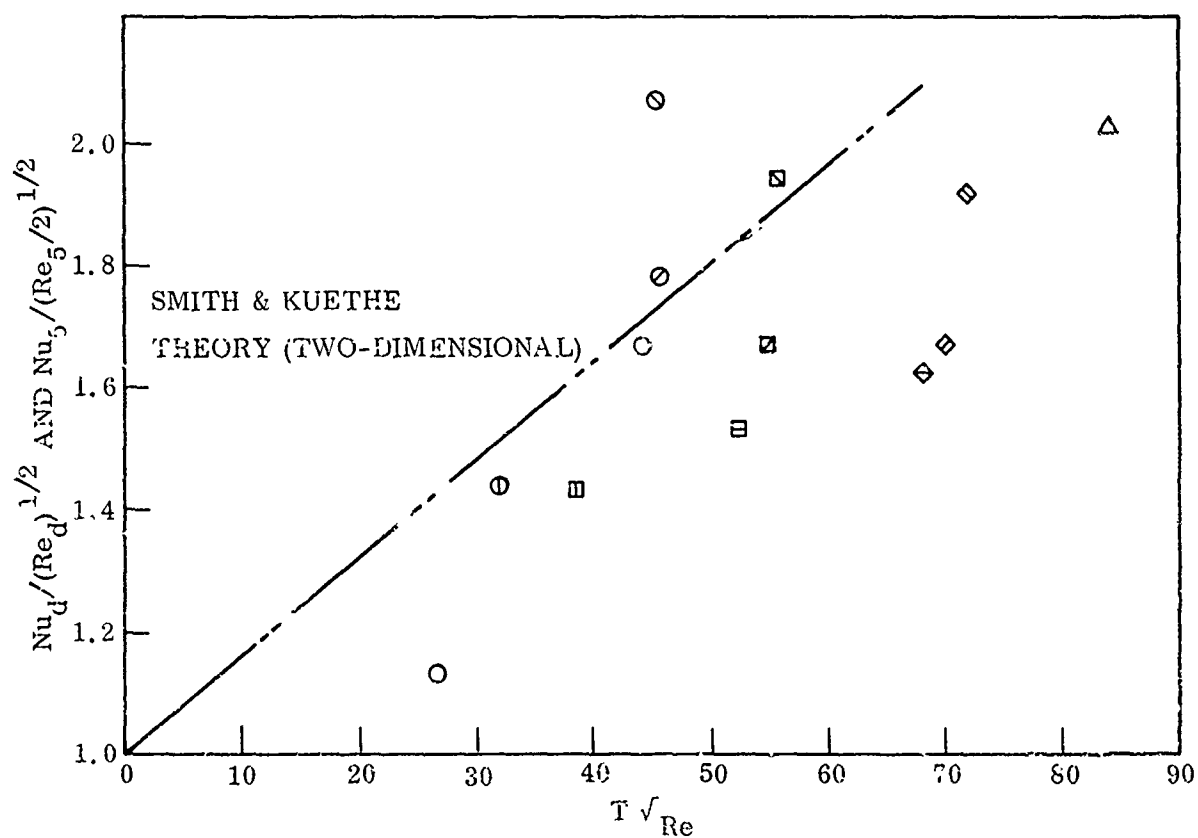
Figure 14   Comparison of Measured Heat Transfer for the Axisymmetric
Impinging Jet with that Predicted by the Two-Dimensional
Theory of Smith & Kuethe
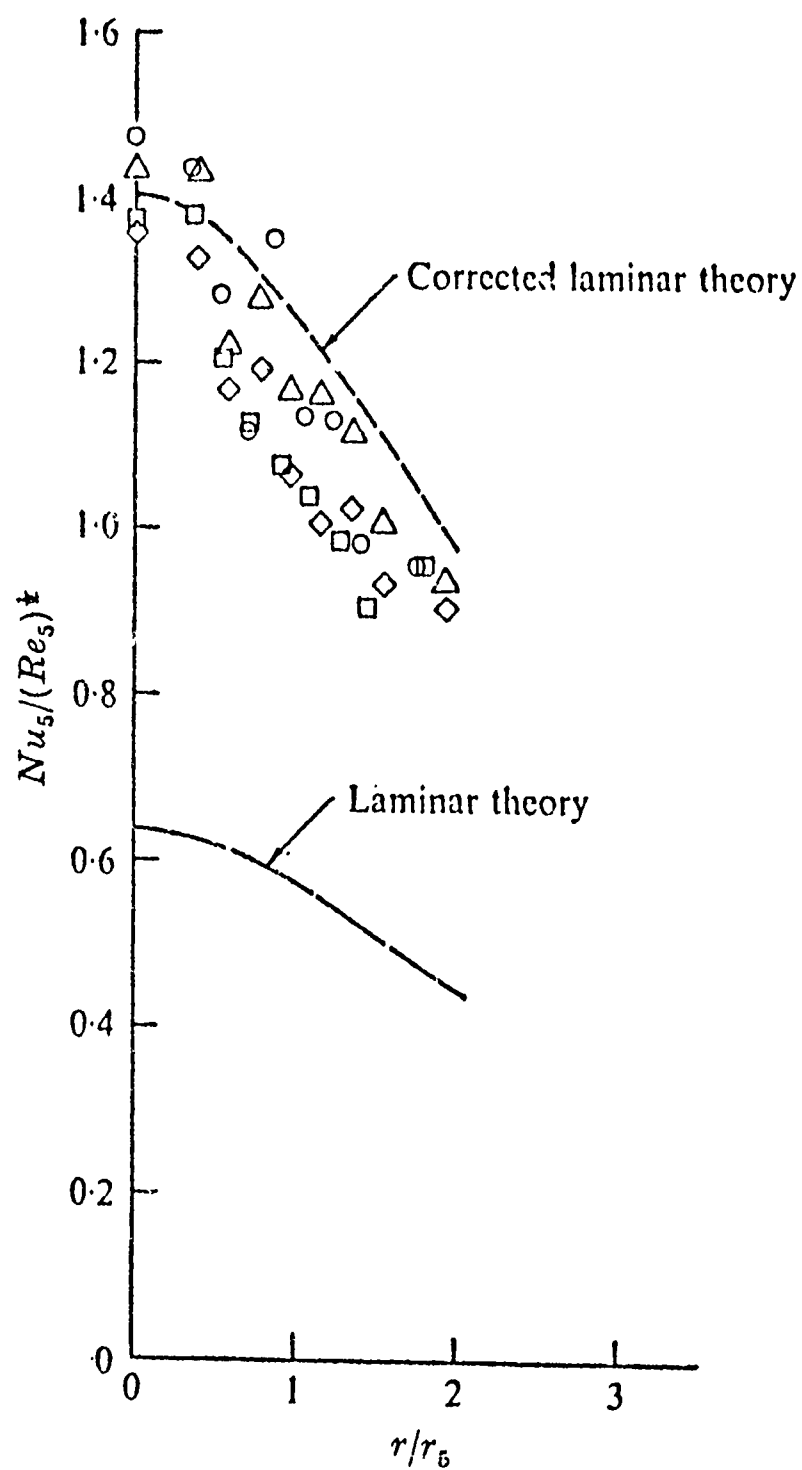
Figure 15   Heat transfer close to the Stagnation Point
$z/d_N = 30$
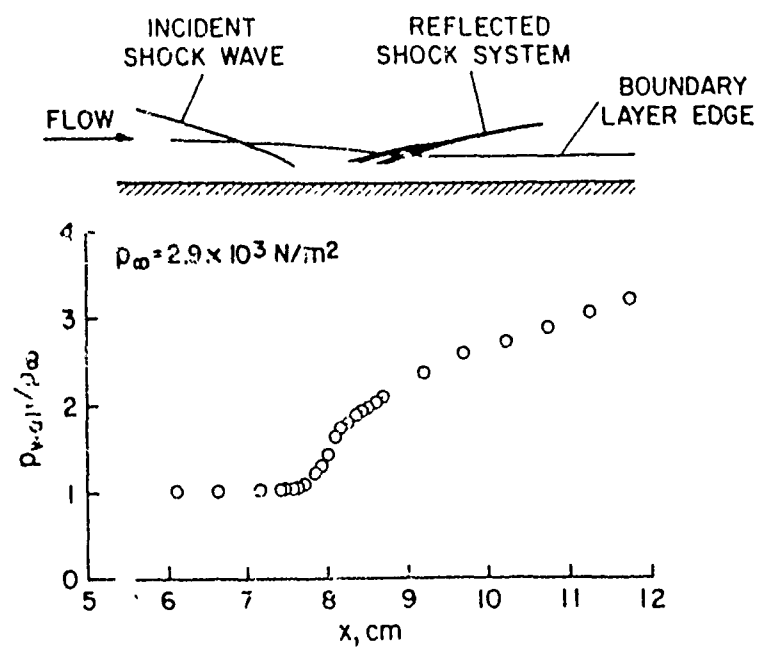
Figure 16   Shock Wave Locations and Surface Static
Pressure   Distribution

For these particular experimental conditions, the pressure rise across the
shock wave was 2.5 times the free stream value. The static pressure rise
in the RENT facility for the 1.11", Mach 1.8 nozzle is 3.4 times the up-
stream value followed by a further rise of a 1.25 factor going towards
the stagnation point. The results shown in Figure 17 indicate that the
fluctuation level before the shock wave/boundary layer interaction was
about 5% and after the shock was 7 or 8%. This is not a spectacular
change, but only serves to show that shock waves can increase at least
some components of turbulent flow. Other results for temperature and
density fluctuations may not be directly applicable to the RENT situation
because of dissociation and other real gas effects.

Of course, detailed turbulent measurements are much more difficult in
very high enthalpy streams, but the effects of turbulence of heat transfer
can be inferred from some reasonable fluid mechanical aspects of these
flows. An example is data taken from the inpingement of a "plasma" torch
onto a large vertical plate as shown in Figure 18 from Roma-Abu (Ref.
4-10).
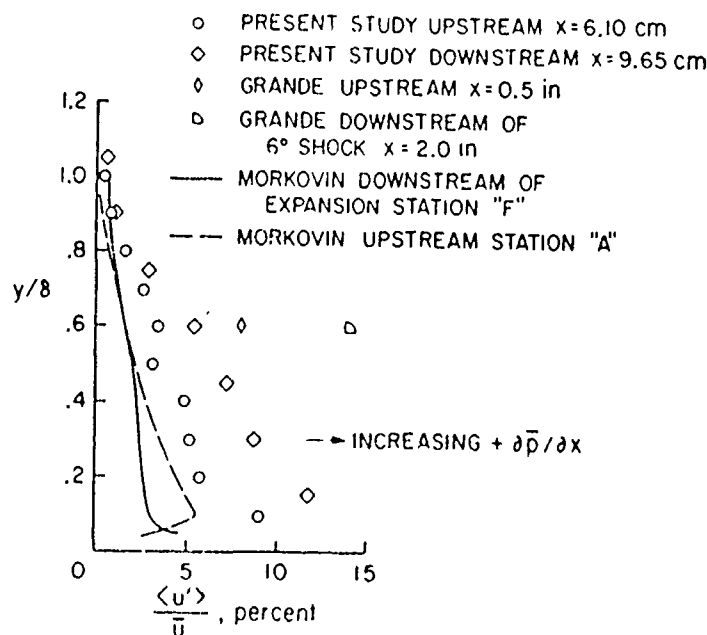
Figure 17 Effect of Pressure Gradients on Velocity Fluctuations

------

Ref. (4-10) Roma'Abu, M.M., "Heat Pipe Colorimetry for Plasma Stagnation-
Point Heat Transfer", AIAA Journal 10, No. 3, pp. 313-316 (1972)
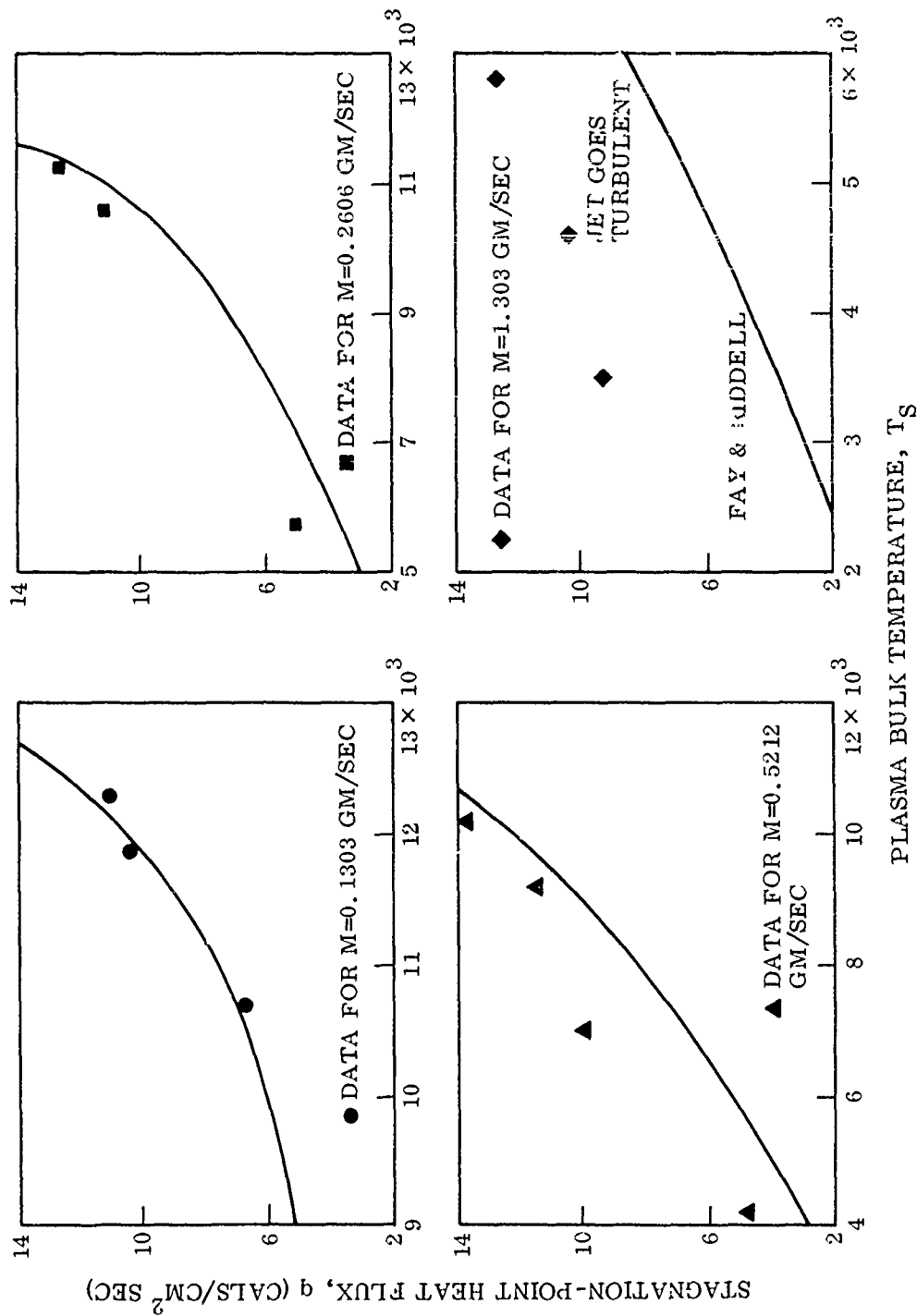
Figure 18   Comparison Between Heat-Transfer Laminar Flow Predictions and Experimental Data

-37-

These heat transfer data were taken with a plasma jet of argon which operated in the fully laminar, transitional, and fully turbulent jet regime as judged from the Reynolds number at the jet exit. The correlation used was that developed by Incropera, F., and Leppert, G., (Ref. 4-11) which related transition to turbulence with large increases in emitted acoustic radiation. The top two figures show good agreement with Fay & Riddell theory. As the flow rate is increased, transition occurs and finally complete turbulent transition in the jet is observed. For these circumstances, at a plasma bulk temperature of $5000^{\circ}K$ (approximately one of the RENT operating values) experimental heat transfer values are 1.6 times those predicted from the Fay & Riddell formula.

Another relevant "hot flow" situation is that described by O'Connor, et al (Ref. 4-12). These authors use a 1.5 megawatt arc heated facility to produce a high subsonic flow of pure nitrogen. This fluid is allowed to impinge on a vertical plate which can move to various axial locations. At each axial location, the heat transfer, static and total pressure, and independently, stream enthalpy were measured. These quantities were then used in the Fay & Riddell correlation and found to underpredict the observed heat transfer by a factor of about 2.5. These results are shown in Figure 19 where the stagnation point heat transfer is plotted versus the nondimensional axial distance x/r. The solid curve uses an empirical correction factor $(x/r_1)^{.5}$ in the Fay & Riddell correlation type of equation, viz:

$$q_{stag} = 0.442 \left(\frac{\rho_w \mu_w}{\rho_e \mu_e}\right)^{.1} (\rho_e \mu_e \; \frac{u_c}{r_5} \; \frac{x}{r_1})^{1/2}$$
$$\left(1 + (L_e^{.5} -1) \frac{h_D}{h_e}\right) (h_e - h_w)$$

Ref. (4-11) Incropera, F., and Leppert G., "Flow Transition Phenomena for a Subsonic Plasmajet", AIAA Journal 4, No. 6, pp. 1087-1088 (1966)

Ref. (4-12) O'Connor, T. J., "Turbulent Mixing of Axisymmetric Jets of Partially Dissociated Nitrogen with Ambient Air", AVCO Tech Report RAD-TR-65-18 (1968) AVCO Corp., Wilmington, Mass.

$$q_s = 0.442 \left[\left(\frac{\rho_w \mu_w}{\rho_e \mu_e} \right)^{0.10} \left(\rho_e \mu_e \frac{u_c}{r_5} \frac{x}{r} \right) \right]^{1/2}$$

$$\left(1 + (Le^{0.52} - 1) \frac{h_p}{h_e} \right) \left(h_e - h_w \right) \Big]$$

○ EXPERIMENT
△ PREDICTED
FAY & RIDDELL

$(h_{s_i} - h_o) = 4328$ BTU/LB

$M_1 = 0.782$

COLD WALL STAGNATION HEAT FLUX (BTU/FT²-SEC)

x/r_i
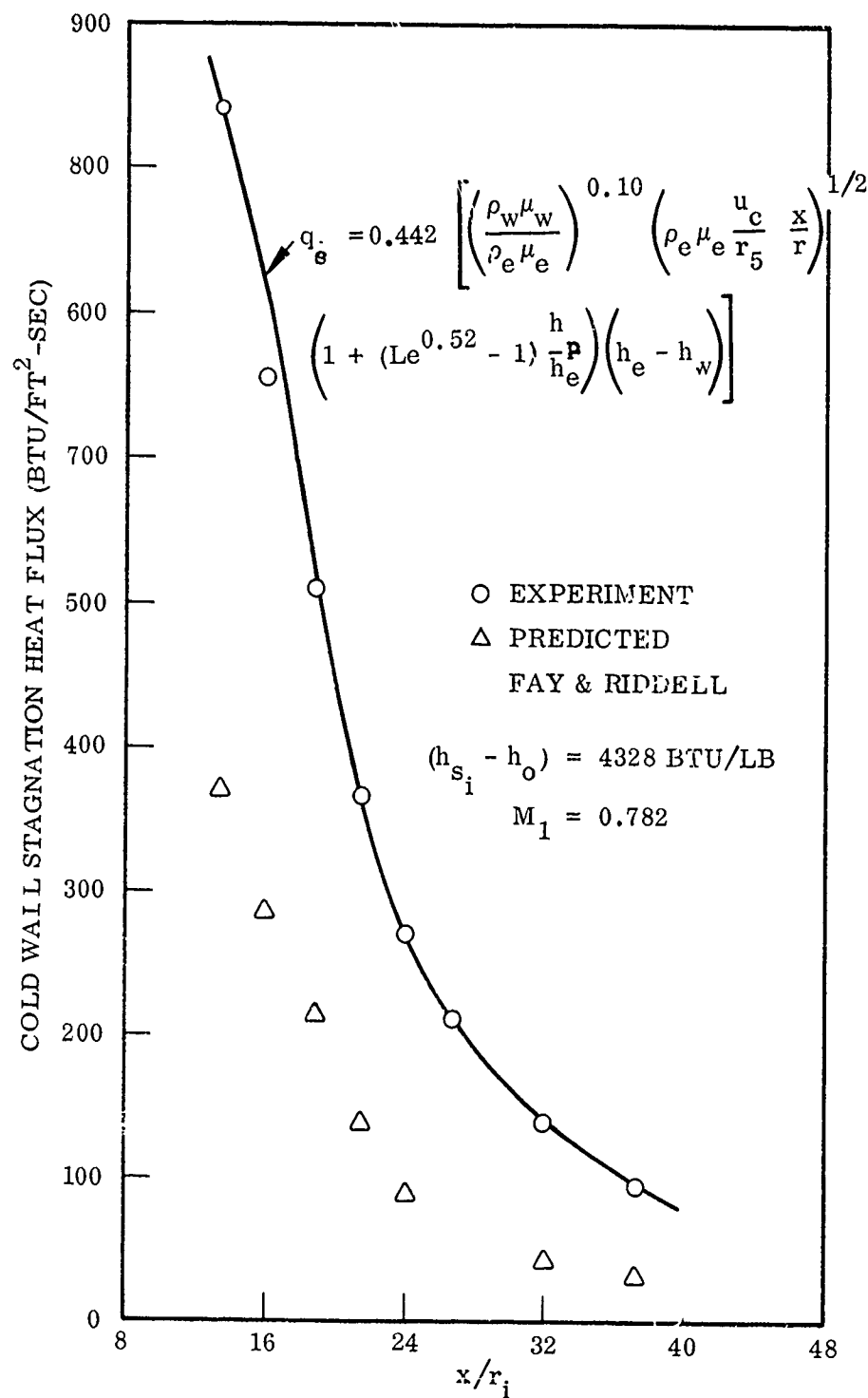
Figure 19   Jet Impingement Heat Transfer to a Vertical Plate

(r_5 is the jet radius where the velocity is 1/2 its centerline value. It is a function of the axial coordinate x). The condition of total enthalpy equal to 4328 BTU is similar to RENT operation. The Mach number 0.782 is lower.

4.3 Rough Estimate of RENT Turbulence Level

Because of the demonstrated importance of turbulence (taken together with high model Reynolds numbers) it is appropriate to try and estimate the turbulence level in the RENT facility. Only very limited information on fluctuations is available. If velocity fluctuations occur, then some fluctuations in total pressure would result. If the small fluctuations given by Brown-Edwards (Ref. 4-13 in Figures 1a, 1b, 1c are viewed to represent such fluctuations, then several simple models may be used to infer the shock layer turbulence level. A result from incompressible, homogeneous turbulence theory (quoted in Ref. 4-8) is that

$$\sqrt{\frac{\overline{P_o^2}}{\rho U^2}} = .58 \left(\frac{U'}{U}\right)^2$$

If ρ and U are evaluated behind the shock wave and $\sqrt{p_o^2} = 13$ psig for the 1.11" Mach 1.8 nozzle (a crude estimate by inspection of the figures in Ref. (4-13) then $U'/U_2 = .36$. This 36% level which appears to be very high, would produce the maximum (i.e., about 1.8) effect in the heat transfer. Another way is to use the compressible form of Bernouillis' equation for the high subsonic flow between the shock and stagnation point. A fluctuation in measured total pressure would then relate to a velocity fluctuation immediately behind the shock by an easily derivable relation ship:

Ref. (4-13) Brown-Edwards, E.G., "Fluctuations in Heat Flux as Observed in the Expanded Flow From the RENT Facility Arc Heater", Tech Rep't AFFDL TR-73-102 (Nov. 1972) A.F. Flight Dynamics Laboratory

$$
\frac{U'}{U_2} = \left[\frac{p_2^{\frac{\gamma-1}{\gamma}} \, p_o^{\frac{1-\gamma}{\gamma}}}{(\frac{2\gamma}{\gamma-1})(1 - p^{\frac{\gamma-1}{\gamma}} p_o^{\frac{1-\gamma}{\gamma}})} \right] \frac{\Delta p_o}{p_o}
$$

Taking the static pressure behond the shock to be 61.2 atm (from standard tables), p_o the stagnation pressure to be 76.5 atm and $\gamma = 1.26$ (its average value) we obtain for the 1.11" nozzle

$$
\frac{U'}{U_2} = 2.2 \, \frac{\Delta p_o}{p_o}
$$

Since $\Delta p_o = (13 + 14.7)/14.7 = 1.88$ atm and $p_o = 76.5$ atm (slightly lower than actually measured) we obtain finally:

$$
\frac{U'}{U_2} = .054
$$

or about 5.4% turbulence level, a somewhat more realistic figure. This makes the parameter $T\sqrt{Re} = 37.8$ which would give a 50% increase in heat transfer rate.

The only other indications of fluctuating flow (aside from heat transfer) are given by Bader (Ref. 4-14). He obtained fluctuations in the intensity of copper line spectrometer measurements. No power spectral densities of the signal were obtained so that it is not possible to say whether the flow was fully turbulent, i.e., a complete distribution of scales of motion following established decay laws.

4.4 Theoretical Predictions

Theoretical results which attempt to predict the large observed effects of turbulence on laminar, stagnation point heat transfer have used the simple model of subsonic, incompressible, ideal fluid flow. The specific

----

Ref. (4-14) Bader, J., "Time Resolved Absolute Intensity Measurements of the 5106 Angstrom Copper Atomic Spectral Line in the AFFDLL RENT Facility", Tech Report AFFDL TR-75-33 (Feb. 1975) Air Force Flight Dynamics Laboratory

form of the turbulence law has been mixing length (Ref. (4-4, 4-15) or
an adaptation of turbulent kinetic energy models (Ref. 4-16). In all
these models an added term representing the eddy diffusivity of heat and
momentum is used. In the simple "eddy" law

$$\epsilon_m = kU'y$$

where k is a constant, U' is the free stream fluctuation level and y
the normal coordinate. In the more complex methods $\epsilon_m = e/\omega$ where "e"
is turbulent energy and "ω" is pseudovorticity and differential equations
must be solved for each of these quantities. The more complex theory has
the advantage of being able to be extended to compressible flow and, more
importantly, to account for the correlation lengths in the flow. Some
typical results from the mixing length type of theory are shown in
Figure 20. Figure 14 shows the theory of Ref. (4-4).

The theory continues to rise with $T\sqrt{Re}$ whereas the experiments reach
an asymptotic value. The more complex theories are shown in Figure 21.
They appear to better predict the trend of the experimental results. Note
that the correlation length ℓ_t appears as the parameter $(\ell_{t/D})\sqrt{Re_D}$.
Results of both of these types of theories for spheres give about the same
numerical values, although the experiments tend to show somewhat lower
influence of turbulence on heat transfer augmentation.

Ref. (4-15) Galloway, T.R., "Enhancement of Stagnation Flow Heat and
             Mass Transfer Through Interactions of Free Stream Turbulence",
             AICHE Journal, 19, No. 3., pp. 608-617 (May 1973)
Ref. (4-16) Traci, R.M., and Wilcox, C.D., "Analytical Study of Free-
             stream Turbulence Effects on Stagnation Point Flow and Heat
             Transfer", AIAA Paper 74-515, 7th Fluid & Plasma Dynamics
             Conference, Palo Alto, Calif., June 1974
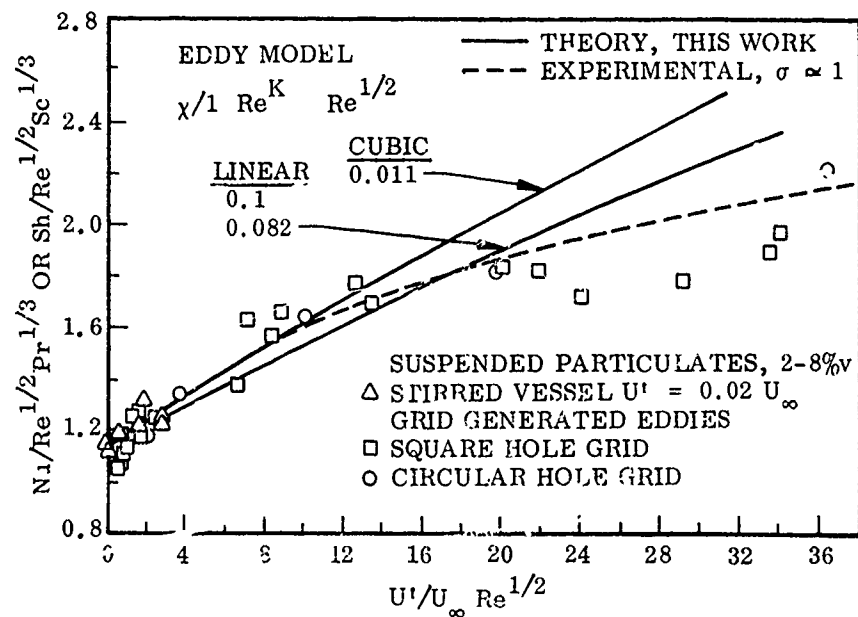
Figure 20   Augmentation of Forward Stagnation Point Transport,
              Comparison with Experiments Involving Circular Cylinders (Ref. 4-15)
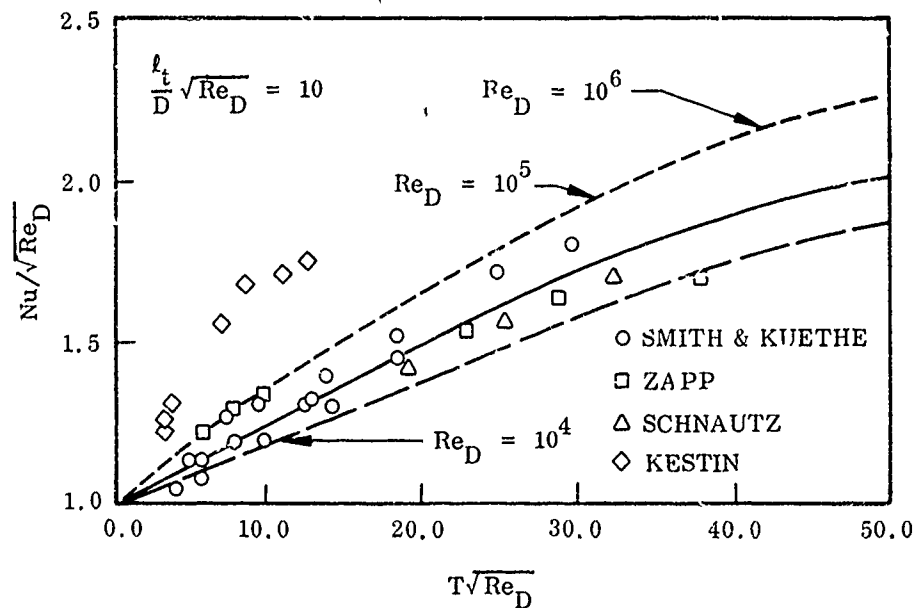
Figure 21   Stagnation Point Heat Transfer to a Cylinder in a
              Turbulent Cross Flow (Ref. 4-16)

Another approach of studying the effect of free stream turbulence on the stagnation point heat transfer is the so-called vorticity amplification theory advanced by Sutera (Ref. (4-17) and (4-18)). This theory suggests that vorticity amplification due to stretching of vortex filaments in the strongly diverging stagnation point flow is the essential mechanism underlying the strong influence of free stream turbulence on heat transfer. The development of this theory was based on the study of incompressible two-dimensional stagnation point flow. In this study, the free stream turbulence was modeled by a distributed, unidirectional vorticity in the form of a simple sinusoidal perturbation of a unique wave number k. The axis of this added vorticity is perpendicular to the surface streamline which is, according to the vorticity amplication theory, the only direction susceptible to amplification by stretching in the stagnation point flow.

It was found (Ref. 4-17) that amplification depends on the wavelength or scale of the added vorticity. Only those vorticity components with a wave length λ greater than a certain neutral wavelength λ_o (or $k < 1$) amplify and can therefore affect the boundary layer. For $\lambda < \lambda_o$ or $k > 1$, the vorticity is dissipated, for $\lambda = \lambda_o$ or $k = 1$, the vorticity is convected toward the wall with no net amplification. It is important to emphasize that in this theory, the nature of the vorticity contained in the oncoming flow is imposed on the flow.

Sutera (Ref. 4-18) has made calculations for the stagnation flow near a cylinder in cross flow by choosing $k = 1.5$. Increased heat transfer due to the added vorticity was found. It was also found that the mean temperature profile is much more responsive to the added vorticity than the mean velocity profile. The solutions obtained, however, depend on a

------

Ref. (4-17) S. P. Sutera, R. F. Maeder, and J. Kestin, "On the Sensitivity of Heat Transfer in the Stagnation Point Boundary Layer to Free-Stream Vorticity", J. Fluid Mech., Vol. 16, part 4, p. 497, 1963

Ref. (4-18) S. P. Sutera, "Vorticity Amplification in Stagnation Point Flow and Its Effect on Heat Transfer", J. Fluid Mech., Vol. 21, part 3, p. 513, 1965

so-called amplification parameter A, which is a free parameter not provided by the theory.

Based on Sutera's work, Weeks (Ref. 4-19) has applied the vorticity amplification theory to study the effect of free stream turbulence on hypersonic stagnation point heat transfer. In Weeks' study, the dissipation term was included in the energy equation, the wave number k was again taken to be 1.5, and the amplification parameter A was related to the turbulent intensity by

$$A = \frac{3.8(1.7)}{0.15} \frac{|v|}{V_o}$$

Where V_o is the mean longitudinal velocity ahead of the probe shock and $|v|$ is the velocity fluctuation. Based on the Klebanoff (Ref. 4-20) values of longitudinal turbulence intensity, the heat transfer through a hypersonic nozzle boundary layer was calculated and compared with data as shown in Figure 22. It is seen from this figure that the calculated value agrees qualitatively with the data and that the heat transfer with free stream turbulence (q) is greater than that without free stream turbulence (q_b). Stagnation point heating in a plasma jet was also calculated by Weeks and compared with data as shown in Figure 23. Again, qualitative agreement was found between the measured and the calculated heat transfer rates.

Ref. (4-19)   T. M. Weeks, "Influence of Free Stream Turbulence on Hypersonic Stagnation Zone Heating", Tech Rept. AFFDL-TR-67-195, May 1968

Ref. (4-20)   M. V. Lowson, "Pressure Fluctuations in Turbulent Boundary Layers", NASA TN D3156, 1965
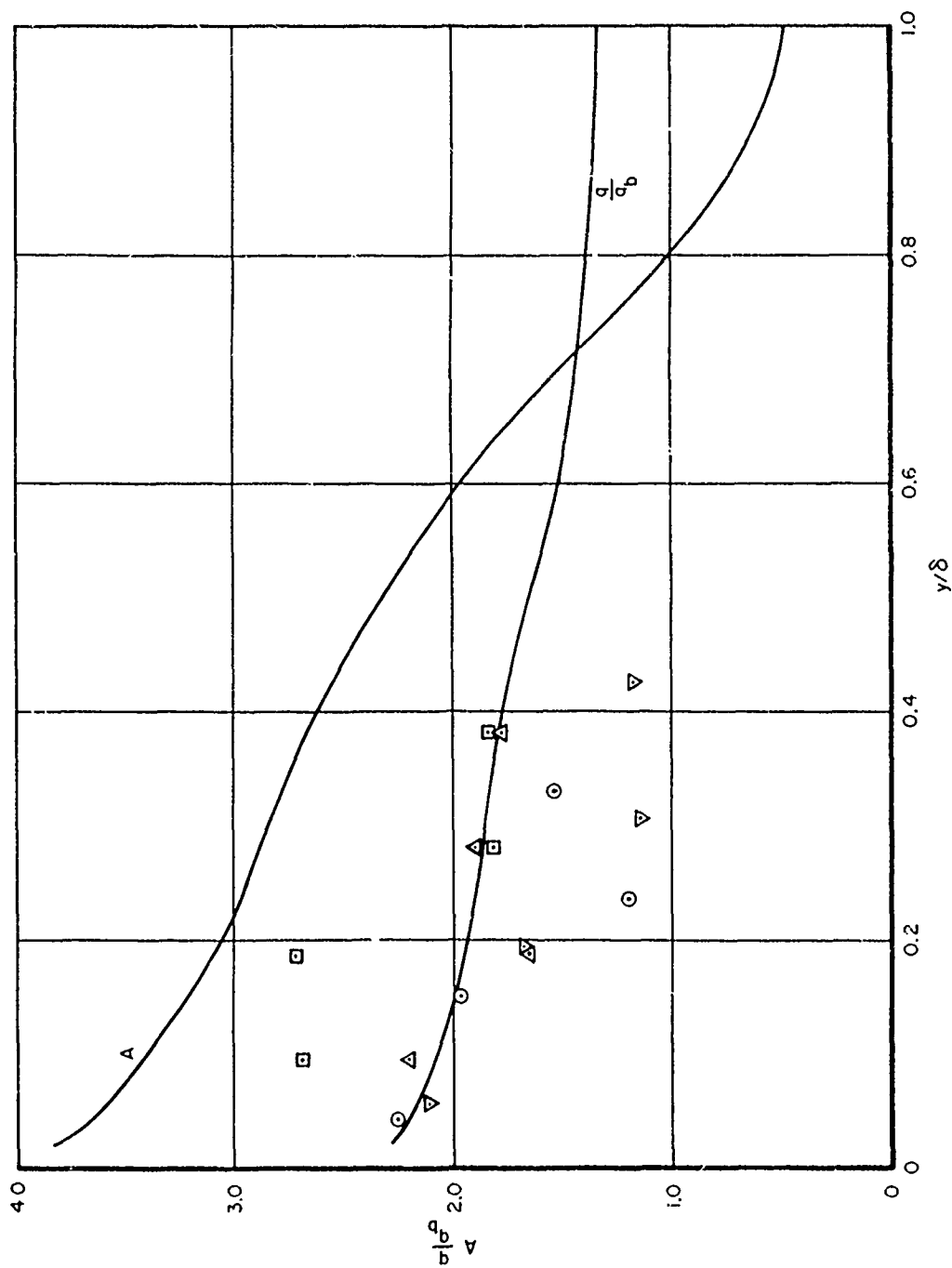
Figure 22   Variations of Stagnation Point Heat Transfer Through a Turbulent Boundary Layer
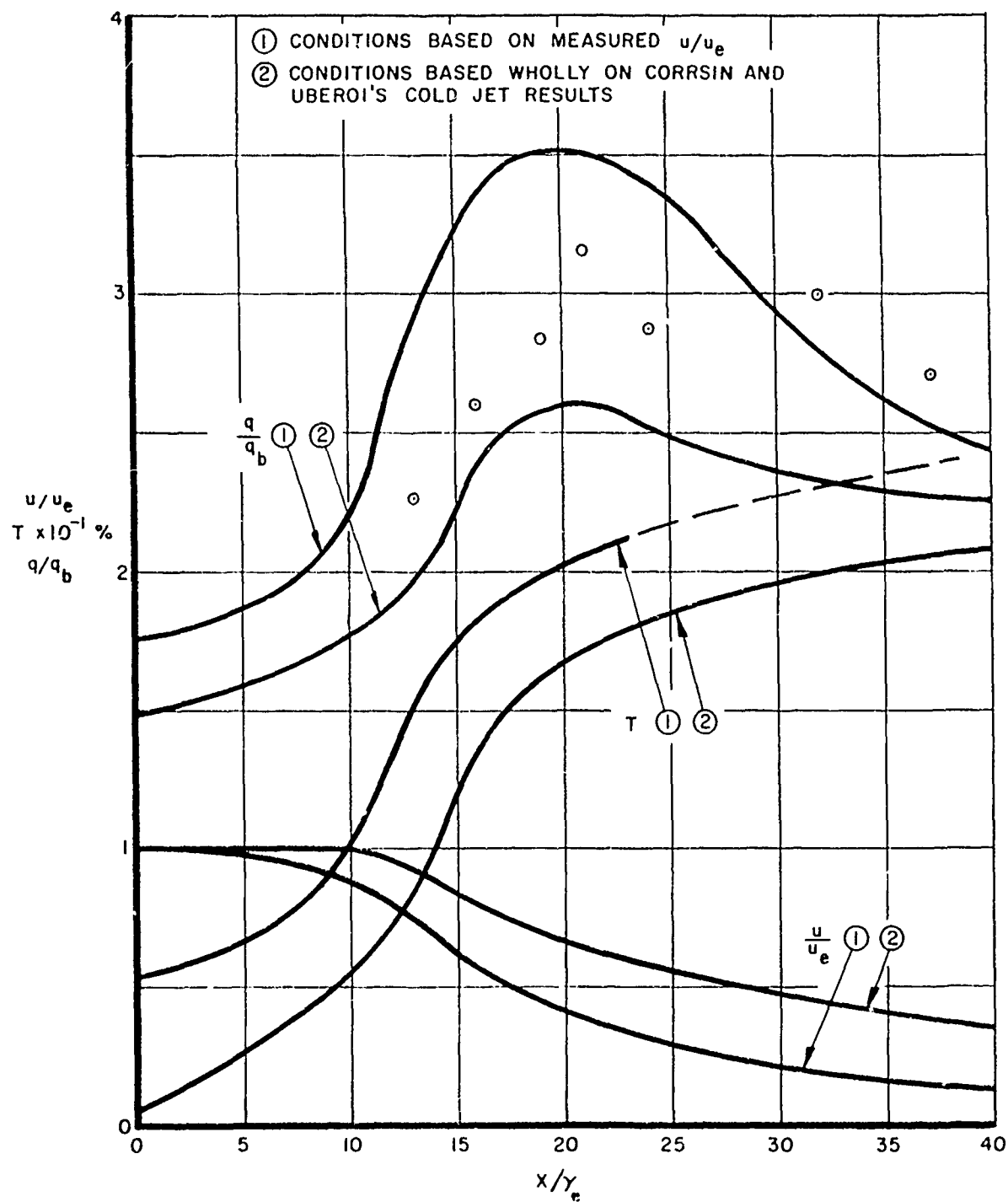
Figure 23 Stagnation Point Heat Transfer Rate Along the Centerline
of a Nitrogen Plasma Jet

The successful application of vorticity amplification theory to a given flow problem depends largely on the choice of wave number k and the relationship of the parameter A to the turbulent intensity. The theory predicts qualitatively correct results as shown by Weeks. It seems, however, difficult to obtain quantitatively accurate results due to the lack of any universal or rigorous method in determining the two parameters k and A. It should be pointed out that the vorticity amplification mechanism, which is certainly one of the important mechanisms in the enhancement of heat transfer due to free stream turbulence is included in some of the modern turbulence models such as the turbulent kinetic energy model. Such a model will be less restrictive in its application than the theory of vorticity amplification.

From all of these theoretical and experimental results it is clear that any free stream turbulence in the exit jet of the RENT facility will have (because of the large Reynolds numbers) a substantial effect on measured values of stagnation point heat transfer. It would be worth-while to have some direct measurement (from say the spectrum of fluctuating radiation) of its existence and furthermore to extend the classical heat transfer results of Fay & Riddell to include effects of turbulence. This should be done using a modern formulation of turbulent-transport which will allow inclusion of pertinent (to the RENT conditions) real gas effects.

Section 5

COPPER PARTICLE IMPINGEMENT

In order to determine the enhancement of stagnation point heat transfer due to particle impingement, it is necessary to have data or information on particle mass loading and particle size distribution. In the absence of this information, only an upper bound estimate can be made. An upper bound estimate was made based on the following two basic assumptions: (a) the injection rate of copper particles from the electrodes is 0.1 percent by weight of the gas flow rate (Ref. 5-1); (b) the number density of gas phase copper in the model shock layer is 10^{16} part/cm^3 for the 1.11 inch nozzle. Ths gas density in the model shock layer for the 1.11 inch diameter nozzle is approximately 2.8×10^{-3} gm/cm^3, hence, the gas phase copper concentration in the model shock layer corresponds to 0.017 percent by weight. For other size nozzles the ratio of gas phase copper density to the gas density in the shock layer is assumed to be the same as the 1.11 inch nozzle.

Let us denote ρ_c as the particle density in front of the shock, V_i as the particle impact velocity and E_c as the collection efficiency defined as the percentage of ρ_c that can reach the stagnation region. For unit energy accommodation coefficient, the heat transfer from particle impingement $\dot{q}_{imp}$ is

$$\dot{q}_{imp} = E_c \rho_c V_i^3 /2 \qquad (5-1)$$

Both E_c and V_i are functions of particle size (Ref. 5-2, 5-3). Consider first the case of uniform particle size. By assuming an approximate

------

Ref. 5-1 "The 50 Megawatt Facility" by Thermomechanic Branch, Flight Mechanics Division, Air Force Flight Dynamics Laboratory, Tech Memorandum TM-71-17 FXE, Oct. 1971

Ref. 5-2 G. D. Waldman and W. G. Reinecke, "Particle Trajectories, Heating, and Breakup in Hypersonic Shock Layers", AIAA J., Vol. 9, No. 6, June 1971

Ref. 5-3 R. F. Probstein and F. Fassio, "Dusty Hypersonic Flows", AIAA J., Vol. 8, No. 4, April 1970

heating and evaporation process, together with the known injection rate
and shock layer copper number density, this size can be determined by
the conservation of copper mass as described below.

In the arc heater, we assume that the particles are spheres, that
the particle material immediately reaches its boiling temperature as it
comes out from the electrode, absorbs its latent heat and evaporates
without altering the local heat transfer rate, and that they retain
their spherical shape as they evaporate. With these assumptions, net
energy conservation for a particle subject to an average heat transfer
rate q gives

$$q = - \sigma Q \frac{dr}{dt} \tag{5-2}$$

where σ is the particle material density, r is the particle radius,
and Q = latent heat of sublimation for solid particle and Q = latent
heat of evaporation for liquid particle.

For copper $\frac{(\sigma Q) \text{ solid}}{(\sigma Q) \text{ liquid}}$ 1.12. Hence in the determination of par-
ticle size, there is little difference between solid and liquid particles.
Solid particles in the heater section will result in slightly larger
particles in the shock layer and therefore will have a higher impact
velocity and higher collection efficiency. For the purpose of estimating
the upper bound, we will consider solid particles only.

Assuming that the particle velocity is in equilibrium with the gas
velocity, or equivalently, that the Reynolds number based on the particle-
gas slip velocity is small, then from Ref. (5-4) we have the Nusselt
number $N_u \approx 2$. From the definition of Nusselt number, Eq. (5-2) can be
written as

Ref. (5-4)   T. Yuge, "Experiments on Heat Transfer from Spheres Including
             Combined Natural and Forced Convection", Journal of Heat
             Transfer, Aug. 1960

-50-

$$\frac{d\left(\frac{r}{r_o}\right)^2}{dt} = \frac{-4k(T_o - T_b)}{\sigma Q r_o^2} \tag{5-3}$$

where r_o is the radius of the particle ejected from the electrode (at $t = 0$), k is the heat conductivity of air, T_o is the average core temperature in the arc heater, T_b is the copper boiling temperature. Assume $T_o \approx 6000°K$, which is approximately the temperature in the gas cap over the blunt model. At $6000°K$, $k = 1.516 \times 10^{-3} \frac{watts}{cm°K}$. The boiling temperature for copper at 100 atm pressure is $4240°K$. For copper, $\sigma = 8.9 \ gr/cm^3$ and $Q = 8.14 \times 10^4$ cal/mole. Using these numbers, Eq. (5-3) can be written as

$$\left(\frac{r}{r_o}\right) = \sqrt{1 = 2.15 \times 10^{-4} \frac{t}{r_o^2}} \tag{5-4}$$

The residence time of the particle in the heater is estimated as X/U_o, where U_o is the average gas velocity in the heater and X is taken to be the length of the subsonic portion of the nozzle. This time is estimated to be one msec. From Eq. (5-4), the particle size in front of the model shock, r_e, is

$$r_e = r_o\sqrt{1 - 2.15 \times 10^{-7}/r_o^2} \qquad (r_o \text{ in cm}) \tag{5-5}$$

The density of copper vapor immediately behind the shock due to the evaporation of copper in the arc heater is

$$\rho_{cu(g)} = 0.001 \ \rho_{s_o}\left[1 = \left(1 - \frac{2.5 \times 10^{-7}}{r_o^2}\right)^{3/2}\right] \tag{5-6}$$

where ρ_{s_o} is the gas density immediately behind the shock.

Let us consider, for the time being, that heating in the shock layer is negligible. In this case, we have from the assumption (b) mentioned before that $\rho_{cu(g)} \approx 0.17 \times 10^{-3} \ \rho_{s_o}$ (5-7)

Substituting Eq. (5-7) into Eq. (5-6), r_o can be determined. Consequently from Eq. (5-5), we obtain the particle size in front of the shock as $r_e = 12.8 \ \mu m$.

The particle density before the shock is therefore

$$\rho_c = 0.83 \times 10^{-3} \ \rho_e \tag{5-8}$$

where ρ_e is the gas density before the shock. Equation (5-8) is assumed to be applicable to all nozzle sizes.

In order to make certain that heating of the particle in the shock layer is indeed negligible, a close examination into the heating mechanism in the shock layer is made. The heating of a particle in the shock layer is governed by two parameters H_e and K_{se} defined as (Ref. 5-2).

$$H_e = E\Delta/\sigma Q V_e r_e^{3/2}$$

$$K_{se} = 3C_D \rho_{so} \Delta 8 \sigma r_e \qquad (5-9)$$

$$E = 2\left(\frac{\rho_e}{\rho_o}\right) M_e^{3.5} \quad [\text{BTU}/\text{ft}^{3/2}\text{-sec}]$$

where V_e is the gas velocity and M_e is the Mach number in front of the shock, Δ is the shock stand-off distance, $\rho_o = 2.498 \times 10^{-3}$ slug/ft^3 and C_D is the drag coefficient of particle based on particle cross-sectional area. C_D can be approximated by the formula (Ref. 5-3)

$$C_D = ae^{-n}$$

for

$$
\begin{array}{lll}
Re < 1 & a = 24 & n = 1 \\
1 < R_e < 10^3 & a = 24 & n = \dfrac{2}{5} \\
Re > 10^3 & a = 0.44 & n = 0
\end{array}
\qquad (5-10)
$$

where Re is the particle Reynolds number based on the particle-gas slip velocity and the particle diameter.

The particle impact radius r_i/r_e is plotted as a function of H_e and K_{se} in Figure 24 (from Ref. 5-2). The collection efficiency $E_c (= \frac{m_r}{m_e})$ and the particle impact velocity V_i are also plotted in Figures 25 and 26, respectively (from Ref. 5-2). In Figure 25, ϵ is the density ratio across the shock $\epsilon = \frac{\rho_e}{\rho_{so}}$.

For a 12.8 μm particle, H_e is of the order of 10^{-3} and K_{se} is of the order of 10^{-2} for all nozzle conditions. In this case, we see, from Figures 24 and 26 that not only is the heating negligible, but also that the effects of the shock layer on particle trajectory are negligible small,
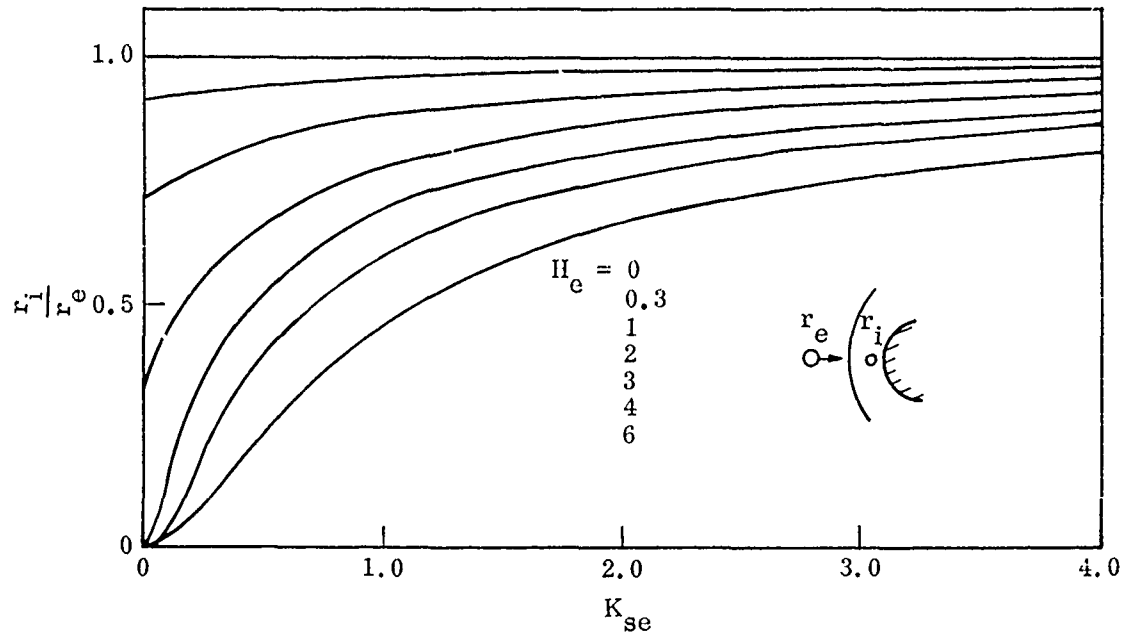
Figure 24 Particle Radius at Impact, Including Mass Loss by Heating
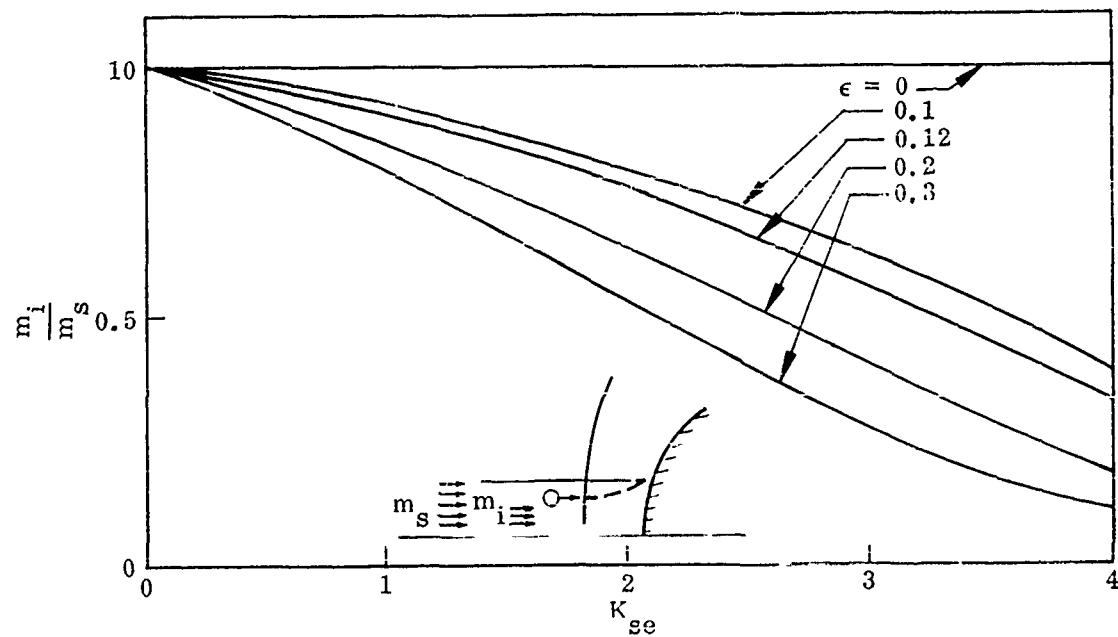
Figure 25 Collection Efficient for Spherical Nose
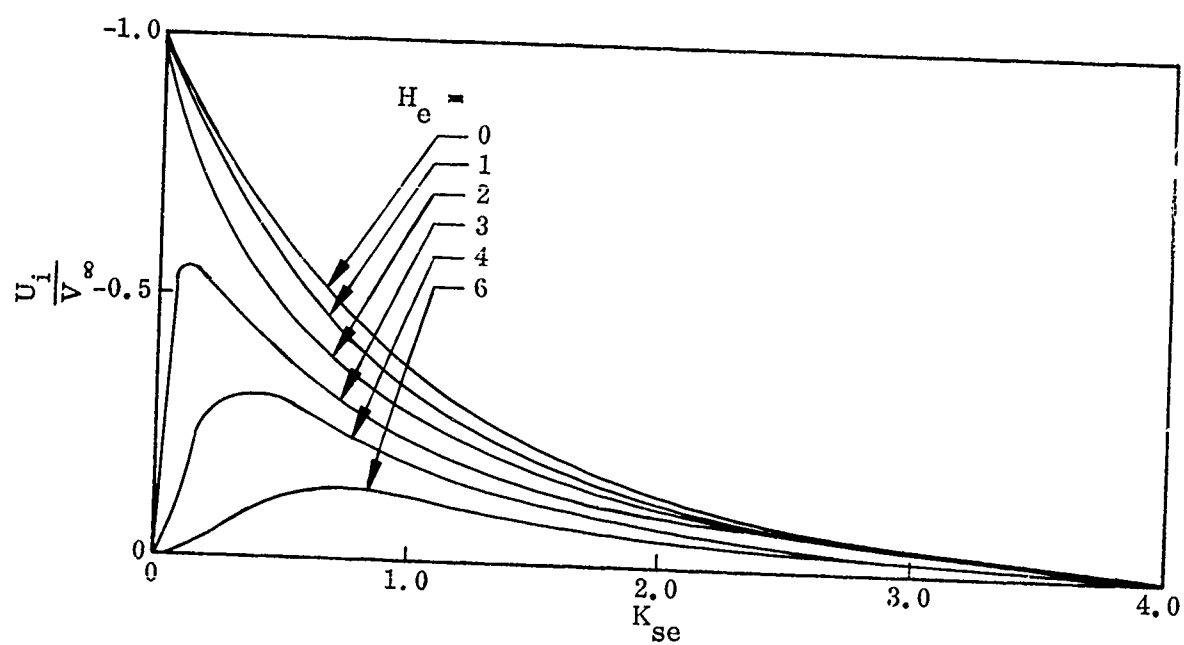
Figure 26   Particle Velocity at Impact, Including Mass Loss by Heating

(i.e., $E_c = 1$, $V_i = V_e$). In fact, shock layer heating will not become important until the particle size is 0.1 μm or less. Also the particle trajectory will not be altered appreciably in the shock layer until the particle size is 1 μm or less. Based on these considerations, we assume

$$E_c = 1, \qquad V_i = V_e \qquad\qquad (5\text{-}11)$$

The particle density ρ_c and the particle impact velocity V_i are plotted in Figures 27 and 28, respectively for various nozzle exit diameters and at various stream enthalpys. The heat transfer due to impingement $\dot{q}_{imp}$ (from Eqs. (5-1), (5-8), and (5-11)) is presented in Figure 29 along with the range of observed convective heat transfer $\dot{q}_c$. It is seen that within the estimated range of the stream enthalpy (from 2000 to $6000\frac{BTU}{lb}$), the impingement heat transfer is about 5% of the observed convective heat transfer.

The results of Figure 29 represent an upper bound due to Eq. (5-11). The effect of the particle size distrubution and the uncertainty in the estimated particle residence time in the heater can only reduce both the collection efficiency and the impact velocity. Therefore, we conclude that the effect of copper particle impingement is at most 5 percent. This conclusion is based on the assumption that the total copper mass fraction is 0.1 percent and that 17 percent or 0.017 percent by mass is in the vapor state. If the copper mass fraction in the solid phase is higher, the impingement heat transfer would be proportionately higher. It is therefore desirable to obtain data on copper mass loading in the RENT flow field.

One possible method for obtaining this data is to capture the copper particles and perhaps the copper vapor on a membrane filter placed in an enthalpy probe at a point where the gas temperatures are sufficiently low to enable the filter to survive. The copper mass captured on the filter could be determined by emission spectroscopy or atomic absorption.
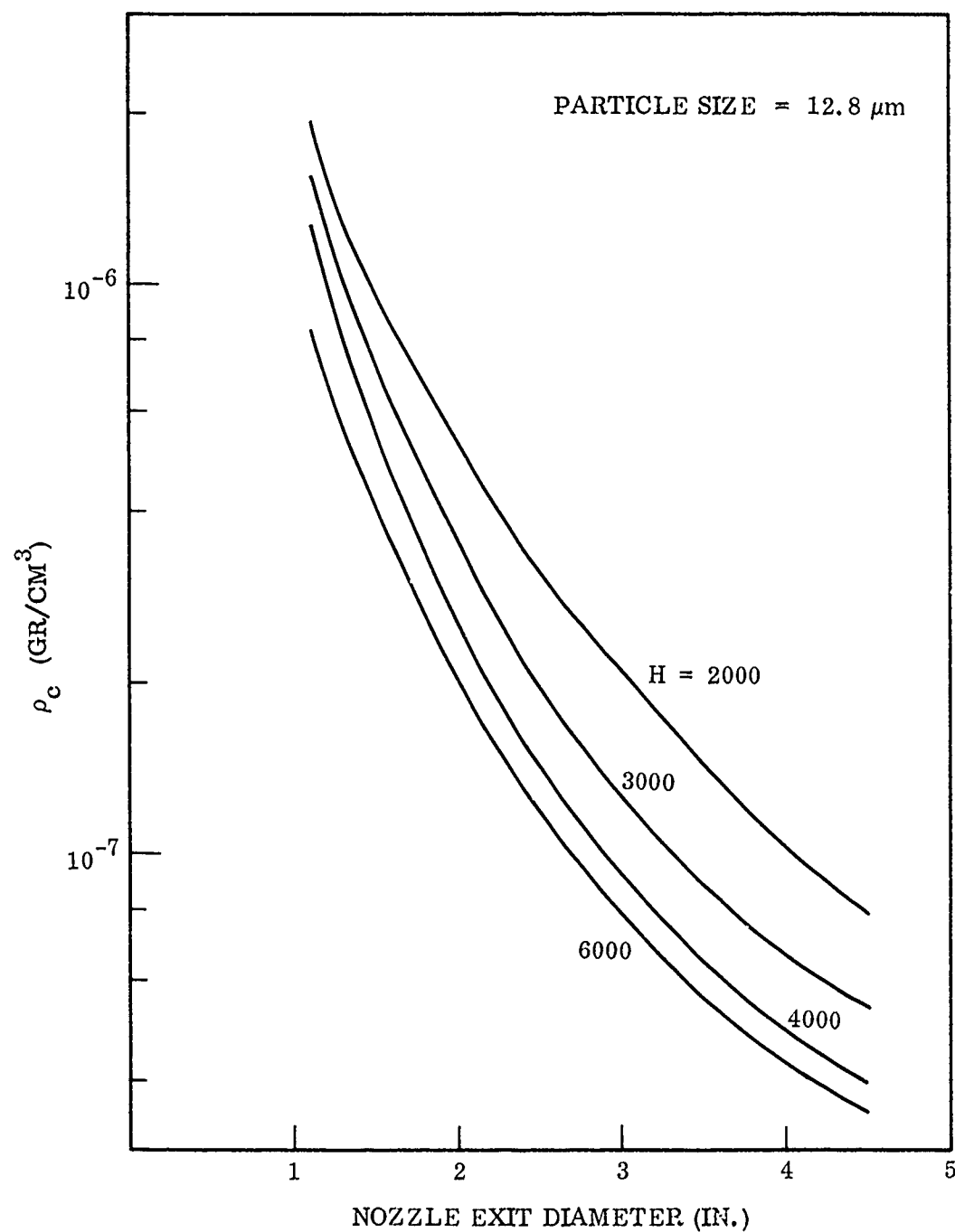
Figure 27 Particle Density
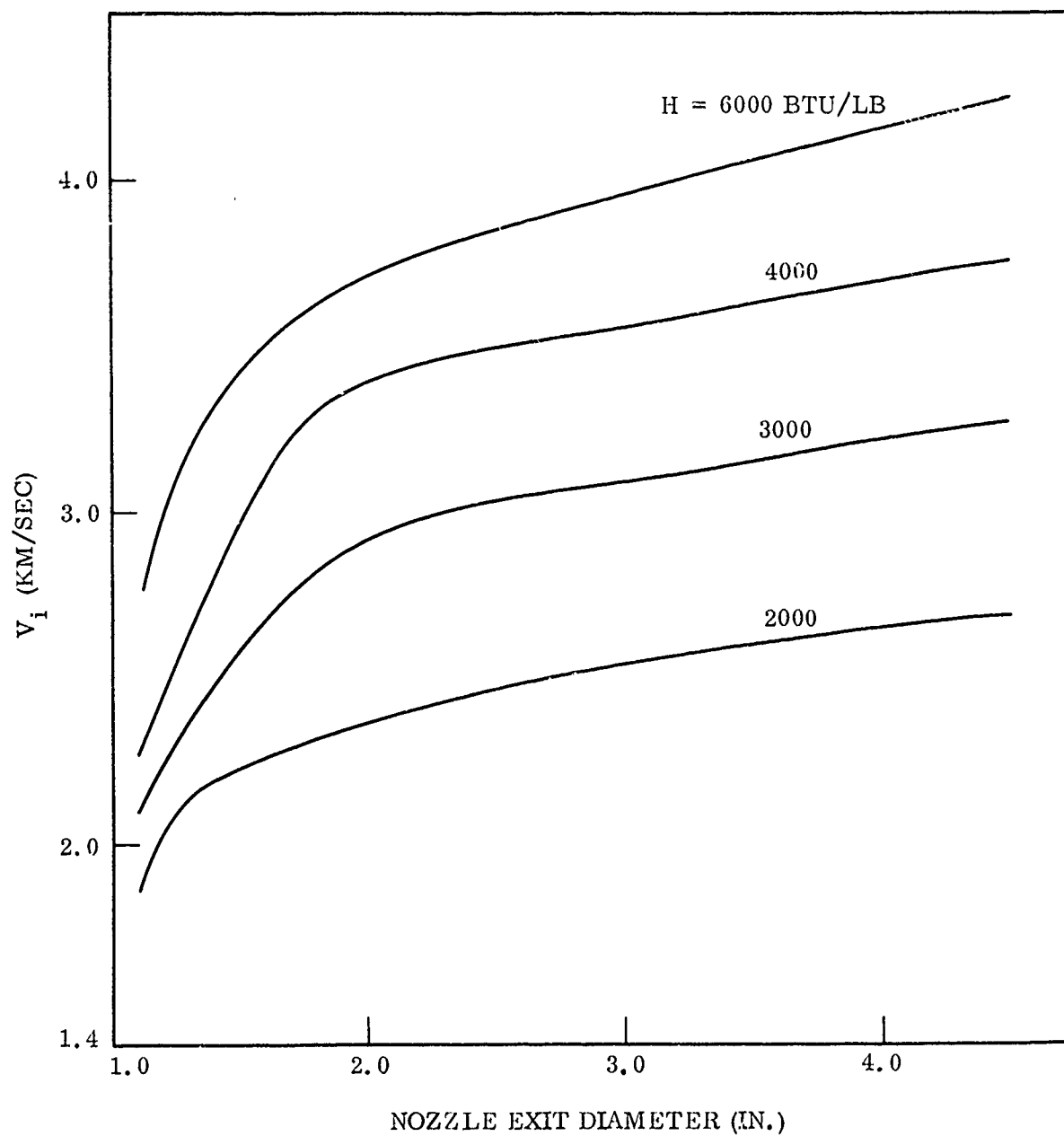
Figure 28 Particle Impact Velocity
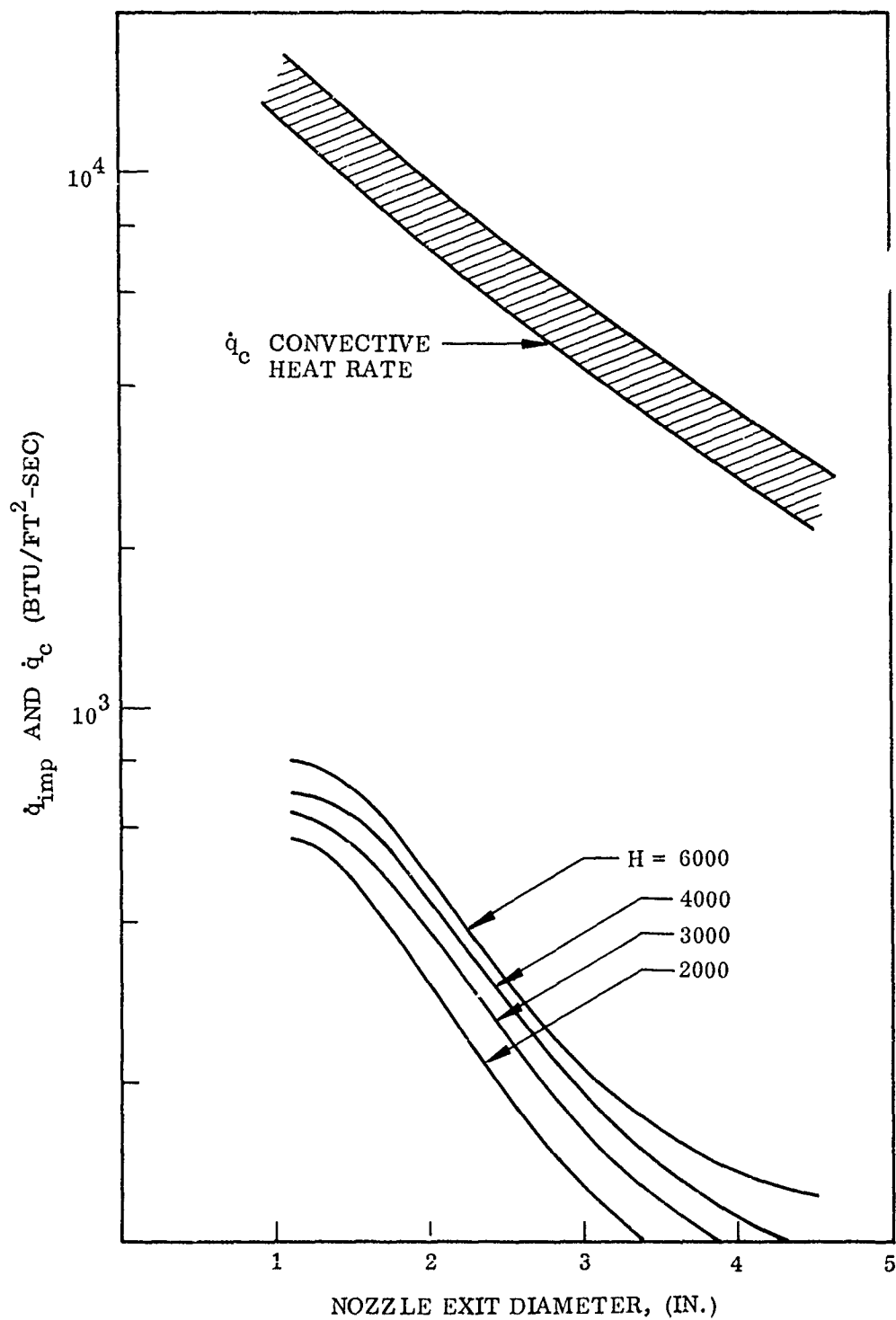
Figure 29 Copper Particle Impingement Heat Rate

Section 6
ENTHALPY FLUCTUATIONS AND GRADIENTS

In this section the effects of free stream enthalpy fluctuations and enthalpy gradients on stagnation point heat transfer are discussed. Analysis of the effect of timewise fluctuations of flow variables and the effect of spatial enthalpy gradients on stagnation point heat transfer were performed to assess the importance of these effects in the RENT facility. Details of these analyses are presented in Appendix A and B, respectively. The results of these analyses are summarized in this section.

The RENT flow field contains both timewise fluctuations and radial spatial gradients in the stream enthalpy as demonstrated by the heat transfer measurements results shown in Figures 30 and 31 (Ref. 6-1). The heat transfer results shown in Figure 30 were obtained with the model held fixed near the nozzle centerline. Heat transfer models are normally swept across the nozzle to prevent destruction by excessive heating. The results shown in Figure 30 were obtained when the traverse carriage malfunctioned and the model stopped for about 40 msec. Heat transfer data from swept models normally contain the effects of radial gradients as well as timewise fluctuations. When the radial gradients are large, as is the case in Figure 31, the timewise fluctuations can be seen to be superimposed on the radial gradient.

In Appendix A, the effect of timewise fluction of flow properties on stagnation-point heat transfer is investigated by considering the unsteady, one-dimensional boundary layer energy equation. The total enthalpy and free stream velocity are approximated by periodic oscillations. An analytic solution to the unsteady energy equation is obtained by the method of successive approximations up to first order. After considerable analysis and manipulations, the final result for the increase in heat transfer due to timewise fluctions is developed and is given by the following relation

------

Ref. (6-1) Brown-Edwards, E.G., "Fluctuations in Heat Flux as Observed in the Expanded Flow from the RENT Facility Arc Heater", AFFDL-TR-73-102, Nov. 1973
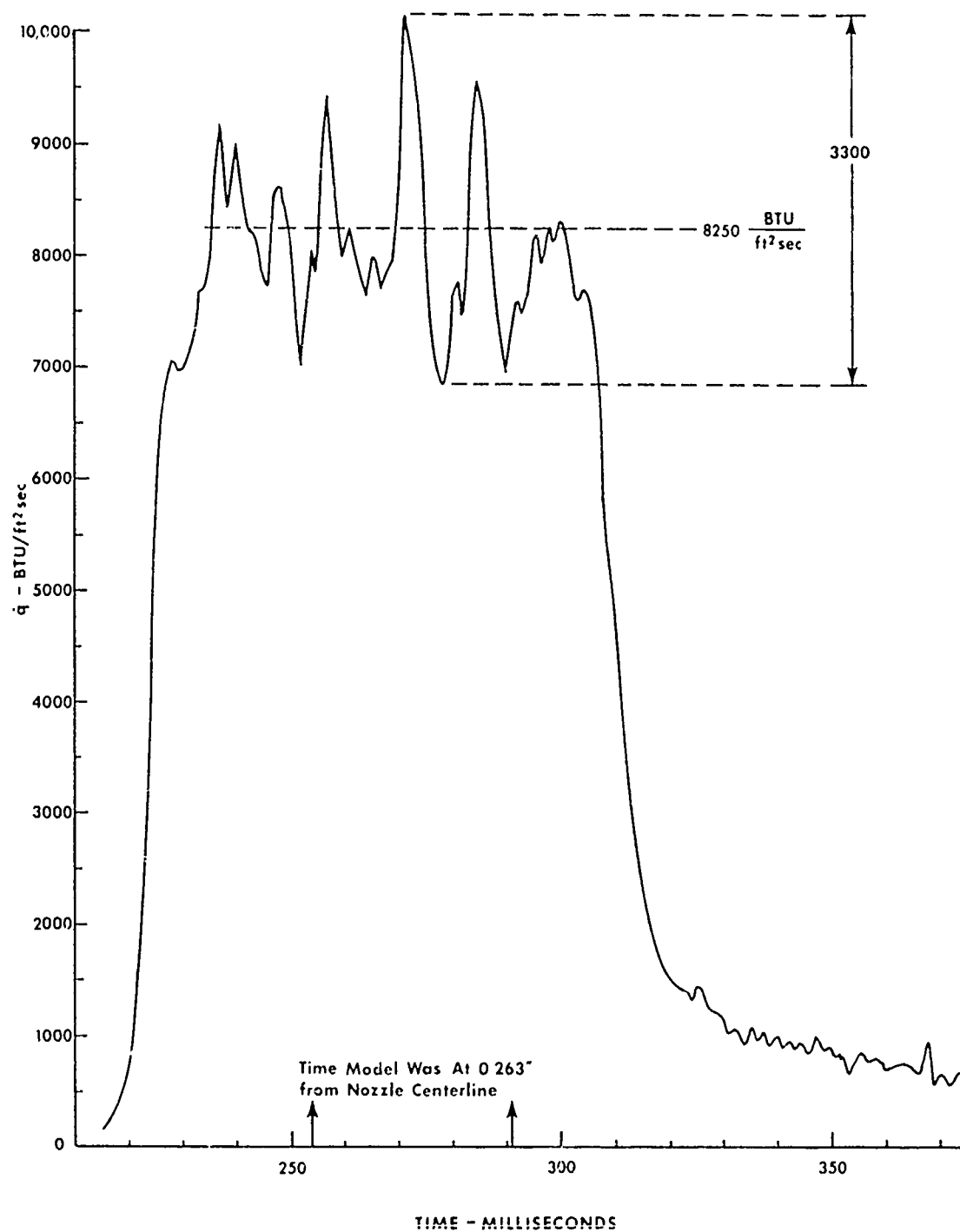
Figure 30   Heat Flux Variation in the 1.11 Inch Nozzle with
Calorimeter Held at 0.26" from Nozzle Centerline
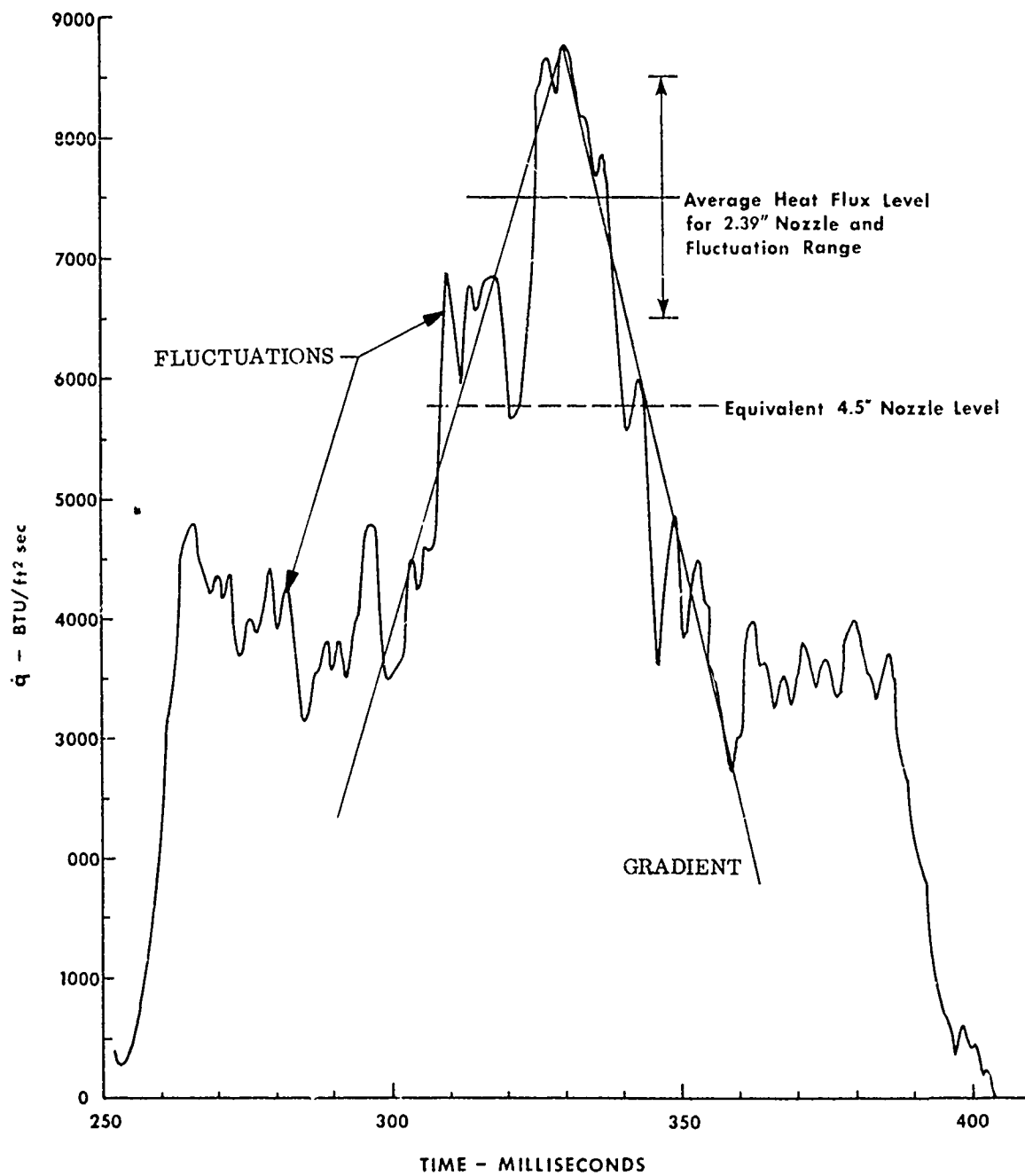
Figure 31   Radial Heat Flux Profile in the 2.39 Inch Nozzle
            at X = 0.1"

$$\frac{\overline{q_w(t)}}{q_w(\bar{H}_e)} = 1 - (1 - H_w)\,(q_w')^2\,\Gamma$$

Tn the above expression:

$\overline{q_w(t)}$ = time averaged heat transfer rate

$q_w(\bar{H}_e)$ = heat transfer rate corresponding to the mean total enthalpy

q'_w = heat transfer fluctuation normalized to $\overline{q_w(t)}$

Γ = heating enhancement factor (function of the dimensionless frequency, B_t.)

In the Rent facility, the heat transfer fluctuation, q_w', is of the order of $\pm$ 20% at a frequency of about 100 Hz (Ref. 6-1). For these conditions the increase in heat transfer is 2%. For the same value of q_w' and a frequench of 10^5 Hz, the increase in heat transfer is 1.7%. It is therefore concluded that enthalpy fluctuations in the RENT facility will not increase the measured stagnation point heat transfer results by more than a few percent.

An analysis of the effect of spatial enthalpy gradients on stagnation point heat transfer was also carried out. This analysis is presented in Appendix B a·d the results presented below.

By considering the compressible energy equation, it is shown that the increase in stagnation point heat transfer due to total enthalpy gradients is

$$\frac{\bar{q}_w'}{\bar{q}_w} = \frac{1 + 0.18\theta_o\,[1 + 0.52\,\theta_o]\,[\frac{dH_s}{d\theta}\Big|_o^+ - \frac{dH_s}{d\theta}\Big|_o^-]}{1 + 0.25\theta_o[\frac{dH_s}{d\theta_o}\Big|_o^+ - \frac{dH_s}{d\theta}\Big|_o^-]}$$

$$\approx 1 = 0.07\theta_o[\frac{dH_s}{d\theta}\Big|_o^+ - \frac{dH_s}{d\theta}\Big|_o^-] + 0(\theta_o)^2$$

where

$$\dfrac{q_w'}{} = \text{average heat flux over calorimeter with } dH_s/d\theta \neq 0$$

$$\dfrac{\overline{q_w}}{} = \text{average heat flux over calorimeter with } dH_s/d\theta = 0$$

$$\theta_o = \text{body angle subtended by calorimeter radius, } 0(1^o)$$

$$\left.\dfrac{dH_s}{d\theta}\right|_o^{+} = \text{total enthalpy slope in positive } \theta \text{ direction}$$

$$\left.\dfrac{dH_s}{d\theta}\right|_o^{-} = \text{total enthalpy slope in negative } \theta \text{ direction}$$

The above equation yields some interesting results on the effects of total enthalpy gradients on stagnation point heat transfer. Note first of all that since θ_o, the body angle subtended by the calorimeter, is generally less than 0.1 radian, the change in enthalpy will have to be rather large before there is a significant increase in heat flux. (The total enthalpy is normalized to the value corresponding to $dH_s/d\theta = 0$). Secondly, the gradients must be of opposite sign around the stagnation point or the effect of the gradients will cancel. Thirdly, it is possible to obtain no change, an increase or a decrease in the stagnation point heat flux. The possibilities are illustrated in Figure 32 .

In Figure 32a the total enthalpy gradient is a constant so that the effect of the gradients cancel according to the above equation. In this case the heat flux, when total enthalpy gradients are present, is equal to the heat flux corresponding to the average total enthalpy across the calorimeter. For the case shown in Figure 32b, the gradient is negative for positive θ and vice versa for negative θ so that the effect is an increase in heat flux. In this case, the actual heat flux is greater than the heat flux corresponding to the total enthalpy averaged over the calorimeter surface. Figure 32c shows the case where the effect of total enthalpy gradients is to decrease the heat flux.
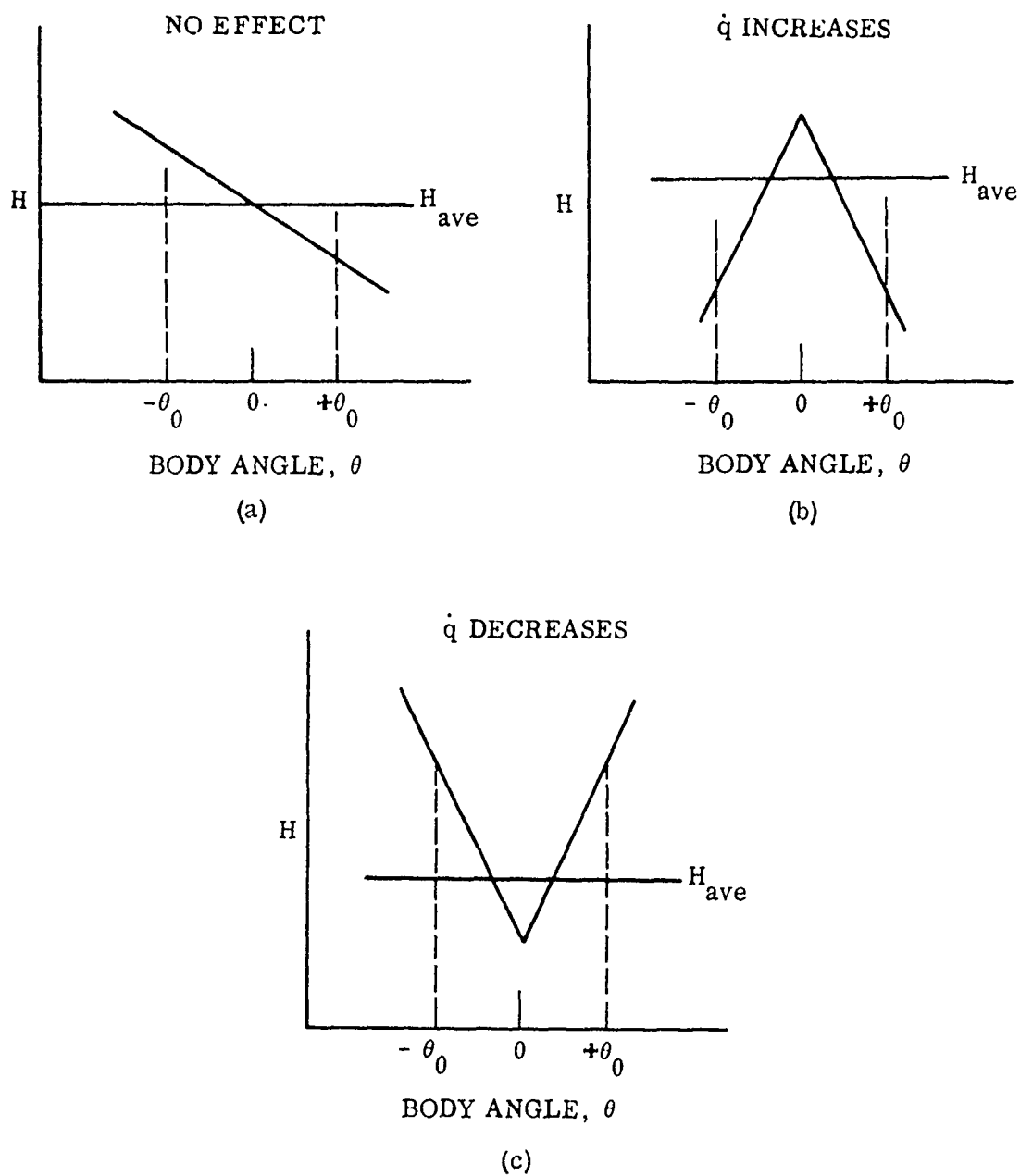
Figure 32   Possible Effect of Total Enthalpy on Stagnation
Point Heat Flux

The gradients shown in Figure 31 can increase the peak heat rate by about 0.5%. The heat rate gradients shown in Figure 31 are typical of RENT data and it is therefore concluded that spatial enthalpy gradients have a negligible effect on heat transfer.

Section 7
SWIRLING FLOW

In the present context, swirling flow refers to the uniform free stream with solid body rotation. Nonuniform flow aspects are considered in Section 4. The intent here is to investigate the effect of a swirl component in an otherwise uniform flow. An analysis of the effect of swirl has been performed and is presented in Appendix C. The results of this analysis show that swirling flow effects are small. Subsonic heat transfer data to a rotating sphere (Ref. 7-1) were located which confirm the results of the analysis. These data are shown in Figure 33 where

$$R_{e_R} = \frac{RV_r \rho}{\mu}$$

$$R_e = \frac{RV_x \rho}{\mu}$$

$V_r = R\omega$

R = model nose radius

ω = flow angular velocity, rad/sec

V_x = stream velocity

It is assumed that the angular velocity in the free stream is equal to the angular velocity in the arc chamber, which was estimated to be 10^3 rad/sec, the ratio of R_{e_R}/R_e is of the order of 10^{-2}. It is seen from Figure 31 that the effect of circumferential flow on heat transfer is negligible.

Ref. 7-1 Eastop, T.D., "The Influence of Rotation on the Heat Transfer from a Sphere to an Air Stream", Int. J. Heat Mass Transfer, Vol. 16, pp. 1954-1957, 1973
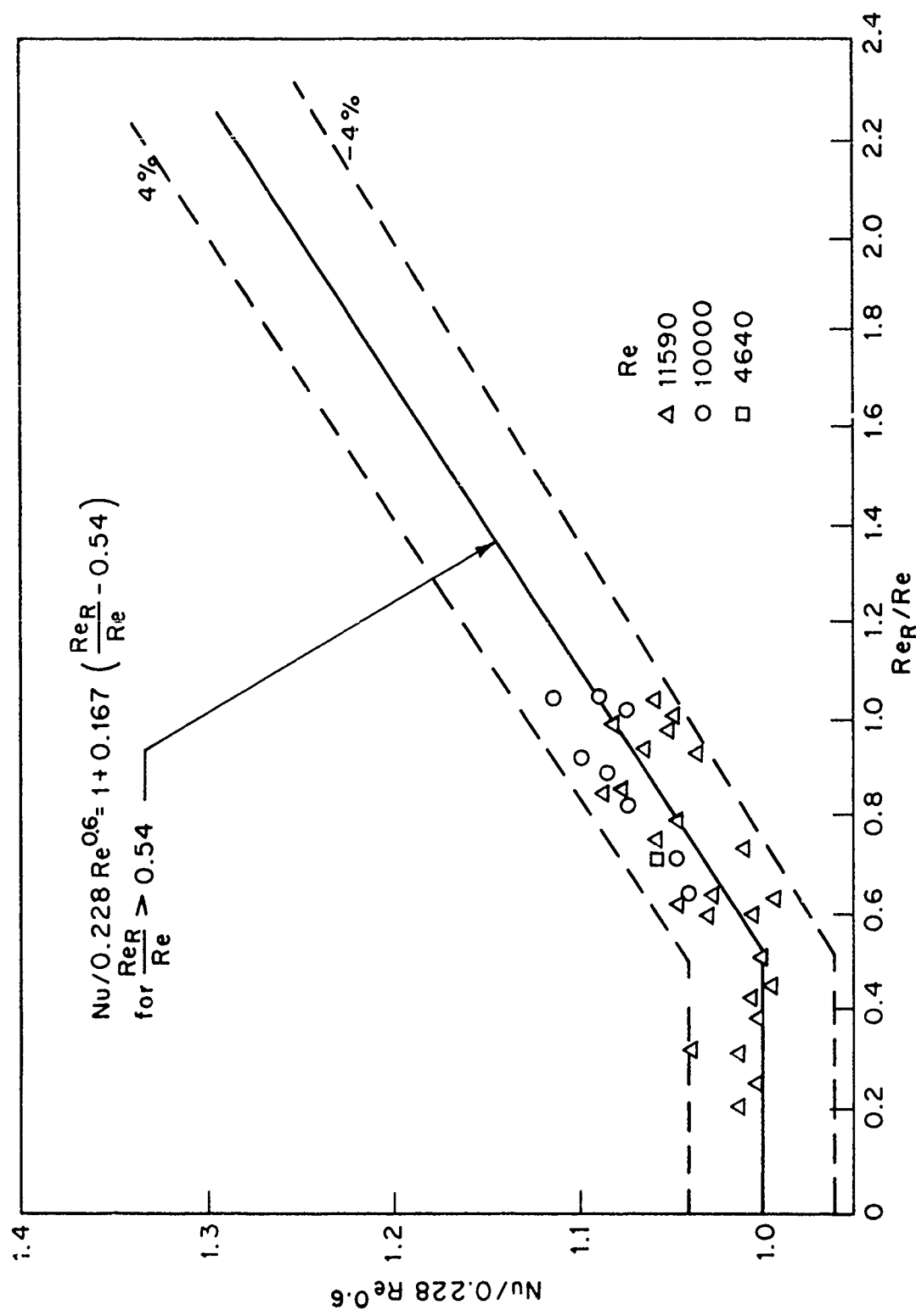
Figure 33 Effect of Rotation on Heat Transfer to a Sphere

$$\frac{Nu}{0.228\ Re^{0.6}} = 1 + 0.167 \left(\frac{Re_R}{Re} - 0.54 \right)$$

$$\text{for } \frac{Re_R}{Re} > 0.54$$

Re
△ 11590
○ 10000
□ 4640

4%

-4%

$\frac{Re_R}{Re}$

$\frac{Nu}{0.228\ Re^{0.6}}$

Section 8
CHEMICAL NONEQUILIBRIUM

Based on our review, it seems certain that any RENT nonequilibrium effects are exceedingly small. There would at most by only a very slight blocking of some heat transfer resulting in an underestimate of the total enthalpy from Fay & Riddell's formula. The magnitude of the effect is less than 5%.

In general, several requirements must be met for a nonequilibrium blocking effect to be significant. a) A major portion of the stagnation point enthalpy must be associated with dissociation or ionization. b) Homogeneous chemical times, that is, times required for the atoms or ions to recombine in the gas phase must be greater than boundary layer flow times. c) Finally, unless there is considerable ionization, a noncatalytic surface is required to prevent atom recombination on the wall which otherwise gives a heating rate nearly equivalent to the equilibrium case. With ionization, there can be large differences in heat transfer even with a perfectly catalytic wall (Ref. 8-1).

Tables 8-1 and 8-2 provide the information needed to address Points a) and b). Table 8-1 gives a summary of equilibrium stagnation point properties for "low", "nominal", and "high" values of RENT total enthalpy and both high and low expansion ratio nozzles. Flow data were determined from the hypervelocity air flow charts of Jorgensen (Ref. 8-2), compositions

----

Ref. 8-1   Fay, J. A., and N. H. Kemp, "Theory of Stagnation-Point Heat Transfer in a Partially Ionized Diatomic Gas", AIAA J., 1, 12, 2741-2751 (Dec. 1963)

Ref. 8-2   Jorgensen, L. H., and Baum, G. M., "Charts for Equilibrium Flow Properties of Air in Hypervelocity Nozzles", NASA TN D-1333 (Sept. 1962)

Table 8-1   RENT STAGNATION POINT PROPERTIES SUMMARY

	Total Enthalpy (B/lb)	Nozzle No.	Exit Mach No.	T_s (°K)	P_s (atm)	Z	Equilibrium Stagnation Conditions			
							O-Atom Mole Fraction	N-Atom Mole Fraction	Fraction of Energy in Dissoc't'n	Ion Mole Fraction NO+
"Low"	2000	09111P	1.8	3500	80	1.02	0.02	-	0.04	-
	2000	09450C	4.2	3500	5.9	1.03	0.06	-	0.13	-
"Nominal"	4500	09111P	1.8	5000	80	1.11	0.18	-	0.16	-
	4500	-	-	5000	50	1.12	0.20	-	0.18	-
	4500	09450C	4.0	5000	6.3	1.18	0.29	0.01	0.26	-
"High"	6000	09111P	1.8	7100	80	1.24	0.29	0.10	0.41	3×10^{-4}
	6000	09450C	3.9	7100	6.5	1.41	0.29	0.25	0.67	5×10^{-4}

Table 8-2 Damkohler Numbers (Flow Time/Chemical Time for Atom Recombination in Stagnation Point Flow

|	Total Enthalpy (B/lb)	Nozzle No.	Gas Reaction Damkohler Number		Surface Reaction Damkohler No. ζ_w	
			Γ_s $T = T_s$	Γ_{wall} $T = 1000°K$	$\gamma_w = 1$	$\gamma_w = 0.1$*
"Low"	2000	09111P	2.9	1.2×10^2	4.3×10^2	4.3×10^1
	2000	09450C	3×10^{-2}	1.3	1.1×10^2	1.1×10^1
"Nominal"	4500	09111P	7.0	8.9×10^2	3.8×10^2	3.8×10^1
	4500	-	3.0	3.8×10^2	2.9×10^2	2.9×10^1
	4500	09450C	6×10^{-2}	7.5	9.6×10^1	9.6
"High"	6000	09111P	3.3	1.2×10^3	3.2×10^2	3.2×10^1
	6000	09450C	2×10^{-2}	7.1	7.9×10^1	7.9

-----

*γ_w = Catalytic efficiency of surface material

are from the Hilsenrath (Ref. 8-3) tables. As can be seen from Table 8-1,
the RENT environment is fairly mild with respect to a). Ionization is
negligible in all cases and dissociation is mostly limited to oxygen except
in the high enthalpy, high expansion ratio case where about 1/3 of the
nitrogen is in atomic form.

Dissociative kinetics are generally fast so that equilibrium in the
shock layer is a good assumption; however, as atoms diffuse into the cold
BL they must recombine by 3-body reactions. If the gas is sufficiently
rarefied, the recombination process will be slow, thus locking up some
chemical enthalpy and reducing the heat transfer. Table 8-2 lists gas
phase Damkohler numbers (flow time/chemical time) for the stagnation con-
ditions outside the BL and at an assumed wall temperature of $1000^{\circ}K$. Here
the flow time t_f is the time for a particle in the free stream to move
one nose radius r_n (Ref. 8-4).

$$t_f = r_n \left[\frac{2(P_s - P_\infty)}{\rho_s} \right]^{-\frac{1}{2}}$$

where P_s and ρ_s are stagnation pressure and density, respectively, and
∞ refers to free stream conditions. Since oxygen is the main atomic
species the chemical time t_{chem} is the characteristic time for 0-atoms
to recombine via

$$0 + 0 + M \overset{\vec{k}}{\rightarrow} 0_2 + M$$
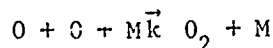
and is given by

$$t_{chem} = \frac{1}{kX_0[M]^2}$$

where $k = 3.8 \times 10^{-30} T^{-1} \exp(\frac{-170}{T}) \; cm^6 \; molecules^{-2} sec^{-1}$

= reaction rate constant

$[M]$ = total concentration $(\frac{molecules}{cm^3})$ (Ref. 8-5)

Ref. (8-3) Hilsenrath, J., and M. Klein, "Tables of Thermodynamic Properties
of Air in Chemical Equilibrium Including Second Virial Correc-
tions from $1500^{\circ}K$ to $15,000^{\circ}K$," AEDC-TR-65-58, (March 1965)

Ref. (8-4) Fay, J.A. and Riddell, F.R., "Theory of Stagnation Point Heat
Transfer in Dissociated Air", J. Aeronaut. Sci., 25, 121, 73-85,
(1958)

Ref. (8-5) Johnston, H.S., "Gas Phase Reaction Kinetics of Nuetral Oxygen
Species", NSRDS-NBS20, U.S. Depart. Commerce (Sept. 1968)

X_o = mole fraction of o-atoms outside Bl

The Damkohler number $\Gamma \equiv t_f/t_{chem}$ will vary as T^3 in the BL due to
the combined effect of [M] and the rate constant temperature dependence.
As Table 8-2 indicates with high expansion ratio nozzles one has slow
kinetics ($\Gamma < 1$) in the free stream, but still fast gas kinetics ($\Gamma > 1$)
at the cold wall. The wall region is most important in determining
heat transfer so we might suspect that while detailed profiles might deviate
from equilibrium in the outer edgs of the BL the heat transfer effects
would be minimal as long as $\Gamma_{wall} > 1$. This is borne out by the boundary
layer computations of Inger (Ref. 8-6) or Fay (Ref. 8-4) which show almost
no difference between equilibrium and nonequilibrium for $\Gamma_s > 10^{-1}$.
Figure 34 taken from Inger illustrates this and shows that to achieve
the full nonequilibrium blocking effect required $\Gamma_s < 10^{-5}$.

Finally, it is likely that even the small (5%) blocking effects
potentially possible according to Figure 34 for $\Gamma_s = 2 \times 10^{-2}$ (high
expansion, high enthalpy case) will not be achieved because of relatively
high surface catalytic efficiencies (γ_w) of the copper models. γ_w has
the microscopic interpretation as the fraction of atoms striking the
geometric surface of the model that undergo heterogeneous recombination.
There is some question as to the exact value of γ_w to use for copper,
but available data indicate it is in the range of 0.1 - 1.0, probably
with the higher values applying to unoxidized surfaces (Wise, Ref. 8-7;

Ref. (8-6) Inger, G.R., "Nonequilibrium Stagnation Point Boundary Layers
            with Arbitrary Surface Catalycity", AIAA J. Vol. 1, No. 8,
            pp. 176 - 178, Aug. 1973
Ref. (8-7) Wise, H., and B. J. Wood, "Reactive Collisions between Gas
            and Surface Atoms", Adv. in Atomic and Molecular Physics. 3,
            (D. R. Bates, ed., 291-353, Academic Press, 1967)
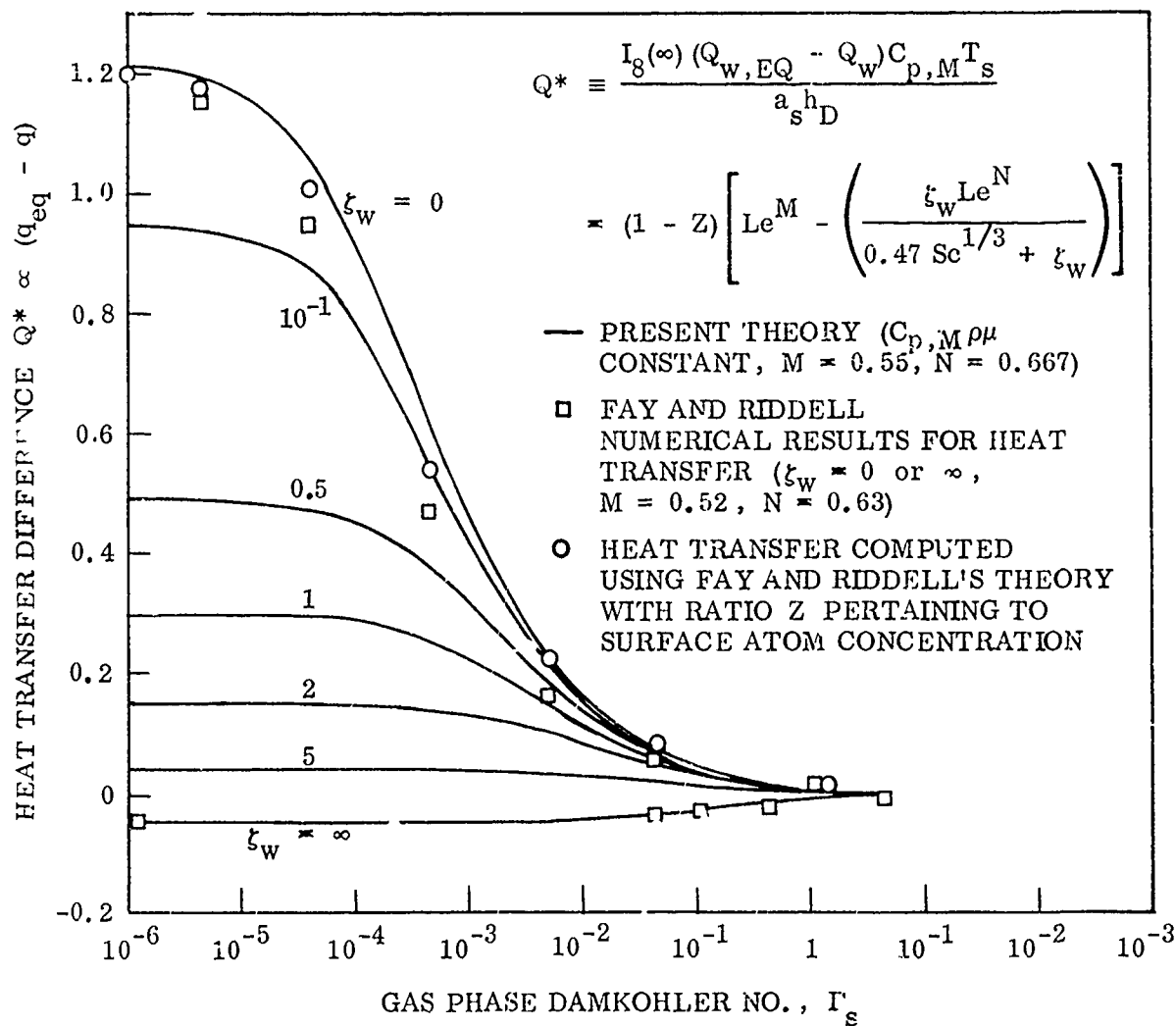
Figure 34 Nonequilibrium Stagnation Point Heat Transfer Results (Inger,
Ref. 8-6) ζ_w is a Heterogeneous Reaction Damkohler No;
$\zeta_w = 0$ Corresponds to a Noncatalytic Wall and $\zeta_w = \infty$ is
Perfectly Catalytic

Carden, Ref. (8-8); Anderson, Ref. (8-9); Pope, Ref. (8-10).

A Damkohler number ζ_w for the heterogeneous recombination process is expressed as: (Rosner, Ref. 8-11)

$$\zeta_w = k_w \rho_w Sc^{2/3} [\frac{\rho_s \mu_s}{r_n} (\frac{2(P_s - P_\infty)}{\rho_s})^{\frac{1}{2}}]^{-\frac{1}{2}}$$

where

$$k_w = \gamma_w (\frac{RT_w}{2\pi M_A})^{\frac{1}{2}}$$

= surface reaction rate constant

γ_w = surface catalytic efficiency or fraction of atoms striking surface which will recombine

R = universal gas constant

T_w = wall temperature

M_A = mole wt. of atoms

μ = viscosity

Sc Schmidt number $\mu/\rho D$

The ζ_w's for the range of RENT conditions have been computed and are also shown in Table 8-2; as can be seen the minimum ζ_w is approximately 8. Refering again to Figure 8-1 it is apparent that ζ_w = 8 would behave nearly as a perfectly catalytic wall in terms of heat transfer.

In conclusion, the combination of relatively modest dissociation, no ionization, and fast gas or surface reaction kinetics should make it a certainty that there will be no significant nonequilibrium effects on the RENT heat transfer with copper models. Even with models with completely non-catalytic coatings and the most extreme conditions (H_o = 6000 B/lb, P_s = 6.5 atm) it is doubtful if a blocking effect could be detected.

Ref. (8-8)   Carden, W.H., Heat Transfer in Nonequilibrium Dissociated Hypersonic Flow with Surface Catalysis and Second-Order Effects", AIAA J., 4, 10, 1704-1711 (Oct. 1966)

Ref. (8-9)   Anderson, L.A. "Effect of Surface Catalytic Activity on Stagnation Heat-Transfer Rates", AIAA J., 11, 5, 649-655 (May 1973)

Ref. (8-10) Pope, R.B., "Stagnation-Point Convective Heat Transfer in Frozen Boundary Layers", AIAA J., 6, 4, 619-626 (Apr. 1968)

Ref. (8-11) Rosner, D.E., "Scale Effects and Correlations in Nonequilibrium Convective Heat Transfer", AIAA J., 1, 7, 1550-1555 (July 1963)

Section 9
TRANSPORT PROPERTIES

In order to qualitatively assess the importance of molecular transport on the magnitude of stagnation point heat transfer, it was first necessary to establish some baseline enthalpy level. Study of Ref. 9-1 shows that a level of 4,500 BTU/lb at a chamber pressure of 100 atm is an appropriate mean upper value. For these circumstances the static pressure behind the shock wave and temperature were found for the Mach = 1.8 nozzle (1.11" diameter), to be about 61 atm and $5240^\circ K$. The stagnation conditions are about 77 atm and $5460^\circ K$. For these conditions, the gas consists of nitrogen molecules and oxygen atoms and some oxygen molecules with only a small amount of atomic nitrogen. The high pressure effectively suppresses the dissociation of nitrogen molecules. The relevant mole fractions of the major species are:

$$[O] = .261$$
$$[N_2] = .692$$
$$[O_2] = .043$$

For these equilibrium stagnation point conditions the mole fraction of electrons is negligible and the conductivity of the gas is less than 0.1 mho/cm.

Heat Transfer Formulations:

As given in Ref. 9-2 the standard form of the Fay & Riddell correlation for heat transfer from a simple dissociated gas mixture is for frozen flow

------

Ref. 9-1 Brown-Edwards, E.G.,"Fluctuations in Heat Flux as Observed in the Expanded Flor from the RENT Facility Arc Heater", AFFDL-TR-73-102, Nov. 1973

Ref. 9-2 Dorrance, W.H., "Viscous Hypersonic Flow", p. 302, McGraw-Hill Book Company, New York (1962)

in the boundary layer, (catalytic wall)

$$(-q_w)_{eq} = 0.763 \ Pr^{-0.6} (\rho_e \mu_e)^{1/2} \left[\left(\frac{dU_e}{ds} \right)_o \right]^{1/2} \frac{(\rho_w \mu_w)^{0.1}}{\rho_e \mu_e}$$

$$x(H-h_w) \left[1 + (L^{0.63}-1) \frac{h_D}{H} \right]$$

The only difference for completely equilibrium flow is a very small change
in the numerical value of the exponent on the Lewis number, L, from 0.63
to 0.52.

Effect of Non-Unity Lewis Number:

Evidently if the Lewis number is unity, the added contribution to the
heat transfer from the degree of free stream dissociation, expressed as the
fraction h_D/H of total energy appearing in dissociated gas, is eliminated.
Based on the calculated shock layer composition this quantity is estimated
to be 0.241. The Lewis number is a function of the degree of dissociation
as shown in Figure 35 taken from Ref. 9-2. The value L_o is taken to be
1.4. For the given stagnation conditions the Lewis number is then found
to be equal to 1.25. This gives only a 3% additional heat transfer rate.
The largest value of Lewis number is 1.464 corresponding to the 100 atm
pressure in the arc chamber with no dissociation. This value gives only
a + 5% increment in heat transfer. If all oxygen were dissociated, the
fraction of energy in this form would rise to 28% of the total. If the
largest value of Lewis number is used, i.e., 1.464, a maximum increase of
6.1% would occur. These conclusions are repeated in Table 9-1.

Table 9-1 Effect of Non-Unity Lewis Number of Heat Transfer

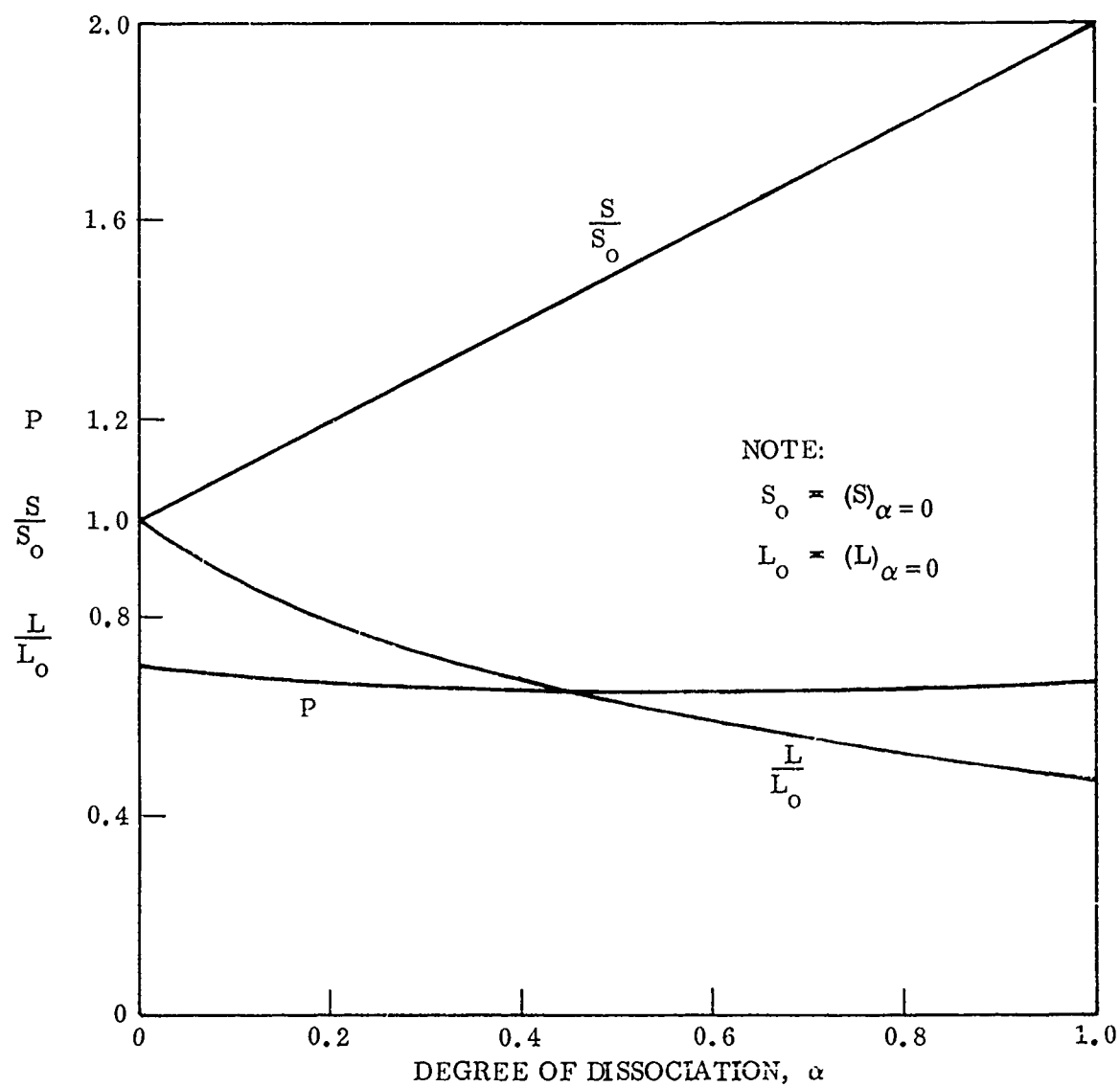| Condition	Heat Transfer Increase
Equilibrium at Stag. Point Best Value of Lewis Number	+3%
Equilibrium Stagnation Point Largest Value of Lewis Number	+5%
Frozen Dissociation Level at Reservoir Conditions Largest Value of Lewis Number	+6.1%

Figure 35   Variation of Prandtl number p, Schmidt number S, and Lewis number
             L with degree of Dissociation for a Dissociating Diatomic Gas

Effect of Density-Viscosity Product Variations:

A natural quantity that occurs during analysis of boundary layers by means of similarity variables is the product of density and viscosity. Different investigators have used various assumptions about how this quantity may vary across a boundary layer. Sibulkin (Ref. 9-3) assumed $\rho\mu = $ constant (or $\mu \alpha T^{-1}$) so that the ratio is unity between wall and free stream conditions. His results including the 0.763 value of the constant are the same as those of Fay & Riddell if $\rho_w\mu_w/\rho_e\mu_e = 1$ and $L_e = 1$. Therefore it is reasonable to assume that the form of heat transfer correlation is not affected by the details of the variability of $\rho\mu$ across the boundary layer.

Fay & Riddell use a Sutherland type viscosity-temperature law so that $\mu\alpha T^{.76}$ or $\rho\mu\alpha T^{-.24}$. The term $[\rho_w\mu_w/\rho_e\mu_e]^{.1}$ is then proportional to $(\frac{T_e}{T_w})^{.024}$. The largest value this temperature ratio could have is given by the ratio of shock layer temperature to ambient temperature which corresponds to the heat transfer gage not rising in temperature. This ratio is 17:1 so that the effect of neglect of this term is to underestimate heat transfer by 7%.

Effects of Viscosity:

The "edge" viscosity appears in the heat transfer equation raised to the 0.4 power. Dorrance (Ref. 9-2) shows typical results for viscosity as a function of temperature as reproduced in Figure 36. It can be argued that one should use the value of viscosity which was employed to derive a particular form of heat transfer correlation. In the case of the Fay & Riddell formula this corresponds to Curve (2) of Figure 36, the Sutherland viscosity law. If, however, (at $5000^\circ K$), the other values of viscosity were to be used, then relative to the Fay & Riddell formulation the heating rate could be (predicted) 16% higher or 9% lower. This effect is essentially the variation of "nose" Reynolds number because of variations in viscosity. Of course, for the simple equilibrium conditions taken in this case, the density is given very accurately by the perfect gas law applied to a dissociating gas.

Ref. 9-3 Sibulkin, M., J. Aeronautical Sciences 19, No. 8, pp. 570-571 (1952)
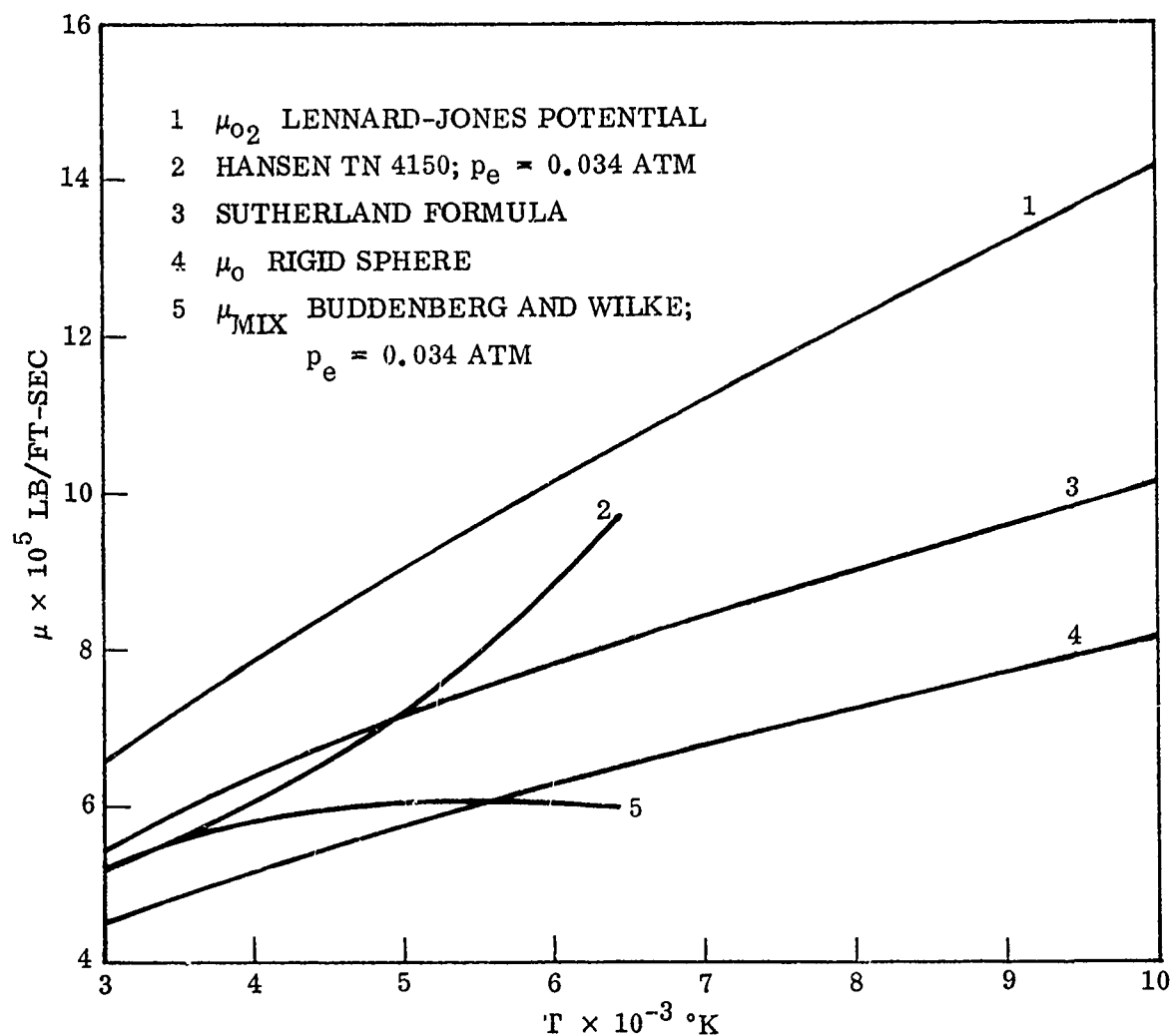
Figure 35 Comparison of Various Calculations of Viscosity at High
Temperature. (After Sinclaire M. Scala and Charles W.
Baulknight, ARS J., Vol. 30, No. 4, pp. 329-336, 1960)

Sutton (Ref. 9-4) treats general gas mixtures and uses a form $\mu \alpha T^{.65}$ which falls within the stated results.

The Prandtl number, which appears to the -0.6 power, produces no effects worth discussion, since the thermal conductivity has the same type of temperature dependence as viscosity. It varies with degree of dissociation very slightly as shown in Figure 35 with a value of 0.7 being generally applicable.

The conclusion can be drawn that for the assumed conditions of equilibrium at the stagnation point the variation in transport properties has very little effect on the theoretical heat transfer and that assuming Lewis number of unity has no serious numerical consequences. These conclusions would have to be altered in the face of any non-equilibrium effects. For example, a large excess of electrons could, if their temperature were elevated, produce an additional heat transfer.

Ref. 9-4 Sutton K., and Graves, R., "A General Stagnation Point Convective Heating Equation for Arbitrary Gas Mictures"

Section 10

CONCLUSIONS

The results of the studies performed during this program lead to the following conclusions:

a) The discrepancy between the bulk enthalpy obtained from an arc chamber heat balance and that computed from heat transfer and stagnation pressure measurements appears to be significant.

b) Free stream turbulence can account for this discrepancy if the turbulence level in the RENT facility is of the order of a few percent

c) Heat transfer enhancement by copper particle impingement is negligible if the copper mass loading is about 0.1% and of major importance for mass loadings of the order of 1%

d) Timewise flow property fluctuations, radial enthalpy gradients, swirling flow, chemical nonequilibrium, and transport property uncertainties individually have a negligible effect on heat transfer in the RENT facility. Taken in total, these phenomena may have a noticeable effect on heat transfer.

APPENDIX A

EFFECT OF TIMEWISE FLUCTUATIONS OF FLOW VARIABLES ON STAGNATION HEAT TRANSFER

A.1 FORMULATION

To study the effect of timewise fluctuations of flow variables on stagnation heat transfer, consider the unsteady, one-dimensional boundary-layer energy equations, which, after neglecting the viscous heating term, can be written as

$$\frac{\partial H}{\partial t} + \frac{\partial H}{\partial y} - \frac{1\partial}{\rho\partial y}\left(\frac{\mu}{Pr}\frac{\partial H}{\partial y}\right) = \frac{1}{\rho}\frac{\partial p_e}{\partial t} \tag{A-1}$$

where p_e is the pressure at boundary layer edge, H is the total enthalpy, ρ is the density, v is the velocity in the y direction, which is the outward normal to the surface, Pr is the Prandtl number and μ is the viscosity. In order to simplify Eq. (A-1), we assume Pr = constant, $\mu = \mu_e$, $\rho = \rho_e$, and that v is given by the constant density inviscid solution for sphere near the wall, i.e.,

$$v \sim -2V_\infty\sqrt{\frac{8\epsilon}{3}}\frac{y}{R_N}$$

where V_∞ is the free stream velocity, R_N is the nose radius, and $\epsilon = \dfrac{\rho_\infty}{\rho_s}$ (density ratio across a normal shock).

In this inviscid flow, it is assumed that the isentropic condition is not violated. In this case, we have from the second law of thermodynamics

$$\frac{dh_e}{dt} \bigg/ \frac{dP_e}{dt} = \frac{1}{\rho_e} \tag{A-2}$$

and since $\dfrac{v_e}{V_\infty} << 1$, we can write $h_e = H_e + O\left(\dfrac{v_e}{V_\infty}\right)^2$

thus

$$\frac{dH_e}{dt} \simeq \frac{1}{\rho_e}\frac{dP_e}{dt} \tag{A-3}$$

Assuming a perfect gas, we have

$$\rho_e = \frac{\gamma-1}{\gamma} \, p_e h_e \simeq \frac{\gamma-1}{\gamma} p_e H_e \tag{A-4}$$

From Eqs. (A-3) and (A-4) it can be shown that

$$\rho_e = C \, H_e^{\frac{1}{\gamma-1}} \tag{A-5}$$

where C is a constant, and

$$\frac{1}{\rho_e} \, \frac{\partial p_e}{\partial t} = \frac{\partial H_e}{\partial t} \tag{A-6}$$

In General, H_e and V_∞ can be represented by Fourier Series as

$$V_\infty = (V_\infty)_o \left[1 + \sum_{n=1}^{\infty} V'_{1n} \cos nft + V'_{2n} \sin nft \right] \tag{A-7}$$

$$H_e + (H_e)_o \left[1 + \sum_{n=1}^{\infty} H'_{1n} \cos nft + H'_{2n} \sin nft \right]$$

where f is the normal frequency.

It is prohibitive to solve Eq. (A-1) for the general case as described by Eq. (A-7), instead, we consider the simplified case of periodic motion as given by

$$V_\infty = (V_\infty)_o \left[1 + V' \cos ft \right] \tag{A-8}$$

$$H_e = (H_e)_o \left[1 + H' \cos ft \right]$$

Assuming

$$\mu \sim T^{1/2} \sim H_e^{1/2} \text{ , we may write}$$

$$\mu_e + (\mu_e)_o \left[1 + \frac{H'}{2} \cos ft \right]$$

From Eqs. (A-5) and (A-8) we may write

$$\rho_e = (\rho_e)_o \left(1 + \frac{H'}{\gamma-1} \cos ft \right) \tag{A-9}$$

Now normalize H by $(H_e)_o$, v by $(V_\infty)_o$, t by $\frac{1}{f}$ and y by $R_N / \sqrt{R_e Pr}$, where R_e is the Reynolds number defined as

$$R_e = \frac{(\rho_e)_o (V_\infty)_o R_N}{(\mu_e)_o}$$

In nondimensional form, Eq. (A-1), after using Eqs. (A-6) and (A-9) becomes

$$\beta_t \frac{\partial H}{\partial t} - 2 \sqrt{\frac{3\epsilon}{3}} y \, (1 + v' \cos t) \frac{\partial H}{\partial y} - (1 + \frac{H'(\gamma-3)}{2(\gamma-1)} \cos t)$$

$$\cdot \frac{\partial^2 H}{\partial y^2} = -\beta_t H' \sin t \tag{A-10}$$

where

$$\beta_t = \frac{R_N f}{(V_\infty)_o} \tag{A-11}$$

Assuming H' and v' to be small, Eq. (A-10) can be solved by the method of successive approximation. To illustrate this method, we rewrite Eq. (A-10) as

$$\beta_t \frac{\partial H}{\partial t} - 2 \sqrt{\frac{8\epsilon}{3}} y \frac{\partial H}{\partial y} - \frac{\partial^2 H}{\partial y^2} + \beta_t H' \sin t = 2 \sqrt{\frac{8\epsilon}{3}} y \, v' \cos t \cdot \frac{\partial H}{\partial y}$$

$$+ \frac{H'}{2} \frac{(\gamma-3)}{(\gamma-1)} \cos t \frac{\partial^2 H}{\partial y^2} \tag{A-12}$$

The zeroth order solution is found by neglecting the right hand side terms of Eq. (A-12), the first order solution is obtained by evaluating the right hand side of Eq. (A-12) based on zeroth order solution. Similar procedures are applied for higher order solutions. We will solve Eq. (A-12) up to the first order. Write

$$H = H_o + H_1 \tag{A-13}$$

H_o satisfies the following equation

$$\beta_t \frac{\partial H_o}{\partial t} - 2 \sqrt{\frac{8\epsilon}{3}} y \frac{\partial H_o}{\partial y} - \frac{\partial^2 H_o}{\partial y^2} = \beta_t H'_1 \sin t \tag{A-14}$$

A further approximation is made to simplify the equation by replacing the coefficient in front of the second term of Eq. (A-14) by unity. This approximation implies the velocity in the boundary layer is assumed to be a constant evaluated at a distance y_o given by $2\sqrt{\frac{8\epsilon}{3}}\, y_o = 1$. This approximation will not affect the conclusion of this study, but will enable us to obtain an analytic solution.

Equation (A-14) therefore becomes

$$\beta_t \frac{\partial H_o}{\partial t} - \frac{\partial H_o}{\partial y} - \frac{\partial^2 H_o}{\partial y^2} = -\beta_t H' \sin t \qquad (A-15)$$

$$y = 0,\ H_o = H_W \quad ;\quad y \to \infty \quad H_o = 1 - H' \cos t$$

Similarly H_1 is governed by the following equations

$$\beta_t \frac{\partial H_1}{\partial t} - \frac{\partial H_1}{\partial y} - \frac{\partial^2 H_1}{\partial y^2} = v'\cos t \cdot \frac{\partial H_o}{\partial y} + \frac{H'}{2}\frac{(\gamma-3)}{(\gamma-1)}\cos t \frac{\partial^2 H_o}{\partial y^2} \qquad (A-16)$$

$$y = 0 \quad H_1 = 0 \quad y \to \infty \quad H_1 = 0$$

The heat transfer toward the surface is given by

$$q_w(t) = k\frac{\partial T}{\partial y}$$

In our nondimensional form, it can be shown that

$$q_w(t) = \sqrt{R_e P_r}\ \left.\frac{\partial H}{\partial y}\right)_{y=0}$$

where $q_w(t)$ is normalized by $(\rho_e)_o (V_\infty)_o (H_e)_o$. The purpose of the present study is to obtain the time average of the unsteady heat transfer $\overline{q_w(t)} = \int_o^{2\pi} q_w(t)\, dt$ and to compare it with the steady heat transfer based on the average free stream enthalpy $q_w \overline{(H_e)}$. The ratio of $\overline{q_w(t)}$ to $q_w(\overline{H_e})$ will determine the effect of time fluctuations on heat transfer.

A.2 SOLUTIONS

Eq. (A-15) is linear, it is convenient to adopt the complex notation to write Eq. (A-15) in the form

$$\beta_t \frac{\partial H_o}{\partial t} - \frac{\partial H_o}{\partial y} - \frac{\partial^2 H_o}{\partial y^2} = i\,\beta_t\, H'\, e^{it} \qquad\qquad (A-17)$$

$$y = 0 \quad H_o = H_w \,, \quad y \to \infty \quad H_o = 1 + H' e^{it}$$

The solution to Eq. (A-15) will be the real part of the solution to Eq. (A-17). Write

$$H_o = (H_o)_1 + (H_o)_2\, e^{it} \,; \quad \text{where } (H_o)_1 \text{ and } (H_o)_2 \text{ are functions of } y \qquad (A-18)$$
only

Substituting Eq. (A-18) into Eq. (A-17) yields

$$\frac{\partial^2 (H_o)_1}{\partial y^2} + \frac{\partial (H_o)_1}{\partial y} = 0 \qquad\qquad (A-19)$$

$$y = 0, (H_o)_1 = H_w, \quad y \to \infty \quad (H_o)_1 = 1$$

$$i\beta_t (H_o)_2 - \frac{\partial (H_o)_2}{\partial y} - \frac{\partial^2 (H_o)_2}{\partial y^2} = i\beta_t H' \qquad\qquad (A-20)$$

$$y = 0, \quad (H_o)_2 = 0, \quad y \to \infty \quad (H_o)_2 = H'$$

The solutions to Eqs. (A-19) and (A-20) are

$$(H_o)_1 = (1 - H_w)(1 - e^{-y}) + H_w$$

$$(H_o)_2 = H'\,[1 - e^{-(k_2 + ik_1)y}]$$

Hence

$$H_o = (1 - H_w)(1 - e^{-y}) + H_w + H'\,[\cos(t) - e^{-k_2 y}\cos(t - k_1 y)] \qquad (A-21)$$

with

$$k_1 = \frac{r_o}{2}\sin\frac{\theta_o}{2} \,, \quad k_2 = \tfrac{1}{2}(1 + r_o\cos\frac{\theta_o}{2}) \,, \quad r_o = [1 + (4\beta_t)^2]^{\frac{1}{4}} \,,$$

$$\theta_o = \tan^{-1} 4\beta_t$$

By using Eq. (A-21) and after some manipulations, Eq. (A-16) becomes

$$\beta_t \frac{\partial H_1}{\partial t} - \frac{\partial H_1}{\partial y} - \frac{\partial^2 H_1}{\partial y^2} = e^{-y}(1 - H_w)\,(v' - \frac{H'(\gamma - 3)}{2(\gamma - 1)})\cos \quad + H' e^{-k_2 y} \cdot$$

$$\cdot [\alpha_1 (1 + \cos 2t) + \alpha_2 \sin 2t] \qquad\qquad (A-22)$$

with

$$\alpha_1 = \tfrac{1}{2}\left\{\left[\frac{H'(\gamma-3)}{2(\gamma-1)}(k_1^2-k_2^2) + K_2 v'\right]\cos k_1 y + \left[v'k_1 - k_1 k_2 \frac{H'(\gamma-3)}{(\gamma-1)}\right]\sin k_1 y\right\}$$

$$\alpha_2 = \tfrac{1}{2}\left\{\left[k_1 k_2 \frac{H'(\gamma-3)}{(\gamma-1)} - v'k_1\right]\cos k_1 y + \left[\frac{H'(\gamma-3)}{2(\gamma-1)}k_1^2 - k_2^2) + v'k_2\right]\sin k_1 y\right\}$$

We again write H_1 in complex notation as

$$H_1 = (H_1)_o + (H_1)_1 e^{it} + (H_1)_2 e^{2it}$$

Since we are only interested in the time average heat transfer, it is only necessary to determine $(H_1)_o$. The other two terms make no contribution to the average heat transfer.

The governing equation for $(H_1)_o$ is

$$\frac{\partial (H_1)_o}{\partial y} + \frac{\partial^2 (H_1)_o}{\partial y^2} = -H' e^{-k_2 y}\alpha(y) \tag{A-23}$$

$$y = 0, \quad (H_1)_o = 0, \quad y \to \infty, \quad (H_1)_o = 0$$

The solution is

$$(H_1)_o = c(1-e^{-y}) - H'\int_o e^{-y} dy \int_o^{y-} e^{-(k_2-1)y}\alpha_1 (y) dy \tag{A-24}$$

where

$$c = H'v'\theta_1(\beta_t) + \theta_2(\beta_t)(H')^2 \frac{(\gamma-3)}{2(\gamma-1)}$$

$$\theta_1(\beta_t) = \tfrac{1}{2}$$

$$\theta_2(\beta_t) = \frac{k_1^2[k_1^2 + k_2^2 + 2k_2(k_2-1)] - k_2[(k_2-1)(k_1^2-k_2^2)]}{2(k_1^2 + k_2^2)[(k_2-1)^2 + k_1^2]}$$

$$+ \frac{(k_1^2 - k_2^2)(k_2-1) - 2k_1^2 k_2}{2[(k_2-1)^2 + k_1^2]} \tag{A-25}$$

From Eqs. (A-21) and (A-24) we obtain the average heat transfer ratio as

$$\frac{\overline{q_w(t)}}{q_w(H_e)} = 1 + \frac{H'v'\theta_1 + \frac{(H')^2}{2}\theta_2\left(\frac{\gamma-3}{\gamma-1}\right)}{1 - H_w} \tag{A-26}$$

It is interesting to find that θ_1 turns out to be a constant independent of frequency.

Equation (A-26) states that the timewise fluctuation will increase the time averaged heat transfer to the wall, the amount of increase is proportional to the fluctuation square as $H'v'$ and $(H')^2$. It is very desirable to relate these fluctuations to the heat flux fluctuations. This will be discussed in the following.

For high Mach numbers, velocity fluctuations are proportional to the square root of total pressure fluctuations. Assuming v' small, then v' can be approximated as

$$v' \simeq \tfrac{1}{2} P_t'$$

where P_t' is the total pressure fluctuation. For isentropic flow of a perfect gas, the total enthalpy fluctuation is directly related to P_t', i.e., $P_t' + H'$, therefore, we have

$$v' = \tfrac{1}{2}H' \tag{A-27}$$

In order to relate H' to the heat flux fluctuation q_w' consider the zeroth order solution. From Eq. (A-21) we obtain

$$q_w \sim \left.\frac{\partial H_o}{\partial y}\right)_{y=0} = (1-H_w)\left[1 + \frac{k_2 H'}{1-H_w}\cos t + ---\right] \tag{A-28}$$

Write

$$q_w = (q_w)_o\left[1 - q_w' \cos t\right] \tag{A-29}$$

By comparing Eq. (A-28) and (A-29) we find

$$H' = \frac{(1-H_w)\, q'_w}{k_2} \tag{A-30}$$

By using Eqs. (A-27) and (A-30), Eq. (A-26) finally becomes

$$\frac{\overline{q_w(t)}}{q_w(\bar{H}_e)} = 1 + (1-H_w)(q'_w)^2\, \Gamma \tag{A-31}$$

where Γ is the heating enhancement parameter defined as

$$\Gamma = \frac{1 + \frac{2(\gamma-3)}{\gamma-1}\theta_2}{4k^2_2} \qquad\qquad\text{(A-32)}$$

Γ is plotted in Figure A-1 as a function of dimensionless frequency β_t.

A.3 CONCLUSIONS

It has been shown that when the free stream enthalpy and velocity fluctuations can be approximated by periodic oscillations, the time averaged stagnation heat transfer is increased over that obtained without oscillation. The amount of increase is a weak function of frequency and is proportional to the square of the heat flux fluctuation.

In the case that the free stream fluctuations are highly irregular, these fluctuations should then be considered as turbulence.

According to Ref. A-1, q'_w found in RENT was 20% at a frequency of 100 Hz. Under this condition, we find that $\beta_t = 2 \times 10^{-4} << 1$, and the effect of this fluctuation on $\bar{q}_w$ is 6.7%, which is small. Frequencies as high as 10^5 Hz were observed in Ref. A-2, and for this frequency, $\beta_t = 0.2$. Again assume a 20% heat flux fluctuation and the effect of this fluctuation on $\bar{q}_w$ is found to be 6.4%. Therefore, for 20% heat flux fluctuation, the effect on $\bar{q}_w$ is small.

Ref. A-1 G. G. Brown-Edwards, "Fluctuations in Heat Flux as Observed in the Expanded Flow from the RENT Facility Arc Heater", AFFDL-TR-23-102, Nov. 1973

Ref. A-2 Daniel M. Parobek, "AFFDL Developments in the H_o and q' Measurements in High Energy Arc Flow", presented 40th Semiannual Meeting of the Supersonic Tunnel Association, 24-26 Sept. 1973
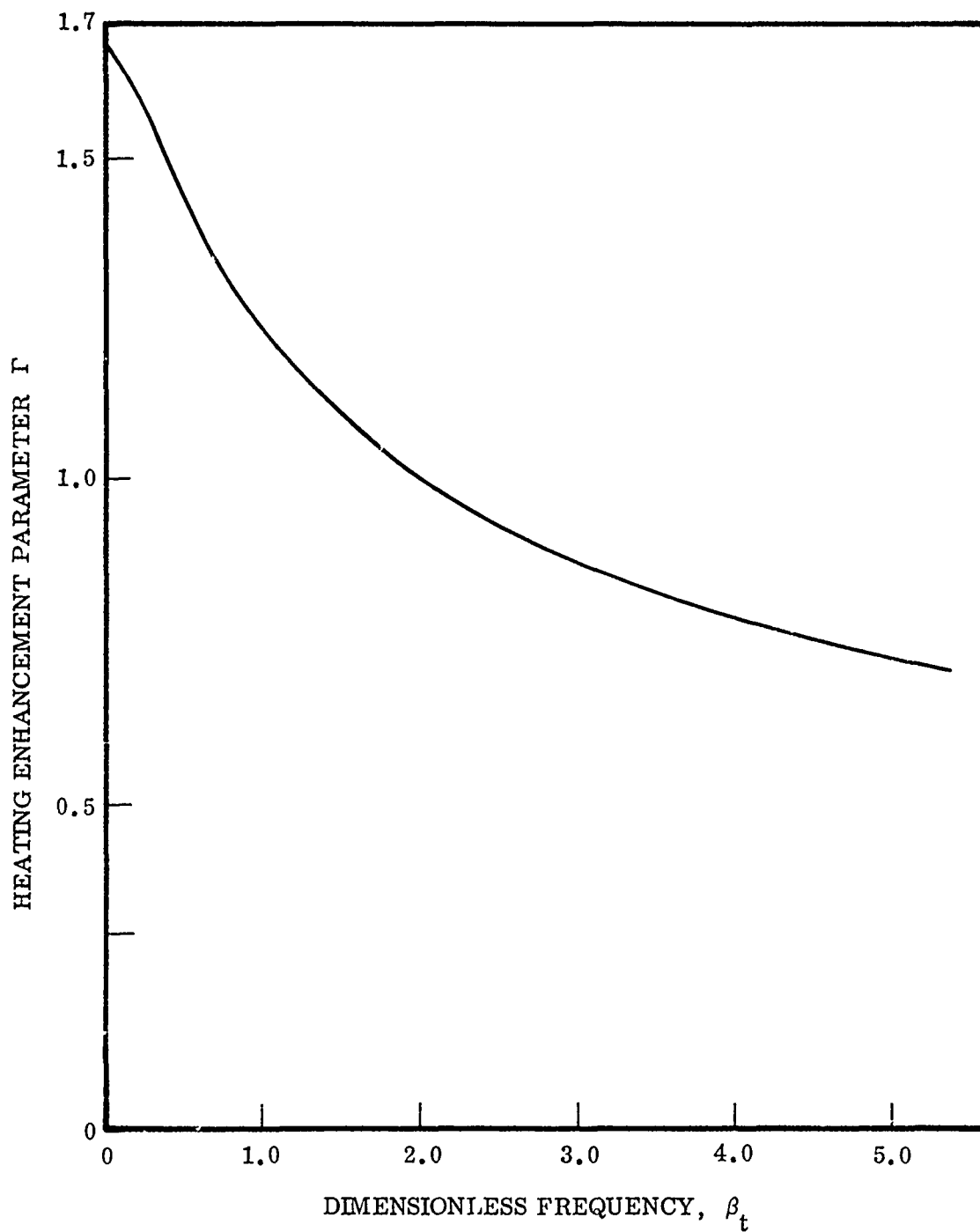
Figure A-1 Heating Enhancement Parameters vs Dimensionless Frequency

APPENDIX B

EFFECT OF TOTAL ENTHALPY VARIATION ON STAGNATION POINT HEAT TRANSFER

In this appendix, we will demonstrate the effect of spatial variation of total enthalpy over the surface of the heat transfer gauge on the stagnation point heat transfer. We assume that the velocity vield is not affected by the spatial nonuniformity of enthalpy. Therefore, we will consider only the energy equation.

The dimensionless shock layer energy equation for a compressible gas with constant Prandtl number written in a set of similarity variables (ξ,η) is: (Ref. B-1)

$$\frac{\partial}{\partial\eta}(f\frac{\partial H}{\partial\eta}) + 2R_e P_r(\frac{r_s}{U_s}\frac{dr_s}{d\xi})\eta\frac{\partial H}{\partial\eta} = U_s^2(1-P_r)\frac{\partial}{\partial\eta}(f^2\frac{\partial f}{\partial\eta}) + R_e P_r\frac{r_s^2}{U_s}H_\xi \qquad (B-1)$$

where

$$f = \frac{U}{U_s}, \quad R_e = \frac{\rho_s(0)U_\infty a}{\mu_s(0)}, \quad P_r = \frac{\mu c_p}{k},$$

U is the tangential velocity in the shock layer, U_s is the tangential velocity immediately behind the shock and $\rho_s(0)$ and $\mu_s(0)$ are the density and viscosity immediately behind the shock at the stagnation line, respectively. The total enthalpy H is normalized by that behind the shock at the stagnation line. A sketch of the geometry is shown in Fig. B-1. Due to the normalization, the shock position is at $\eta = 1$ and $\eta = 0$

Ref. B-1 Y. S. Chou, "Locally Nonsimilar Solutions for Radiating Shock Layer about Smooth Axisymmetric Bodies", NASA CR-1989, March 1972

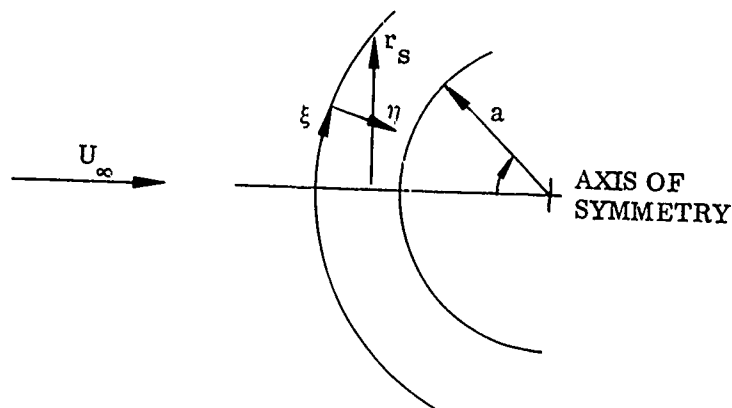is the probe surface. The heat transfer gauge extends from θ_o to $-\theta_o$ ($\theta_o << 1$).

Figure B-1 Flow Geometry

Equation (B-1) can be formally integrated, subject to the boundary conditions that at $\eta = 1$, $H = H_o$ at $\eta = 0$, $H = H_w$, as

$$H = G_1(\eta) + C_1 G_2(\eta) + H_w \tag{B-2}$$

where

$$G_1(\eta) = \int_o^\eta \frac{d\eta}{f} \int_o^\eta [U_s^2(1-Pr)\frac{\partial}{\partial \eta}(f^2 \frac{\partial f}{\partial \eta}) + R_e P_r \frac{r_s^2}{U_s} H_s] \exp[\int_\eta^{\eta'} 2PrR_e \frac{r_s}{u_s} \cdot$$

$$\cdot \frac{dr_s}{d\xi} \frac{\eta''}{f} d\eta''] d\eta'$$

$$G_2(\eta) = \int_o^\eta \frac{1}{f} \exp[-2R_e P_r \frac{r_s}{U_s} \frac{dr_s}{d\xi} \int_o^\eta \frac{\eta'}{f} d\eta'] d\eta$$

and the constant C_1 is given by

$$C_1 = \frac{H_s - H_w - G_1(1)}{G_2(1)} \tag{B-3}$$

It can be shown that the convective heating is related to constant C_1 as

$$q_w = (\frac{U_s}{2R_e r_s}) C_1 \tag{B-4}$$

where q_w is normalized by p_∞, U_∞, H_∞, U_s and r_s are dimensionless quantities, normalized by U_∞ and a respectively. Hence, we obtain

-92-

$$\frac{(q_w)_{\frac{dH_s}{d\theta} \neq 0}}{(q_w)_{\frac{dH_s}{d\theta} = 0}} = \frac{C'_1}{C_1 \bar{H}} = \frac{[H_s - H_w - G'_1(1)]G_2(1)}{[1 - H_w - G_1(1)]G'_2(1)\bar{H}}$$
(B-5)

Where subscript ( )' denotes the solution for the case $\frac{dH_s}{d\theta} \neq 0$.

Note for the constant enthalpy case (i.e., $\frac{dH_s}{d\theta} = 0$), $H_s = 1$ due to the normalization. $\bar{H}$ is the average H over the gauge.

$$\bar{H} = \frac{\int_o^{\theta_o} H \, d\eta}{2\theta_o}$$

Assuming the effect of free stream enthalpy nonuniformity on the velocity field as well as H_ξ can be neglected, we then have

$$G'_1(1) \simeq G_1(1) \quad , \quad G'_2(1) \simeq G_2(1)$$
(B-6)

For small θ we may write
$$H_s = 1 + (\frac{dH_s}{d\theta})_o \theta + ----$$
(B-7)

After using Eqs. (B-6) and (B-7), Eq. (B-5) becomes

$$\frac{(q_w)_{\frac{dH_s}{d\theta} \neq 0}}{(q_w)_{\frac{dH_s}{d\theta} = 0}} = [1 + \frac{\frac{dH_s}{d\theta})\theta}{2R_e \frac{r_s}{U_s} (q_w)_{\frac{dH_s}{d\theta} = 0} G_2(1)}] \frac{1}{\bar{H}}$$
(B-8)

now

$$G_2(1) = \int_o^1 \frac{1}{f} \exp [-2R_e P_r \frac{r_s}{U_s} \frac{dr_s}{d\xi} \int_o^\eta \frac{\eta'}{f} d\eta'] d\eta$$

Assuming $\iota \simeq 1$ then, $G_2(1) \simeq \dfrac{\pi}{2} \dfrac{\mathrm{erf}\left(\sqrt{R_e P_r}\, \dfrac{r_s}{U_s}\, \dfrac{dr_s}{d\xi}\right)}{\sqrt{R_e P_r}\, \dfrac{r_s}{U_s}\, \dfrac{dr_s}{d\xi}}$

for $R_e \gg 1$, $r_s \sim \theta$, $U_s \sim \sin\theta \sim \theta$, $\dfrac{dr_s}{d\xi} \sim \dfrac{dr_s}{d\theta} \sim 1$

Hence for $R_e \gg 1$, $G_2(1) \sim \dfrac{\sqrt{\pi}}{2} \dfrac{1}{\sqrt{R_e P_r}}$

From Ref. B-2, we obtain $\sqrt{R_e}(q_w)_{\frac{dH_s}{d\theta}=0} \simeq 0.65 \pm 0.33\theta$ where (-) sign is for $\theta > 0$ and (+) sign for $\theta < 0$. Equation (B-8) is now reduced to ($P_r = 0.72$)

$$\dfrac{(q_w)_{\frac{dH_s}{d\theta} \neq 0}}{(q_w)_{\frac{dH_s}{d\theta} = 0}} = \left[1 + \dfrac{0.48\left(\frac{dH_s}{d\theta}\right)_o \theta}{0.65 \pm 0.33\theta}\right] \dfrac{1}{\bar{H}} \tag{B-9}$$

The (-) sign in the denominator of Eq. (B-9) is for $\theta > 0$, (+) sign is for $\theta < 0$. Let us write

$$\bar{q}_w = \dfrac{\int_{-\theta_o}^{\theta_o} (q_w)_{\frac{dH_s}{d\theta} \neq 0}\, d\theta}{2\theta_o} \quad , \quad \bar{q}_w = \dfrac{\int_{-\theta_o}^{\theta_o} (q_w)_{\frac{dH_s}{d\theta} = 0}\, d\theta}{2\theta_o}$$

then $\bar{q}_w'$ is the average heat flux over the heat transfer gauge in the

------

Ref. B-2   R. T. Davis and I. Flugge-Lotz, "Second Order Boundary Layer Effects in Hypersonic Flow Past Axisymmetric Blunt Bodies" J. Fluid Mech., Vol. 10, Pt. 4, Dec. 1964

case that $\dfrac{dH_s}{d\theta} \neq 0$ while $\bar{q}_w$ is the average heat flux over the gauge

for $\dfrac{dH_s}{d\theta} = 0$

From Eq. (B-9) we have

$$\bar{H}\,\bar{q}_w^{\,\prime} = \bar{q}_w + \frac{0.48}{2\theta o}\int_{-\theta o}^{\theta o} \frac{\dfrac{dH_s}{d\theta})_o\,(q_w)\,\dfrac{dH_s}{d\theta}=0}{0.65 \; \underset{+}{-} \; 0.33\theta}\;\theta\;d\theta \;\simeq\; \bar{q}_w\,[1 + \frac{0.24}{\theta o}\int_{-\theta o}^{\theta o}$$

$$\frac{\dfrac{dH_s}{d\theta})_o}{0.65 \; \underset{+}{-} \; 0.33\theta}\;\theta\;d\theta\,] \tag{B-10}$$

After θ integration, we finally obtain from Eq. (B-10)

$$\frac{\bar{q}_w}{\bar{q}_w} = \frac{1 + 0.18\;\theta o[1 + 0.52\theta o][-\dfrac{dH_s}{d\theta})_o^{-}]}{1 + 0.25\;\theta o\;[-\dfrac{dH_s}{d\theta})_o^{+}]} \tag{B-11}$$

where $\dfrac{dH_s}{d\theta})_o^{+}$ denotes the slope of H_s in the positive θ direction, $\dfrac{dH_s}{d\theta})_o^{-}$ indicates $\dfrac{dH_s}{d\theta})_o$ in the negative direction. Based on Eq. (B-11) the effect of the total enthalpy spatial variation can be discussed as the following.

a. If the enthalpy varies linearly over the heat transfer gauge as shown in Figure B-2a, there is no net effect on the heat transfer.

b. If the gauge is located on an enthalpy maximum as shown in Figure B-2b, the effect is that the average heat transfer in this case will be greater than that of the constant enthalpy case.

The amount of decrease or increase from the constant enthalpy heat transfer in Cases (b) and (c) obviously depends on the local slope

$\frac{dH_s}{dt_o}+)$ and $\frac{dH_s}{d\theta_o}-)$. This possible change from the constant enthalpy case is small as discussed in Section 6.

NO EFFECT

(a)

$\dot{q}$ INCREASES
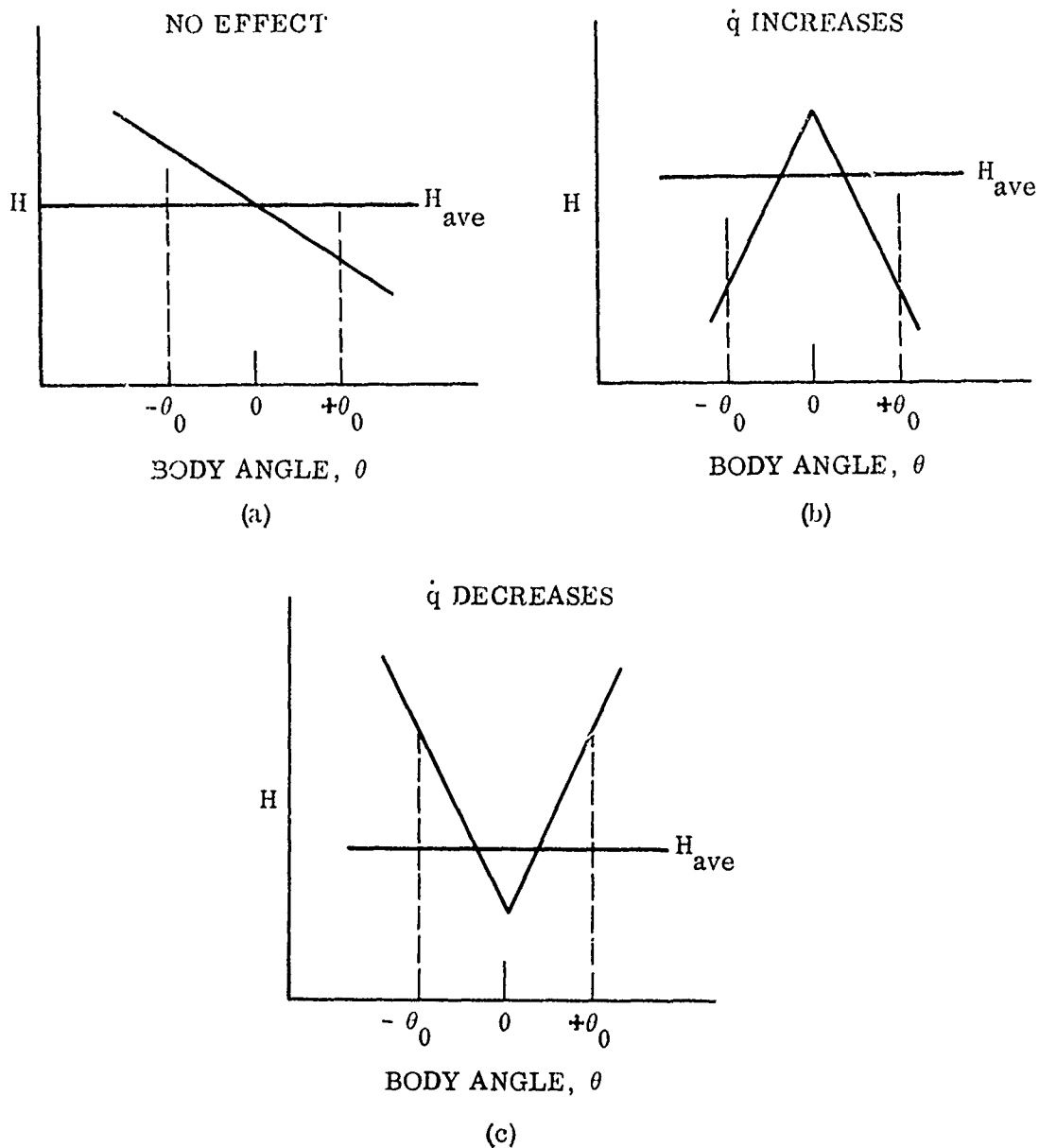

(b)

$\dot{q}$ DECREASES

(c)

Figure B-2 Possible Effect of Total Enthalpy on Stagnation Point
           Heat Flux

APPENDIX C

EFFECT OF SWIRLING FLOW ON STAGNATION POINT HEAT TRANSFER

The effect of free stream swirling motion on stagnation point heat transfer to a blunt body is considered in this Appendix. It is assumed that the effect of coupling between compressibility and swirling motion on heat transfer is negligibly small so that an incompressible analysis will give the correct relative change in heat transfer due to swirl. This analysis is therefore for a viscous incompressible fluid with a swirling motion superimposed on a uniform flow.

For the incompressible swirling motion near an axisymmetric stagnation point, the inviscid velocity components can be written as

$$U = Ar \quad , \quad v = \Omega r, \quad W = 2AZ \tag{C-1}$$

where U is the component in the r direction, Figure C-1, v in the φ direction, W is the component in the negative Z direction.
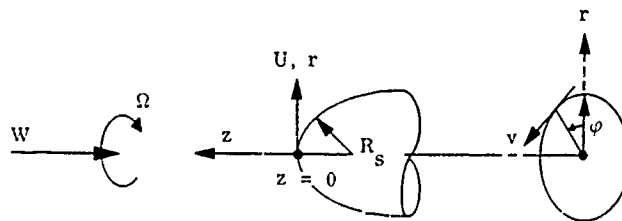

Figure C-1 Coordinate System

Ω is the angular velocity of a solid body, and A is a parameter related to the streamwise velocity gradient at the stagnation point.

$A = \dfrac{\partial U}{\partial r})_{\substack{r = 0 \\ Z = 0}}$. The plane $Z = 0$ is the stagnation plane.

From Eq. (C-1) and the inviscid momentum equation, we obtain the pressure gradient as

$$-\frac{1}{\rho}\frac{\partial p}{\partial r} = (A^2 - \Omega^2)r \quad , \quad -\frac{1}{\rho}\frac{\partial p}{r\partial\varphi} = 2A\Omega r \quad , \quad \frac{\partial p}{\partial Z} \simeq 0 \qquad \begin{array}{l}\text{(Boundary Layer)}\\\text{(approximation)}\end{array}$$

The boundary layer equations in this case can be written as

$$U \frac{\partial U}{\partial r} + W \frac{\partial U}{\partial Z} - \frac{v^2}{r} = (A^2 - \Omega^2)\, r + v\left[\frac{\partial^2 U}{\partial r^2} + \frac{\partial}{\partial r}\left(\frac{U}{r}\right) + \frac{\partial^2 U}{\partial Z^2}\right] \tag{C-2}$$

$$U \frac{\partial v}{\partial r} + W \frac{\partial U}{\partial Z} + \frac{Uv}{r} = 2A\Omega r + v\left[\frac{\partial^2 v}{\partial r^2} + \frac{\partial}{\partial r}\left(\frac{v}{r}\right) + \frac{\partial^2 v}{\partial Z^2}\right] \tag{C-3}$$

$$\frac{\partial U}{\partial r} + \frac{U}{r} + \frac{\partial W}{\partial Z} = 0 \tag{C-4}$$

The boundary conditions are

$Z = 0$, $U = 0$, $W = 0$ (no slip condition)

$Z \to \infty$, $U - Ar$, $v = \Omega r$

Define the dimensionless variable $\zeta = \dfrac{Z\sqrt{A+\Omega}}{v}$ (C-5)

and assume the velocity components in the boundary layer having the form

$$U = r(A + \Omega) F(\zeta) \quad , \quad v = r\Omega G(\zeta) \quad , \quad W = -2\sqrt{(A+r)v}\, H(\zeta) \tag{C-6}$$

We obtain equations for H, G, and F from Eqs. (C-2) - (C-4) as

$$H''' + 2HH'' - (H')^2 + \left(\frac{\Omega}{A+r}\right)^2 G^2 + \frac{A^2 - \Omega^2}{(A+\Omega)^2} = 0 \tag{C-7}$$

$$G'' + 2HG' - 2H'G + \frac{2A}{A+\Omega} = 0 \tag{C-8}$$

$$F = H' \tag{C-9}$$

Where the subscript ( )' denotes differentiation with respect to ζ.
The boundary conditions for H and G are

$$\zeta = 0 \quad H = 0 \quad , \quad H' = 0 \quad , \quad G = 0 \tag{C-10}$$

$$\zeta \to \infty \quad H = \frac{A}{A+\Omega} \qquad\qquad G = 1$$

The solution to Eqs. (C-7) - (C-10) yields the velocity field for a
swirling stagnation point boundary layer.

The stagnation point energy equation can be written as

$$g'' + 2P_r Hg' = 0$$

where $g = \dfrac{T - T_w}{T_{st} - T_w}$, T_w is the temperature at wall and T_{st} the
stagnation temperature behind the normal shock.

The boundary conditions for g are: $\zeta = 0$ $g = 0$, $\zeta \to \infty$ $g = 1$. Now the heat transfer to the wall is

$$q_w = k\frac{\partial T}{\partial Z} = k(T_{st} - T_w) \sqrt{\frac{A+\Omega}{\nu}}g'(0)$$

Hence

$$\frac{q_w}{(q_w)_{\Omega=0}} = \sqrt{\frac{1+\Omega}{A}} \frac{g'(0)}{g'(0)_{\Omega = 0}} \qquad\qquad \text{(C-12)}$$

Since the energy equation, Eq. (C-11), is coupled with Eqs. (C-7) – (C-10) through the velocity function H, $g'(0)$ will be, in general, a function of $\frac{\Omega}{A}$

For small $\frac{\Omega}{A}$ we see that Eq. (C-7) is decoupled from Eq. (C-8) to the order of $(\frac{\Omega}{A})^2$. Also the boundary condition for H as $\zeta \to \infty$ can be approximated as $H' \cong 1$. In this case, the equation for H becomes

$$H''' + 2H\,H'' - (H')^2 + 1 = 0 \qquad\qquad \text{(C-13)}$$

$$\zeta = 0 \quad , \quad H = 0 \quad , \quad H' = 1$$

Equation (C-13) is identical to the equation for the non-swirling case. The solution to Eq. (C-13) is available in Ref. (C-1). Hence, for small $\frac{\Omega}{A}$, we have $H \cong H_{\Omega=0} + 0(\frac{\Omega}{A})$ which implies $g'(0) \cong g'(0)_{\Omega=0} + 0(\frac{\Omega}{A})$ and the effect of swirl on heat transfer for small $\frac{\Omega}{A}$ is

$$\frac{q_w}{(q_w)_{\Omega=0}} = \sqrt{\frac{1+\Omega}{A}} \left[1 + 0(\frac{\Omega}{A})\right] \quad \frac{\Omega}{A} << 1 \qquad\qquad \text{(C-14)}$$

From Ref. (C-2) the parameter A is found to be related to the density across the normal shock as

$$A = (3\epsilon)^{1/2} \frac{W_\infty}{R_s} \quad \text{where} \quad \epsilon = \frac{\rho_\infty}{\rho_S} \quad , \quad R_s - \text{nose radius}$$

We finally obtain

$$\frac{q_w}{(q_w)_{\Omega=0}} = \sqrt{1+ \frac{\Omega R_s}{W_\infty \sqrt{3\epsilon}}} \left[1 + 0\frac{\Omega}{A}\right] \text{ for } \frac{\Omega}{A} << 1 \qquad\qquad \text{(C-15)}$$

From this analysis we see that, physically, the effect of swirling motion
on stagnation point heat transfer is two-fold. The first is to increase
the boundary layer thickness due to the influence of the (positive
direction) swirling secondary flow. This in turn will decrease the
heat transfer. The second effect is to increase the streamwise pressure
gradient at the boundary layer edge due to the centrifugal force. This
will increase the heat transfer. The second effect dominates so that the
net result of these two effects is to increase the heat transfer at the
stagnation point. This increase in heat transfer is small for the RENT
flow conditions as discussed previously.

Ref. C-1 H. Schlichting, "Boundary Layer Theory", 4th edition, McGraw-
          Hill, 1960, pp. 81-83 and pp. 177-179
Ref. C-2 Y. S. Chou, "Inviscid Hypersonic Flow Past Blunt Bodies", AIAA J.
          Vol. 7, No. 1, Jan. 1967